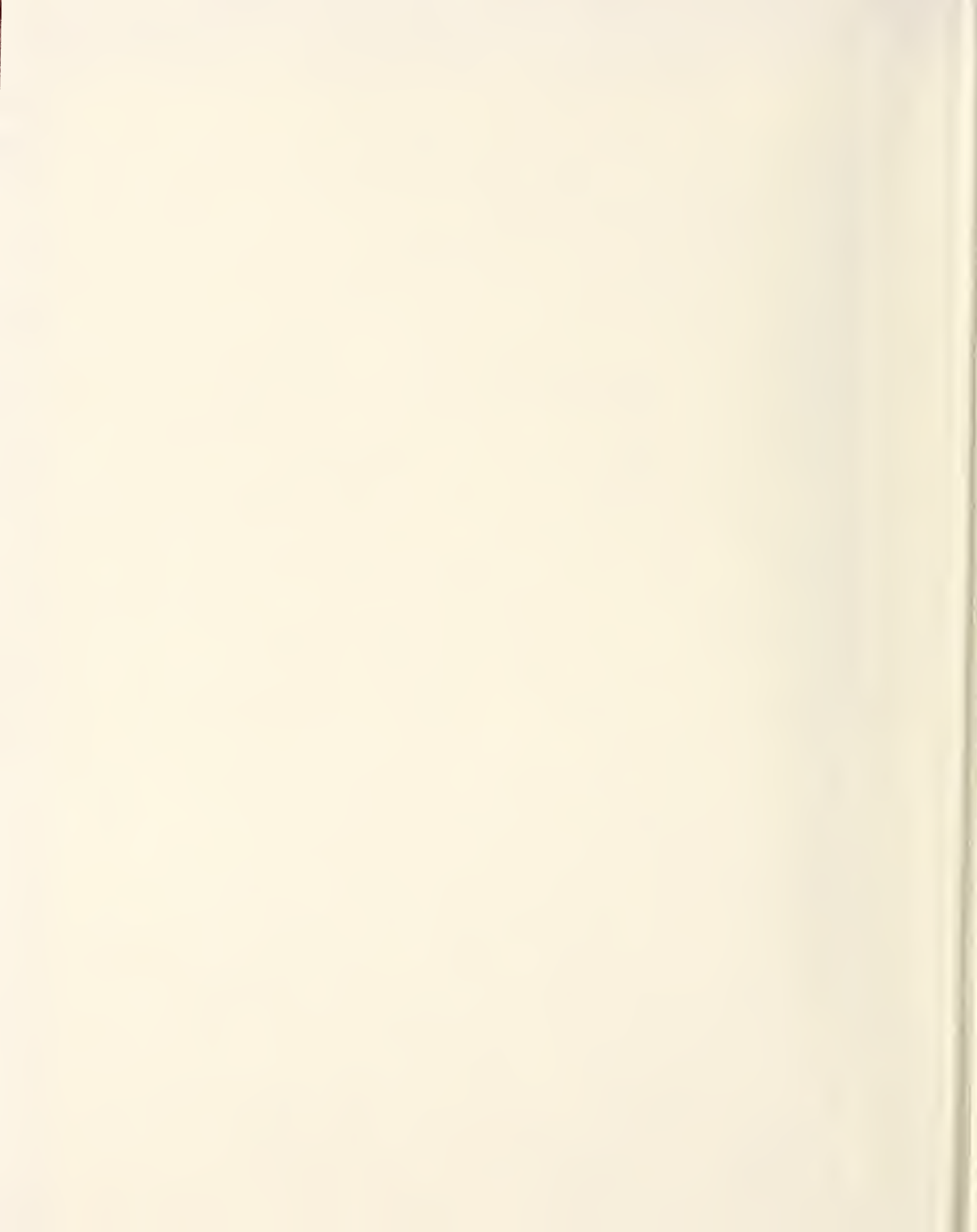


NATL INST. OF STAND & TECH



A11107 209370













National Bureau of Standards  
Library, E-01 Admin. Bldg.

OCT 6 1981

191145

QC

100

.45753

NBS TECHNICAL NOTE 1116

U.S. DEPARTMENT OF COMMERCE / National Bureau of Standards

# SHIELDOSE: A Computer Code for Space-Shielding Radiation Dose Calculations

00  
5753  
p. 1116  
222

## NATIONAL BUREAU OF STANDARDS

The National Bureau of Standards<sup>1</sup> was established by an act of Congress on March 3, 1901. The Bureau's overall goal is to strengthen and advance the Nation's science and technology and facilitate their effective application for public benefit. To this end, the Bureau conducts research and provides: (1) a basis for the Nation's physical measurement system, (2) scientific and technological services for industry and government, (3) a technical basis for equity in trade, and (4) technical services to promote public safety. The Bureau's technical work is performed by the National Measurement Laboratory, the National Engineering Laboratory, and the Institute for Computer Sciences and Technology.

**THE NATIONAL MEASUREMENT LABORATORY** provides the national system of physical and chemical and materials measurement; coordinates the system with measurement systems of other nations and furnishes essential services leading to accurate and uniform physical and chemical measurement throughout the Nation's scientific community, industry, and commerce; conducts materials research leading to improved methods of measurement, standards, and data on the properties of materials needed by industry, commerce, educational institutions, and Government; provides advisory and research services to other Government agencies; develops, produces, and distributes Standard Reference Materials; and provides calibration services. The Laboratory consists of the following centers:

Absolute Physical Quantities<sup>2</sup> — Radiation Research — Thermodynamics and Molecular Science — Analytical Chemistry — Materials Science.

**THE NATIONAL ENGINEERING LABORATORY** provides technology and technical services to the public and private sectors to address national needs and to solve national problems; conducts research in engineering and applied science in support of these efforts; builds and maintains competence in the necessary disciplines required to carry out this research and technical service; develops engineering data and measurement capabilities; provides engineering measurement traceability services; develops test methods and proposes engineering standards and code changes; develops and proposes new engineering practices; and develops and improves mechanisms to transfer results of its research to the ultimate user. The Laboratory consists of the following centers:

Applied Mathematics — Electronics and Electrical Engineering<sup>2</sup> — Mechanical Engineering and Process Technology<sup>2</sup> — Building Technology — Fire Research — Consumer Product Technology — Field Methods.

**THE INSTITUTE FOR COMPUTER SCIENCES AND TECHNOLOGY** conducts research and provides scientific and technical services to aid Federal agencies in the selection, acquisition, application, and use of computer technology to improve effectiveness and economy in Government operations in accordance with Public Law 89-306 (40 U.S.C. 759), relevant Executive Orders, and other directives; carries out this mission by managing the Federal Information Processing Standards Program, developing Federal ADP standards guidelines, and managing Federal participation in ADP voluntary standardization activities; provides scientific and technological advisory services and assistance to Federal agencies; and provides the technical foundation for computer-related policies of the Federal Government. The Institute consists of the following centers:

Programming Science and Technology — Computer Systems Engineering.

<sup>1</sup>Headquarters and Laboratories at Gaithersburg, MD, unless otherwise noted;  
mailing address Washington, DC 20234.

<sup>2</sup>Some divisions within the center are located at Boulder, CO 80303.

APR 25 1980

NOT acc.-C.R.C.

QC 100

UE 753

No. 1116

1980

C.2

# SHIELDOSE: A Computer Code for Space-Shielding Radiation Dose Calculations

Stephen Seltzer

Center for Radiation Research  
National Measurement Laboratory  
National Bureau of Standards  
Washington, DC 20234

Sponsored by:

Office of Naval Research  
Arlington, VA 22217

and

NASA Goddard Space Flight Center  
Greenbelt, MD 20771



*t* Technical note

---

U.S. DEPARTMENT OF COMMERCE, Philip M. Klutznick, Secretary

Luther H. Hodges, Jr., Deputy Secretary

Jordan J. Baruch, Assistant Secretary for Productivity, Technology, and Innovation

NATIONAL BUREAU OF STANDARDS, Ernest Ambler, Director

Issued May 1980

**National Bureau of Standards Technical Note 1116**

Nat. Bur. Stand. (U.S.), Tech. Note 1116, 72 pages (May 1980)  
CODEN: NBTNAE

**U.S. GOVERNMENT PRINTING OFFICE  
WASHINGTON: 1980**

---

For sale by the Superintendent of Documents, U.S. Government Printing Office, Washington, D.C. 20402  
Price \$3.75  
(Add 25 percent for other than U.S. mailing).

Stephen M. Seltzer  
National Bureau of Standards  
Washington, D.C. 20234

A computer code, SHIELDOSE, has been developed for the calculation of absorbed dose as a function of depth in aluminum shielding material of spacecraft, given the electron and proton fluences encountered in orbit. Absorbed dose, for small volumes of the detector materials Al, H<sub>2</sub>O, Si, and SiO<sub>2</sub>, is evaluated in three geometries: (1) in a semi-infinite plane medium, (2) at the transmission surface of a finite-thickness slab, and (3) at the center of a solid sphere. Use of the code is described, and an extensive set of monoenergetic depth-dose data for the various detector materials and geometries is tabulated.

Key words: Computer code; depth-dose data; electrons; electron bremsstrahlung; protons; space shielding.

### 1. Introduction

The ability to predict absorbed dose within a spacecraft due to a specified radiation environment is important for design and planning considerations pertaining to the reliability of electronic components and to the radiological safety of on-board personnel. This report describes the computer code SHIELDOSE, which evaluates the absorbed dose as a function of depth in aluminum shielding material of spacecraft, given the electron and proton fluences encountered in orbit.

---

<sup>1</sup>Work supported by the Office of Naval Research and by the National Space Science Data Center at the NASA Goddard Space Flight Center.

The code makes use of pre-calculated, monoenergetic depth-dose data for an isotropic, broad-beam fluence of radiation incident on uniform aluminum plane media. Such data are particularly suitable for routine dose predictions in situations where the geometrical and compositional complexities of the spacecraft are not known. Furthermore, restricting our consideration to these rather simple geometries has allowed for the development of accurate electron and electron-bremsstrahlung data sets based on detailed transport calculations rather than on more approximate methods. The present version of SHIELDOSE calculates, for arbitrary proton and electron incident spectra, the dose absorbed in small volumes of the detector materials Al, H<sub>2</sub>O (tissue-equivalent detector), Si, and SiO<sub>2</sub>, in the following aluminum shield geometries: (1) in a semi-infinite plane medium, as a function of depth; (2) at the transmission surface of a plane slab, as a function of slab thickness; and (3) at the center of a solid sphere, as a function of sphere radius.

Section 2 defines a number of pertinent quantities used in the calculations and briefly outlines the methods used for integrating the monoenergetic data over the incident flux spectra. Section 3 gives the meanings and required formats of the various input parameters, and other running instructions for SHIELDOSE. Appendix A is a reprint of a report [1]<sup>2</sup> which gives details on the methods with which the monoenergetic depth-dose distributions were calculated. Appendix B comprises tables of the monoenergetic depth-dose data; appendix C gives the input and output listings of a sample run; and appendix D contains a FORTRAN listing of the code.

---

<sup>2</sup>Figures in brackets indicate the literature references at the end of this paper.

## 2. Method

The quantity of interest calculated by SHIELDOSE is the absorbed dose  $\mathcal{D}(z)$ , as a function of depth  $z$  in an aluminum shield, for an arbitrary incident fluence<sup>3</sup> of radiation. The incident fluence can be either protons or electrons. If it is protons, it will be implicitly understood that  $\mathcal{D}(z)$  is the proton dose; if electrons,  $\mathcal{D}(z)$  is calculated separately for the bremsstrahlung component and the "electron" component (by which we mean the distribution of deposited electron energy never converted to bremsstrahlung photons). Results are calculated for three geometries (see fig. 1):

Case 1.  $\mathcal{D}_{\infty}^{\text{det}}(z)$  is the absorbed dose in a thin detector (of material denoted by "det") at a depth  $z$  in a semi-infinite plane aluminium medium. Irradiation is from one side only (the assumed infinite backing effectively insures this).

Case 2.  $\mathcal{D}_{-}^{\text{det}}(z)$  is the absorbed dose in a thin detector at the transmission surface of an aluminum plane slab of thickness  $z$ . Irradiation is from one side only.

Case 3.  $\mathcal{D}_{\cdot}^{\text{det}}(z)$  is the absorbed dose in a small detector volume at the center of a solid aluminum sphere of radius  $z$ . Irradiation is from all directions.

The detector materials Al, H<sub>2</sub>O, Si, and SiO<sub>2</sub> are presently included in the data base.

---

<sup>3</sup>We can use the fluence (number per unit area, per unit energy, per unit solid angle) and the flux (number per unit area, per unit energy, per unit solid angle, per unit time) interchangeably. Use of the fluence leads to absorbed dose, and the flux to dose rate.

We define the following quantities:

$\phi(T_0, \theta)$  is the incident fluence, differential in energy  $T_0$  and angle  $\theta$ , having units of  $\text{cm}^{-2}\text{MeV}^{-1}\text{sr}^{-1}$ . We assume  $\phi$  to be isotropic and drop the explicit dependence on  $\theta$ .

$\psi_{4\pi}(T_0) = 4\pi \phi(T_0)$  is the full-space ( $4\pi$ ) incident fluence, having units of  $\text{cm}^{-2}\text{MeV}^{-1}$ .

$D_{\infty}^{\text{det}}(z, T_0)$  is the depth-dose distribution for irradiation by a monoenergetic, omnidirectional beam with energy  $T_0$  incident on a semi-infinite medium (case 1 geometry).

The depth-dose distribution, normalized to an incident current of  $1 \text{ cm}^{-2}$  (see appendix A, eqs (1-5)), has units of  $\text{MeV cm}^2/\text{g}$ .  $D_{\infty}^{\text{det}}$  is given separately for the proton, electron, and electron-bremsstrahlung components.

$D_{\infty}^{\text{det}}(z, T_0)$  is similar to  $D_{\infty}^{\text{det}}$  but for monoenergetic irradiation of finite-thickness slabs (case 2 geometry), from one side only.

Then

$$D_{\infty}^{\text{det}}(z) = \frac{K}{4} \int_0^{\infty} \psi_{4\pi}(T_0) D_{\infty}^{\text{det}}(z, T_0) dT_0 , \quad (1)$$

where  $K = 1.6022 \times 10^{-8} \text{ rads}/(\text{MeV g}^{-1})$ , and the factor of  $1/4$  comes from the relation between the full-space fluence and the incident current (see eq (5) in appendix A). Because the incident fluence  $\psi_{4\pi}(T_0)$  typically falls off rather steeply with increasing energy, eq (1) is rewritten

$$D_{\infty}^{\text{det}}(z) = \frac{K}{4} \int_{\ln T_{\min}}^{\ln T_{\max}} T_0 \psi_{4\pi}(T_0) D_{\infty}^{\text{det}}(z, T_0) d(\ln T_0) . \quad (2)$$

Equation (2) is evaluated numerically using a Simpson's rule, so that

$$D_{\infty}^{\text{det}}(z) = \frac{K}{4} \frac{\Delta}{3} \sum_{i=1}^N w_i T_i \psi_{4\pi}(T_i) D_{\infty}^{\text{det}}(z, T_i) , \quad (3)$$

where  $w_i = 1, 4, 2, 4, 2 \dots 2, 4, 1$  ( $N$  odd),<sup>4</sup> and  $\ln T_i = \ln T_{\min} + (i - 1)\Delta$  with  $\Delta = (\ln T_{\max} - \ln T_{\min})/(N - 1)$ .

In order to facilitate the interpolation of  $D_{\infty}^{\text{det}}(z, T_0)$  among tabulated values, eq (3) is recast as

$$D_{\infty}^{\text{det}}(z) = \frac{K}{4} \frac{\Delta}{3} \sum_{i=1}^N w_i T_i \psi_{4\pi}(T_i) S^{-1}(T_i) \left\{ S(T_i) D_{\infty}^{\text{det}}[x(z, T_i), T_i] \right\} , \quad (4)$$

for which the scaling functions are

	<u><math>S(T)</math></u>	<u><math>x(z, T)</math></u>
protons	$r_0(T)/T$ , g cm <sup>-2</sup> MeV <sup>-1</sup>	$z/r_0(T)$
electrons	$r_0(T)/T$ , g cm <sup>-2</sup> MeV <sup>-1</sup>	$z/r_0(T)$
bremsstrahlung	$1/T$ , MeV <sup>-1</sup>	$z/T$

and where  $r_0$  is the mean range evaluated in the continuous-slowing-down approximation. Values of the mean range  $r_0$  are given in table 1 for protons [2] and table 2 for electrons [3]. The scaled depth-dose distributions in the curly brackets in eq (4), having a much reduced dependence

---

<sup>4</sup>Any  $N \geq 2$  can be handled, and the weights  $w_i$  are suitably adjusted.

on  $z$  and  $T_0$ , are tabulated in appendix B. Interpolation is accomplished by fitting with natural cubic splines [4], first in  $T$ , then in  $x$ .

Values for  $T_{\min}$  and  $T_{\max}$  (eq (2) above) are often imposed by the available knowledge of the incident electron or proton fluence  $\psi_{4\pi}(T_0)$ . If, in the evaluation of eq (4),  $T_i$  is outside of the energy range for which the scaled, monoenergetic depth-dose distributions are given, then the curly bracket is evaluated for the nearest energy tabulated, and the energy variation is assumed to be taken care of by the term  $S^{-1}(T_i)$ . This procedure should cause little error since the tabulated proton data extend from 2 to 5000 MeV, the electron data from 0.1 to 10 MeV, and the bremsstrahlung data from 0.02 to 20 MeV, and should cover incident spectra encountered in space-shielding problems.

A more likely situation is that information on the incident flux spectra extends only over an energy region more limited than those above. For example, current model predictions of the terrestrial radiation environment [5] typically give spectral information over the energy ranges 0.1 to 10 MeV for electrons 0.5 to 500 MeV for trapped protons, and 10 to 200 MeV for solar-flare protons. If  $\psi_{4\pi}(T_0)$  is entered into SHIELDOSE in numerical form, care should be taken in choosing values of  $T_{\min}$  and  $T_{\max}$  in order to avoid the automatic cubic-spline extrapolation of  $\psi_{4\pi}(T_0)$  which can occasionally result in significant, and quite peculiar, components in the incident energy spectrum. It should be kept in mind that the final results neglect those contributions to the dose from radiation with  $T_0 < T_{\min}$  and  $T_0 > T_{\max}$ . This can be particularly important for depths  $z < r_0(T_{\min})$ . Some results of test calculations using

$$\psi_{4\pi}(T_0) = \frac{1}{\alpha} e^{-T_0/\alpha}, \quad (5)$$

are given in table 3 which shows, at various depths  $z$  and for various values of the e-folding energy  $\alpha$ , the effect on  $D_{\infty}^{A\alpha}(z)$  of different choices of  $T_{\min}$  and  $T_{\max}$ .

The discussion above outlines the calculation of  $D_{\infty}^{\det}(z)$  for a semi-infinite medium. The calculation of  $D_{\infty}^{\det}(z)$  for finite-thickness slabs is similar but based on  $D_{\infty}^{\det}(z, T_0)$ . The results for the dose at the center of a solid sphere of radius  $z$  are obtained from (see also eq (10) in appendix A)

$$D_{\infty}^{\det}(z) = 2 D_{\infty}^{\det}(z) \left\{ 1 - \frac{d \log D_{\infty}^{\det}(z')}{d \log z'} \Bigg|_{z'=z} \right\}, \quad (5)$$

where the logarithmic derivative is evaluated using a cubic-spline fit of  $\log D_{\infty}^{\det}(z)$ . We have found that  $N = 301$  for protons and  $N = 101$  for electrons gives distributions of  $D_{\infty}^{\det}(z)$  sufficiently smooth to give reasonably smooth results for  $D_{\infty}^{\det}(z)$ .

### 3. Input Parameters

The format of the input deck is (using FORTRAN notation):

IDET, NUT, IPRNT	3I6
[scaled monoenergetic depth-dose data set] <sup>5</sup>	not user supplied
IMAX, IUNT	2I6
(Z(I), I=1, IMAX)	6F12.5
EMINS, EMAXS, EMINP, EMAXP, NPTSP, EMINE, EMAXE, NPTSE	4F10.3, I6, 2F10.3, I6

---

<sup>5</sup>This rather lengthy data set, about 13,400 words of information, should be permanently stored on tape or disk. Although its position in the input stream is as indicated above, it is read from unit NUT.

The following block of input data can be repeated for each set of incident spectra:

COMMENT	
JSMAX, JPMAX, JEMAX, EUNIT, TINTER	72H
(EPSS(J), J=1, JSMAX)	3I6, IP2E12.5
(SS(J), J=1, JSMAX)	1P6E12.4
(EPSP(J), J=1, JPMAX)	1P6E12.4
(SP(J), J=1, JPMAX)	1P6E12.4
(EPSE(J), J=1, JEMAX)	1P6E12.4
(SE(J), J=1, JEMAX)	1P6E12.4

The meaning of the input parameters is as follows:

IDET = 1 , detector material is Al.  
2 , detector material is H<sub>2</sub>O.  
3 , detector material is Si.  
4 , detector material is SiO<sub>2</sub>.

NUT is the unit from which the scaled depth-dose data set is read.

IPRNT = 1 , input monoenergetic depth-dose data is listed in printout.  
2 , input monoenergetic depth-dose data is not listed in printout.

IMAX is the number of depths z for which dose calculation is desired (IMAX ≤ 50).

IUNT = 1 , depth z in mils.<sup>6</sup>  
2 , depth z in g/cm<sup>2</sup>.  
3 , depth z in mm.

Z is simultaneously the IMAX depths (case 1 geometry), thicknesses (case 2 geometry), and sphere radii (case 3 geometry) in units specified by IUNT. No Z-value can be 0 because of a log Z interpolation performed in the bremsstrahlung calculation. Furthermore,  $0 < Z \leq 30$  g/cm<sup>2</sup>, due to the extent of the bremsstrahlung data.

EMINS is the lower limit  $T_{\min}$  for the integration over the incident solar-flare-proton spectrum (see eq (2)).

EMAXS is the upper limit  $T_{\max}$  for the integration over the incident solar-flare-proton spectrum (see eq (2)).

EMINP is the lower limit  $T_{\min}$  for the integration over the incident trapped-proton spectrum (see eq (2)).

EMAXP is the upper limit  $T_{\max}$  for the integration over the incident trapped-proton spectrum (see eq (2)).

NPTSP is the number of points used in the numerical evaluation of the integral over the incident proton spectrum, for

---

<sup>6</sup>1 mil = 0.001 inch = 0.0254 mm. For aluminum, with a density of 2.70 g/cm<sup>3</sup>,  
1 mil = 0.00686 g/cm<sup>2</sup>.

which the integration extends from  $\min(\text{EMINS}, \text{EMINP})$  to  $\max(\text{EMAXS}, \text{EMAXP})$ . Note that EMINS, EMAXS, EMINP, and EMAXP may be slightly adjusted to the nearest mesh-energy values. ( $\text{NPTSP} < 301$ , recommend  $\text{NPTSP} = 301$ ).

EMINE is the lower limit  $T_{\min}$  for the integration over the incident electron spectrum (see eq (2)).

EMAXE is the upper limit  $T_{\max}$  for the integration over the incident electron spectrum (see eq (2)).

NPTSE is the number of points used in the numerical evaluation of the integral over the incident electron spectrum ( $\text{NPTSE} < 101$ , recommend  $\text{NPTSE} = 101$ ).

COMMENT is any identifying message.

JSMAX is the number of energies for which the incident solar-flare-proton spectrum is read in ( $\text{JSMAX} < 101$ ). If  $\text{JSMAX} \leq 2$ , no solar-flare-proton results are calculated.

JPMAX is the number of energies for which the incident trapped-proton spectrum is read in ( $\text{JPMAX} < 101$ ). If  $\text{JPMAX} \leq 2$ , no trapped-proton results are calculated.

JEMAX is the number of energies for which the incident electron spectrum is read in ( $\text{JEMAX} < 101$ ). If  $\text{JEMAX} \leq 2$ , no electron and bremsstrahlung results are calculated.

EUNIT is the conversion factor from  $(\text{unit energy})^{-1}$  to  $\text{MeV}^{-1}$ , where  $(\text{unit energy})^{-1}$  pertains to the units in which the incident proton and electron flux spectra are read. For example, if the incident spectra are read in units of  $\text{keV}^{-1}$ , then EUNIT = 1000; if read in units of  $\text{MeV}^{-1}$  then EUNIT = 1 (if the EUNIT field is left blank or if EUNIT  $\leq 0$ , then SHIELDOSE assumes EUNIT = 1).

TINTER is the time interval (e.g., mission duration) for which results are desired. TINTER is in units of  $(\text{unit time})^{-1}$ , where  $(\text{unit time})^{-1}$  pertains to the units in which the incident trapped-proton and electron flux spectra are read. For example, if incident spectra are read in units of  $\text{sec}^{-1}$ , then TINTER = 1 gives the absorbed dose for a 1-sec irradiation; TINTER =  $3.1536 \times 10^7$  gives dose for one year (365 days); etc. If the TINTER field is left blank or if TINTER  $\leq 0$ , then SHIELDOSE assumes TINTER = 1. Note that TINTER does not pertain to the incident solar-flare-proton fluence spectrum which is assumed to be the result of a statistical analysis relating the probability of the incident solar-flare-proton fluence to the mission duration [6].

EPSS are the JSMAX energies in MeV (in ascending order) for which the incident solar-flare-proton fluence spectrum is read. If JSMAX  $\leq 2$ , this array is not read in.

SS are the values (at energies EPSS) of the full-space ( $4\pi$ ), omnidirectional solar-flare-proton incident fluence spectrum in units of  $\text{cm}^{-2}$  (unit energy) $^{-1}$ .

EPSP are the JPMAX energies in MeV (in ascending order) for which the incident trapped-proton flux spectrum is read. If  $\text{JPMAX} \leq 2$ , this array is not read in.

SP are the values (at energies EPSP) of the full-space ( $4\pi$ ), omnidirectional trapped-proton incident flux spectrum in units of  $\text{cm}^{-2}$  (unit energy) $^{-1}$  (unit time) $^{-1}$ .

EPSE are the JEMAX energies in MeV (in ascending order) for which the incident electron fluence spectrum is read.

SE are the values (at energies EPSE) of the full-space ( $4\pi$ ), omnidirectional incident electron fluence spectrum in units of  $\text{cm}^{-2}$  (unit energy) $^{-1}$  (unit time) $^{-1}$ .

Note the following option which pertains to the solar-flare-proton, trapped-proton, and electron incident spectra:

If  $\text{EPS}(1) \leq 0$  (but  $\text{JMAX} \geq 3$ ), then the incident spectrum is assumed to be  $\psi_{4\pi}(T_0) = (C/\alpha) \exp(-T_0/\alpha)$ , with  $\alpha(\text{MeV}) = S(1)$  and  $C = S(2)$ . The units for  $C$  are  $\text{cm}^{-2}$  for the solar-flare-proton fluence spectrum,

and  $\text{cm}^{-2} (\text{unit time})^{-1}$  for the trapped-proton and electron flux spectra. This option may be particularly useful for the solar-flare-proton spectrum for which, in the active years 1977-1983, the spectrum is characterized by  $\alpha = 26.5 \text{ MeV}$  for anomalously large events and by  $\alpha = 63.3 \text{ MeV}$  for ordinary events [6]. Values of  $C$  can be obtained from information on the corresponding integral spectrum  $I(> T_0)$ , via  $C = I(> T_0) \exp(T_0/\alpha)$ . If the entered value  $S(2) \leq 0$ , then SHIELDOSE sets  $C = 1$ .

The code is written to process quickly many incident spectra in a single run. For example, using an IBM 360/91 computer and with  $\text{NPTSP} = 301$ ,  $\text{NPTSE} = 101$  and  $\text{IMAX} = 48$ , approximately 10 sec is required for setting up internal matrices and  $\sim 1$  sec for each input proton and electron spectrum set. The storage requirement is  $\sim 80 \text{ K words}$ .

It is, in general, necessary to suppress underflow diagnostics which interrupt, and can eventually terminate, a run. Underflow conditions are not detected by the code itself and should therefore be suppressed using the appropriate options available at the particular computing installation. For the IBM system used by the author, this is accomplished by the "CALL ERRSET" instruction at the beginning of the main routine listed in appendix D.

## REFERENCES

- [1] Seltzer, S. M., IEEE Trans. Nucl. Science, NS-26, 4896 (1979).
- [2] Barkas, W. H., and Berger, M. J., NASA SP-3013 (1964).
- [3] Berger, M. J., and Seltzer, S. M., NASA SP-3012 (1964).
- [4] Ahlberg, J. H., Nilson, E. N., and Walsh, J. L., The Theory of Splines and Their Applications (Academic Press, New York, 1967).
- [5] Sawyer, D. M., and Vette, J. I., NSSDC 76-06, (Dec. 1976); Teague, M. J., and Vette, J. I., NSSDC 72-10 (Sept. 1972); Teague, M. J., Chan, K. W., and Vette, J. I., NSSDC/WDC-A-R&S 76-04 (March 1976); Stassinopoulos, E. G., Herbert, J. J., Butler, E. L., and Barth, J. L., NSSDC/WDC-A-R&S 79-01; all from the National Space Science Data Center, Greenbelt, Maryland.
- [6] Stassinopoulos, E. G., NSSDC 75-11 (April 1975), National Space Science Data Center, Greenbelt, Maryland.

Table I. Proton range  $r_0(T_0)$  as a function of proton energy  $T_0$ .  
 Values are from reference [2].

$T_0$ (MeV)	$r_0$ ( $\text{g/cm}^2$ )	$T_0$ (MeV)	$r_0$ ( $\text{g/cm}^2$ )
2	$1.147 \times 10^{-2}$	100	9.975
3	$2.181 \times 10^{-2}$	150	$2.026 \times 10^1$
4	$3.500 \times 10^{-2}$	200	$3.320 \times 10^1$
5	$5.094 \times 10^{-2}$	300	$6.547 \times 10^1$
6	$6.974 \times 10^{-2}$	400	$1.043 \times 10^2$
8	$1.157 \times 10^{-1}$	500	$1.482 \times 10^2$
10	$1.703 \times 10^{-1}$	600	$1.959 \times 10^2$
15	$3.458 \times 10^{-1}$	800	$2.994 \times 10^2$
20	$5.739 \times 10^{-1}$	1000	$4.102 \times 10^2$
30	1.177	1500	$7.046 \times 10^2$
40	1.963	2000	$1.010 \times 10^3$
50	2.920	3000	$1.627 \times 10^3$
60	4.039	4000	$2.239 \times 10^3$
80	6.728	5000	$2.843 \times 10^3$

Table 2. Electron range  $r_0(T_0)$  as a function of electron energy  $T_0$ .  
 Values are from reference [3].

$T_0$ (MeV)	$r_0$ (g/cm <sup>2</sup> )	$T_0$ (MeV)	$r_0$ (g/cm <sup>2</sup> )
0.01	$3.519 \times 10^{-4}$	1.0	$5.493 \times 10^{-1}$
0.015	$7.074 \times 10^{-4}$	1.5	$8.825 \times 10^{-1}$
0.02	$1.165 \times 10^{-3}$	2.0	1.212
0.03	$2.356 \times 10^{-3}$	3.0	1.855
0.04	$3.883 \times 10^{-3}$	4.0	2.476
0.05	$5.714 \times 10^{-3}$	5.0	3.076
0.06	$7.822 \times 10^{-3}$	6.0	3.658
0.08	$1.279 \times 10^{-2}$	8.0	4.777
0.10	$1.864 \times 10^{-2}$	10	5.841
0.15	$3.641 \times 10^{-2}$	15	8.305
0.20	$5.772 \times 10^{-2}$	20	$1.054 \times 10^1$
0.30	$1.077 \times 10^{-1}$	30	$1.448 \times 10^1$
0.40	$1.640 \times 10^{-1}$	40	$1.788 \times 10^1$
0.50	$2.243 \times 10^{-1}$	50	$2.087 \times 10^1$
0.60	$2.871 \times 10^{-1}$	60	$2.355 \times 10^1$
0.80	$4.168 \times 10^{-1}$	80	$2.816 \times 10^1$
		100	$3.204 \times 10^1$

Table 3. Fraction of dose  $D_{\infty}^{A\alpha}(z)$  contributed by incident spectral energies below  $T_c$ . The quantity given corresponds to the ratio

$$\int_0^{T_c} D_{\infty}^{A\alpha}(z, T_0) \exp(-T_0/\alpha) dT_0 / \int_0^{\infty} D_{\infty}^{A\alpha}(z, T_0) \exp(-T_0/\alpha) dT_0 ,$$

and is given for various depths  $z$  in  $\text{g/cm}^2$  and for various  $\alpha$  and  $T_c$  in MeV. For any  $z$  and  $\alpha$ , the fraction of the dose contributed by  $T_{\min} \leq T_0 \leq T_{\max}$  is the difference between the value tabulated for  $T_c = T_{\max}$  and that for  $T_c = T_{\min}$ . Results are given for protons, electrons, and bremsstrahlung.

		<u>PROTONS</u>							
$T_c$ (MeV)	$z$ ( $\text{g/cm}^2$ )	2	5	10	200	500	1000	2000	5000
$\alpha = 10 \text{ MeV}$									
0.03	0.00	0.15	0.63	1.00	1.00	1.00	1.00	1.00	1.00
0.3	0.00	0.00	0.00	1.00	1.00	1.00	1.00	1.00	1.00
3	0.00	0.00	0.00	1.00	1.00	1.00	1.00	1.00	1.00
30	0.00	0.00	0.00	0.51	0.92	0.96	0.99	1.00	1.00
$\alpha = 20 \text{ MeV}$									
0.03	0.00	0.10	0.47	1.00	1.00	1.00	1.00	1.00	1.00
0.3	0.00	0.00	0.00	1.00	1.00	1.00	1.00	1.00	1.00
3	0.00	0.00	0.00	1.00	1.00	1.00	1.00	1.00	1.00
30	0.00	0.00	0.00	0.27	0.97	0.99	0.99	1.00	1.00
$\alpha = 50 \text{ MeV}$									
0.03	0.00	0.06	0.31	1.00	1.00	1.00	1.00	1.00	1.00
0.3	0.00	0.00	0.00	0.99	1.00	1.00	1.00	1.00	1.00
3	0.00	0.00	0.00	0.97	1.00	1.00	1.00	1.00	1.00
30	0.00	0.00	0.00	0.10	0.99	1.00	1.00	1.00	1.00
$\alpha = 100 \text{ MeV}$									
0.03	0.00	0.05	0.24	0.96	1.00	1.00	1.00	1.00	1.00
0.3	0.00	0.00	0.00	0.95	1.00	1.00	1.00	1.00	1.00
3	0.00	0.00	0.00	0.86	0.99	1.00	1.00	1.00	1.00
30	0.00	0.00	0.00	0.05	0.95	1.00	1.00	1.00	1.00
$\alpha = 200 \text{ MeV}$									
0.03	0.00	0.03	0.18	0.87	0.98	1.00	1.00	1.00	1.00
0.3	0.00	0.00	0.00	0.83	0.97	1.00	1.00	1.00	1.00
3	0.00	0.00	0.00	0.69	0.95	1.00	1.00	1.00	1.00
30	0.00	0.00	0.00	0.03	0.81	0.99	1.00	1.00	1.00

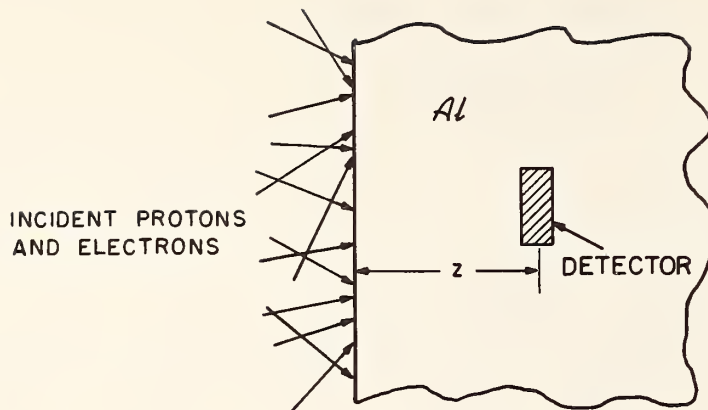
Table 3. (Continued)

		<u>ELECTRONS</u>							
		0.1	0.2	0.5	2	5	10	20	50
$T_c$ (MeV)	$z$ ( $\text{g/cm}^2$ )								
		$\alpha = 0.25 \text{ MeV}$							
0.03	0.00	0.05	0.71	1.00	1.00	1.00	1.00	1.00	1.00
0.3	0.00	0.00	0.00	0.98	1.00	1.00	1.00	1.00	1.00
3	0.00	0.00	0.00	0.00	0.01	1.00	1.00	1.00	1.00
		$\alpha = 0.50 \text{ MeV}$							
0.03	0.00	0.03	0.48	0.98	1.00	1.00	1.00	1.00	1.00
0.3	0.00	0.00	0.00	0.84	1.00	1.00	1.00	1.00	1.00
3	0.00	0.00	0.00	0.00	0.00	1.00	1.00	1.00	1.00
		$\alpha = 1 \text{ MeV}$							
0.03	0.00	0.01	0.29	0.85	0.99	1.00	1.00	1.00	1.00
0.3	0.00	0.00	0.00	0.57	0.98	1.00	1.00	1.00	1.00
3	0.00	0.00	0.00	0.00	0.00	0.95	1.00	1.00	1.00
		$\alpha = 2 \text{ MeV}$							
0.03	0.00	0.01	0.16	0.62	0.92	0.99	1.00	1.00	1.00
0.3	0.00	0.00	0.00	0.33	0.84	0.99	1.00	1.00	1.00
3	0.00	0.00	0.00	0.00	0.00	0.71	1.00	1.00	1.00
		$\alpha = 4 \text{ MeV}$							
0.03	0.00	0.00	0.09	0.39	0.72	0.92	1.00	1.00	1.00
0.3	0.00	0.00	0.00	0.17	0.59	0.89	1.00	1.00	1.00
3	0.00	0.00	0.00	0.00	0.00	0.43	1.00	1.00	1.00

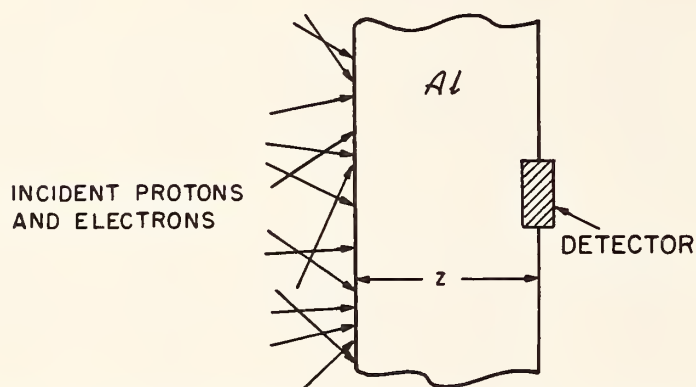
Table 3. (Continued)

BREMSSTRAHLUNG

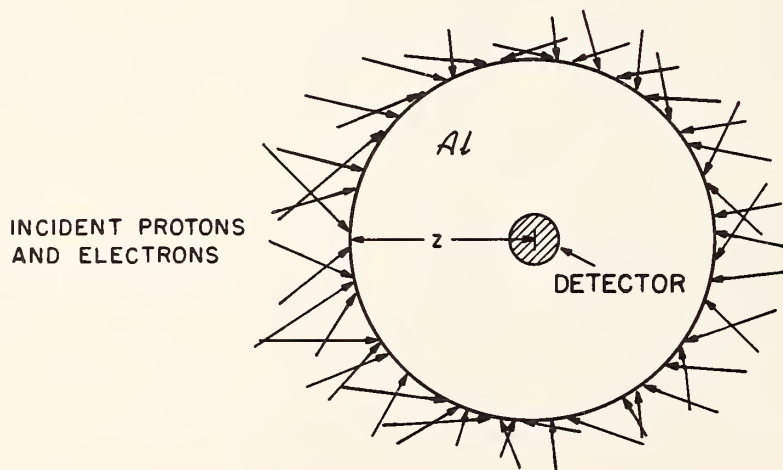
$T_c$ (MeV)	0.1	0.2	0.5	2	5	10	20	50
$z$ (g/cm <sup>2</sup> )	$\alpha = 0.25$ MeV							
0.03	0.02	0.12	0.68	1.00	1.00	1.00	1.00	1.00
0.3	0.01	0.06	0.33	0.99	1.00	1.00	1.00	1.00
3	0.00	0.04	0.30	0.98	1.00	1.00	1.00	1.00
30	0.00	0.01	0.16	0.97	1.00	1.00	1.00	1.00
	$\alpha = 0.50$ MeV							
0.03	0.01	0.05	0.40	0.96	1.00	1.00	1.00	1.00
0.3	0.00	0.01	0.09	0.85	1.00	1.00	1.00	1.00
3	0.00	0.01	0.07	0.74	1.00	1.00	1.00	1.00
30	0.00	0.00	0.03	0.62	0.99	1.00	1.00	1.00
	$\alpha = 1$ MeV							
0.03	0.00	0.02	0.19	0.74	0.98	1.00	1.00	1.00
0.3	0.00	0.00	0.02	0.51	0.95	1.00	1.00	1.00
3	0.00	0.00	0.01	0.29	0.86	1.00	1.00	1.00
30	0.00	0.00	0.00	0.18	0.79	0.99	1.00	1.00
	$\alpha = 2$ MeV							
0.03	0.00	0.01	0.08	0.40	0.97	1.00	1.00	1.00
0.3	0.00	0.00	0.01	0.22	0.70	0.96	1.00	1.00
3	0.00	0.00	0.00	0.07	0.44	0.88	1.00	1.00
30	0.00	0.00	0.00	0.03	0.32	0.82	1.00	1.00
	$\alpha = 4$ MeV							
0.03	0.00	0.00	0.02	0.15	0.41	0.72	0.96	1.00
0.3	0.00	0.00	0.00	0.08	0.34	0.70	0.96	1.00
3	0.00	0.00	0.00	0.01	0.14	0.51	0.92	1.00
30	0.00	0.00	0.00	0.00	0.07	0.37	0.84	1.00



CASE 1. SEMI-INFINITE MEDIUM; ABSORBED DOSE IN DETECTOR DENOTED AS  $D_{\infty}^{\text{det}}(z)$



CASE 2. FINITE-THICKNESS SLAB; ABSORBED DOSE IN DETECTOR DENOTED AS  $D_{-}(z)$



CASE 3. SOLID SPHERE; ABSORBED DOSE IN DETECTOR DENOTED AS  $D_{\bullet}^{\text{det}}(z)$

Fig. 1. Geometries considered in SHIELDOSE calculations. Isotropic, broad-beam fluxes of protons and electrons are assumed incident on aluminum targets; absorbed dose is calculated for small volumes of detector materials Al, H<sub>2</sub>O, Si, and SiO<sub>2</sub>.

ELECTRON, ELECTRON-BREMSSTRAHLUNG AND PROTON DEPTH-DOSE  
DATA FOR SPACE-SHIELDING APPLICATIONS\*

Stephen M. Seltzer  
National Bureau of Standards  
Washington, D.C. 20234

Abstract

A data set has been developed, consisting of depth-dose distributions for omni-directional electron and proton fluxes incident on aluminum shields. The principal new feature of this work is the accurate treatment, based on detailed Monte Carlo calculations, of the electron-produced bremsstrahlung component. Results covering the energy region of interest in space-shielding calculations have been obtained for the absorbed dose ( $\alpha$ ) as a function of depth in a semi-infinite medium, (b) at the edge of slab shields, and (c) at the center of a solid sphere. The dose to a thin tissue-equivalent detector was obtained as well as that in aluminum. Various results and comparisons with other work are given.

Introduction

The longer durations of currently planned and future satellite missions, and the increasing preference for the use of radiation-sensitive CMOS (Complementary Metal-Oxide-Semiconductor) devices, make more acute the problem of predicting the radiation dose at points in the spacecraft.<sup>1</sup> Such predictions depend on (a) knowledge of the spectra of electrons and protons incident on the spacecraft; (b) details of the geometrical and compositional complexities of the spacecraft; and (c) an accurate description of the transport of the radiation through the spacecraft material.

Improvements in space-shielding calculations are desirable in all three of these areas. The uncertainty in the information of the Earth's radiation environment is presently approaching a level of about a factor of two, and should improve further as more comprehensive experimental data are accumulated and theoretical models are refined. The complexities of the spacecraft configuration can, in principle, be taken into account by Monte Carlo transport calculations in complicated geometry<sup>2</sup> or by irradiations of satellite mock-ups. However, a far less costly alternative is the use of approximate methods<sup>3</sup> based on data obtained for simple geometries.

In this paper, calculated results are presented on the penetration of electrons and protons in aluminum, as summarized in terms of depth-dose data, for conditions pertinent to space-shielding problems. The principal new feature of this work is the accurate treatment of the production and transport of electron-produced bremsstrahlung photons which are more penetrating than the electrons themselves. Information on the bremsstrahlung tail can be particularly important for geostationary orbits in which satellites encounter few or no trapped protons, and for which the dose penetrating through thick shields is completely due to the bremsstrahlung.

Although the basic calculations were done for semi-infinite aluminum targets, consideration has been given also to other simple configurations, namely the dose at the edge of finite aluminum slabs and the dose at the center of uniform, solid aluminum spheres. In addition, the dose has been calculated in thin tissue-equivalent detectors embedded in or at the edge of the aluminum target.

Method of Calculation

Electrons and Bremsstrahlung

The electron calculations make use of the Monte Carlo code ETRAN which treats the following processes: i) electron energy loss, including energy-loss straggling (fluctuations) due both to multiple inelastic scattering by atomic electrons and to the emission of bremsstrahlung photons; ii) angular deflections of electrons due to multiple elastic scattering by atoms; iii) penetration and diffusion of the secondary bremsstrahlung photons; and iv) penetration and diffusion of energetic secondary electrons produced in electron-electron knock-on collisions (delta rays) and in the interaction of bremsstrahlung photons with the medium (pair, Compton, and photoelectrons).

Details of the Monte Carlo model and of the cross sections used have been given elsewhere<sup>4-7</sup>, along with numerous comparisons with experimental results. These will not be discussed here, except for the following improvement. The ETRAN bremsstrahlung results, based on the use of a set of empirically-corrected Bethe-Heitler bremsstrahlung cross sections<sup>6</sup>, were adjusted to reflect the exact calculations of the bremsstrahlung production cross section of Pratt, Tseng, et al<sup>8</sup>. Comparisons, using both the ETRAN and Pratt cross-section data sets for aluminum, of the electron mean energy loss per unit pathlength due to the emission of bremsstrahlung (see, e.g., reference 11) and of the total energy radiated in the course of slowing down (in the continuous-slowing-down approximation) give a multiplicative correction factor for the ETRAN results that is very close to unity for electron source energies  $T_0 \geq 1$  MeV, and is 0.96, 0.94, 0.92, 0.89, and 0.82 at 0.5, 0.2, 0.1, 0.05, and 0.02 MeV, respectively.

Protons

The main emphasis on this work was the calculation of the dose from electrons. However, it was considered desirable to include some corresponding results for protons so that one can put the contributions from the two types of radiation into proper perspective. For this purpose, we limited ourselves to a simple treatment that included Coulomb interactions but neglected nuclear interactions. The error incurred by this simplification is generally no greater than 10-20% for shields up to  $\sim 30$  g/cm<sup>2</sup>.

The proton calculations were done in the straight-ahead, continuous-slowing-down approximation using the stopping-power and range data of Barkas and Berger.<sup>9</sup> Alsmiller et al<sup>10</sup> have shown that the neglect of angular deflections and range straggling is negligible in space-shielding calculations.

\* Work supported by the Office of Naval Research and the National Space Science Data Center at the NASA Goddard Space Flight Center.

## Initial and Boundary Conditions

The calculations were made for radiation whose fluence is isotropic and which is incident on a semi-infinite, uniform aluminum plane medium. The radiation is assumed to be incident over a large area, so that the transport problem reduces to a one-dimensional one, with the depth  $z$  as the only spatial variable. Radiation crossing out through the plane boundary ( $z = 0$ ) was considered lost to the medium (backscattered).

Let  $\varphi(T_0, \theta)$  be the incident fluence, differential in initial energy  $T_0$  and in angle  $\theta$ . The fluence, having units of  $\text{cm}^{-2}\text{MeV}^{-1}\text{sr}^{-1}$ , pertains to the number of particles crossing through a unit area perpendicular to the incident particle vector. The current of particles crossing into the medium, per unit area of the plane boundary, is then

$$j(T_0, \theta) = \varphi(T_0, \theta) \cos\theta, \quad 0 \leq \theta \leq \pi/2, \quad (1)$$

where  $\theta$  is the angle of incidence with respect to the normal to the plane. The current  $j$  has the same units as the fluence  $\varphi$ .

For the purposes of normalization, we define the integrated incident  $4\pi$  fluence as\*

$$\Phi_{4\pi} = 2\pi \int_0^\infty dT_0 \int_0^\pi \sin\theta d\theta \varphi(T_0, \theta),$$

or

$$\Phi_{4\pi} = 4\pi \int_0^\infty dT_0 \varphi(T_0), \quad (2)$$

since  $\varphi$  is assumed isotropic.  $\Phi_{4\pi}$  has the units  $\text{cm}^{-2}$ . Only particles with  $0 \leq \theta \leq \pi/2$  cross into a semi-infinite plane medium, so we define the integrated incident  $2\pi$  fluence as

$$\begin{aligned} \Phi_{2\pi} &= 2\pi \int_0^\infty dT_0 \int_0^{\pi/2} \sin\theta d\theta \varphi(T_0, \theta) \\ &= 2\pi \int_0^\infty dT_0 \varphi(T_0) \end{aligned} \quad (3)$$

and the total incident current as

$$\begin{aligned} J &= 2\pi \int_0^\infty dT_0 \int_0^{\pi/2} \sin\theta d\theta j(T_0, \theta) \\ &= 2\pi \int_0^\infty dT_0 \int_0^{\pi/2} \sin\theta d\theta \cos\theta \varphi(T_0, \theta) \\ &= \pi \int_0^\infty dT_0 \varphi(T_0) \end{aligned} \quad (4)$$

Thus,

$$\Phi_{4\pi} = 2\Phi_{2\pi} = 4J \quad (5)$$

## Results for Monoenergetic Radiation

### Electron Component

Electron depth-dose curves and spectra were calculated for incident energies  $T_0 = 0.1, 0.2, 0.5, 1, 2, 3, 5, 7$ , and  $10 \text{ MeV}$ , based on samples of 10,000 incident electrons in each case. The histories of all generations of electrons were followed down to an energy of  $T_0/32$ , at which point the deposition of the small amount of residual energy was treated approximately. Photon histories were followed down to an energy of 2 keV.

In addition to the depth-dose distributions, the electron fluence spectra  $F_e(T, z; T_0)$ , as a function of spectral energy  $T$  and depth  $z$ , set up within the medium were calculated for those electrons traveling in the forward direction (forward fluence denoted as  $F_e^{\text{for}}$ ) as well as for electrons traveling in all directions (total fluence denoted as  $F_e^{\text{tot}}$ ). The data were obtained for depths  $z$  up to the electron mean range  $r_0(T_0)$ , the region in which the energy deposition is dominated by ionization (and excitation) losses of the primary electrons. Typical electron fluence spectra are shown in Fig. 1, for  $T_0 = 1 \text{ MeV}$ , at both a depth near the entrance plane and a depth well into the medium. It can be seen that there is a sizeable backscattered component (the difference between the  $F_e^{\text{tot}}$  and the  $F_e^{\text{for}}$  curves) and a noticeable build-up of low-energy electrons.

Using the notation of Jordan,<sup>12</sup> we let  $D_{\infty}^{A\ell}(z, T_0)$  be the aluminum dose as a function of depth  $z$  in the semi-infinite medium as directly calculated. The dose in thin tissue-equivalent detectors (very thin water layers) was obtained according to\*\*\*

$$\begin{aligned} D_{\infty}^{H_2O}(z, T_0) &= D_{\infty}^{A\ell}(z, T_0) \\ &\times \frac{\int_{\Delta}^T F_e^{\text{tot}}(T, z; T_0) L^{H_2O}(T, \Delta) dT + N(z)\Delta}{\int_{\Delta}^T F_e^{\text{tot}}(T, z; T_0) L^{A\ell}(T, \Delta) dT + N(z)\Delta}, \end{aligned} \quad (6)$$

where  $L(T, \Delta)$  is the electron restricted stopping power<sup>11</sup> which includes only energy transfers less than  $\Delta$  (in our case,  $\Delta = T_0/32$ ). In Eq. 6,  $N(z)$  is the number of electrons per unit depth falling below the cut-off energy  $\Delta$  (the so-called track-ends).

Similarly, the dose  $D_{\infty}(z, T_0)$  at the edge of finite slabs of thickness  $z$  was approximated by

\*\* The mean range, also called the coda range because it is derived in the continuous-slowing-down approximation, is defined as the integral of the reciprocal of the total stopping power over the energy range from the initial energy  $T_0$  down to some very small cut-off energy. Reference 11 contains an extensive tabulation of electron range values.

\*\*\* This expression is closely related to the Spencer-Attix<sup>13</sup> cavity-ionization theory.

\* A factor  $2\pi$  comes from the integration over the azimuthal angle.

$$D_{\infty}^{A\ell}(z, T_0) = \frac{\int_{\Delta}^{T_0} F_e^{\text{for}}(T, z; T_0) L^{A\ell}(T, \Delta) dT + N(z)\Delta/2}{\int_{\Delta}^{T_0} F_e^{\text{tot}}(T, z; T_0) L^{A\ell}(T, \Delta) dT + N(z)\Delta} \quad (7)$$

and by

$$D_{\infty}^{H_2O}(z, T_0) = D_{\infty}^{A\ell}(z, T_0) \frac{\int_{\Delta}^{T_0} F_e^{\text{for}}(T, z; T_0) L^{H_2O}(T, \Delta) dT + N(z)\Delta/2}{\int_{\Delta}^{T_0} F_e^{\text{tot}}(T, z; T_0) L^{H_2O}(T, \Delta) dT + N(z)\Delta} \quad (8)$$

In Eqs. 7 and 8, for the forward-moving electrons we use  $N(z)/2$  in the track-end term since we find that at low spectral energies the fluence is nearly equally divided between the forward- and the backward-moving electrons.

#### Bremsstrahlung Component

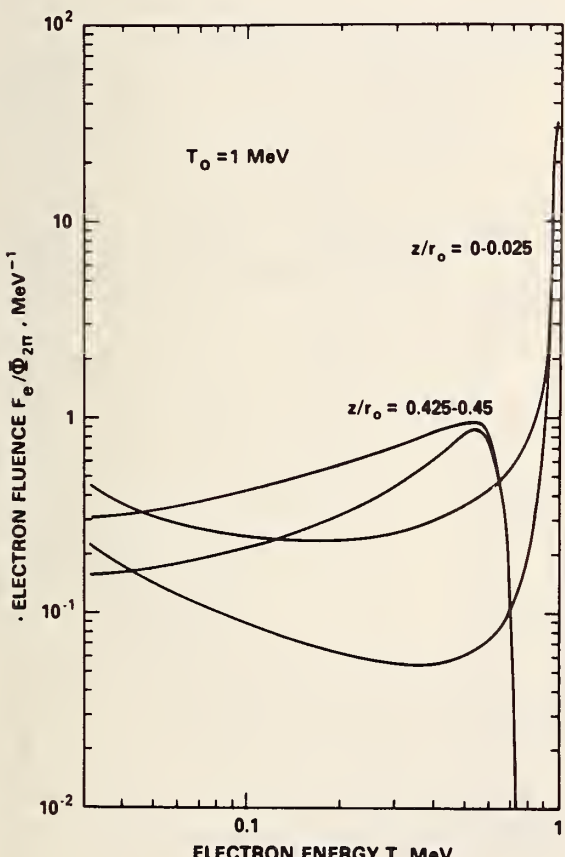


FIG. 1. Electron spectra in a semi-infinite aluminum medium bombarded by a 1-MeV, isotropic electron beam. Calculated spectra  $F_e$ , as a function of electron spectral energy  $T$ , are shown for the depth intervals  $0 < z < 0.025 r_0$  and  $0.425 < z < 0.45 r_0$  where  $r_0$  is the electron mean range. At each depth, the lower curve is for electrons traveling in the forward direction, the upper curve includes electrons traveling in all directions.

In order to obtain statistically significant results for the bremsstrahlung contribution to the dose, this contribution was not taken directly from the output of the ETRAN calculations, but indirectly in the following manner. A feature of the Monte Carlo code was exploited which allows for an arbitrary number of bremsstrahlung photons per electron to be generated. This is compensated by the use of weight factors to correct back to the true production rate. In this way, separate calculations were made of the photon spectrum  $F_Y(k, z; T_0)$  as a function of photon spectral energy  $k$  and depth  $z$  for  $T_0 = 0.02, 0.05, 0.1, 0.2, 0.5, 1, 2, 5, 10$  and  $20 \text{ MeV}$ , and for depths up to  $30 \text{ g/cm}^2$ . These results are based on sample sizes of 10,000 incident electrons and from 115,000 to 160,000 emitted bremsstrahlung photons.

Figure 2 gives typical forward and total photon fluence spectra for  $T_0 = 1 \text{ MeV}$ . At a shallow depth ( $\sim 0.45 \text{ g/cm}^2$ , still within the electron range), soft bremsstrahlung photons are evident in the spectra with energies  $k \lesssim 10 \text{ keV}$ . At larger depths, the spectrum hardens due to the strong photoelectric absorption of low-energy photons.

The bremsstrahlung dose was then obtained from

$$D_{\infty}^{A\ell}(z, T_0) = \int_0^{T_0} F_Y^{\text{tot}}(k, z; T_0) k \frac{\mu_{en}^{A\ell}(k)}{\rho} dk ,$$

$$D_{\infty}^{H_2O}(z, T_0) = \int_0^{T_0} F_Y^{\text{tot}}(k, z; T_0) k \frac{\mu_{en}^{H_2O}(k)}{\rho} dk ,$$

$$D_{\infty}^{A\ell}(z, T_0) = \int_0^{T_0} F_Y^{\text{for}}(k, z; T_0) k \frac{\mu_{en}^{A\ell}(k)}{\rho} dk ,$$

$$D_{\infty}^{H_2O}(z, T_0) = \int_0^{T_0} F_Y^{\text{for}}(k, z; T_0) k \frac{\mu_{en}^{H_2O}(k)}{\rho} dk , \quad (9)$$

where  $\mu_{en}/\rho$  is the photon mass energy-absorption coefficient tabulated by Hubbell<sup>14</sup>.

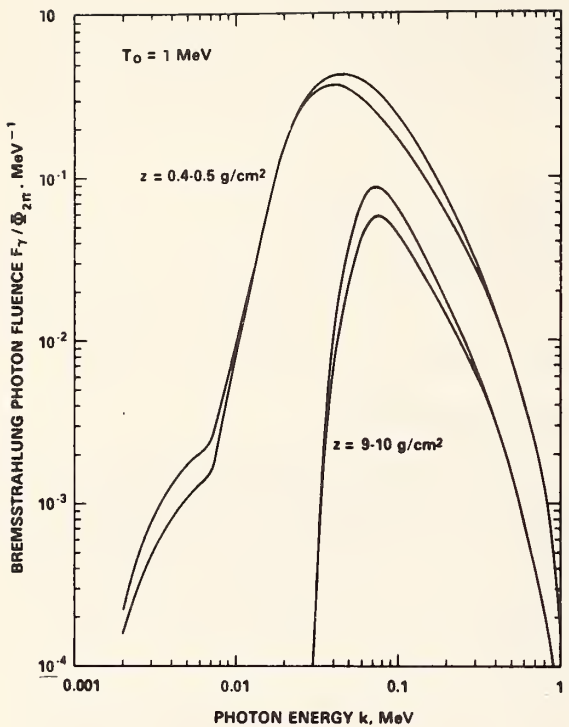


FIG. 2. Bremsstrahlung spectra in a semi-infinite aluminum medium bombarded by a 1-MeV, isotropic electron beam. Calculated spectra  $F_\gamma$ , as a function of bremsstrahlung photon spectral energy  $k$ , are shown for the depth intervals  $0.4 \leq z \leq 0.5 \text{ g/cm}^2$  and  $9 \leq z \leq 10 \text{ g/cm}^2$ . At each depth, the lower curve is for photons traveling in the forward direction, the upper curve includes photons traveling in all directions.

#### Basic Set of Depth-Dose Distributions

Using the methods described above, a set of depth-dose distributions for aluminum shields were generated for monoenergetic sources. The distributions were smoothed in  $z$  and  $T_0$ . The overall uncertainty of the final results, including the uncertainties in cross sections used and those due to statistical fluctuations and smoothing of the Monte Carlo data, is estimated to be 10%.

The aluminum dose expressed in rads\*, as a function of  $T_0$  for fixed depths, is shown for a semi-infinite medium in Fig. 3 for protons\*\* and in Fig. 4 for electrons. The electron curves include contributions from primary and secondary knock-on electrons and from secondary electrons set in motion by bremsstrahlung photons. At  $z = 0$ , the proton dose reduces to the stopping power. However, for the semi-infinite medium, the electron dose at  $z = 0$  is larger than the stopping power due to backscattering from greater depths.

\* A rad =  $10^2 \text{ Gy} = 1.602 \times 10^8 \text{ MeV/g}$ . The detector material will be specified within parentheses in the unit of dose, e.g., rads ( $\text{A}\ell$ ).

\*\* In the straight-ahead approximation,  $D_{\infty} = D_{\text{stop}}$  for protons.

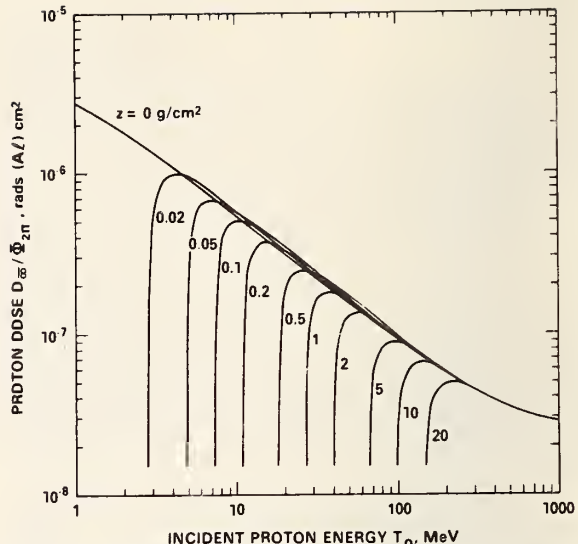


FIG. 3. Proton dose for fixed depths  $z$  in a semi-infinite aluminum medium, plotted as a function of incident energy  $T_0$ . The calculated results  $D_{\bar{\infty}}$  are given in terms of the dose per unit  $2\pi$  isotropic incident fluence.

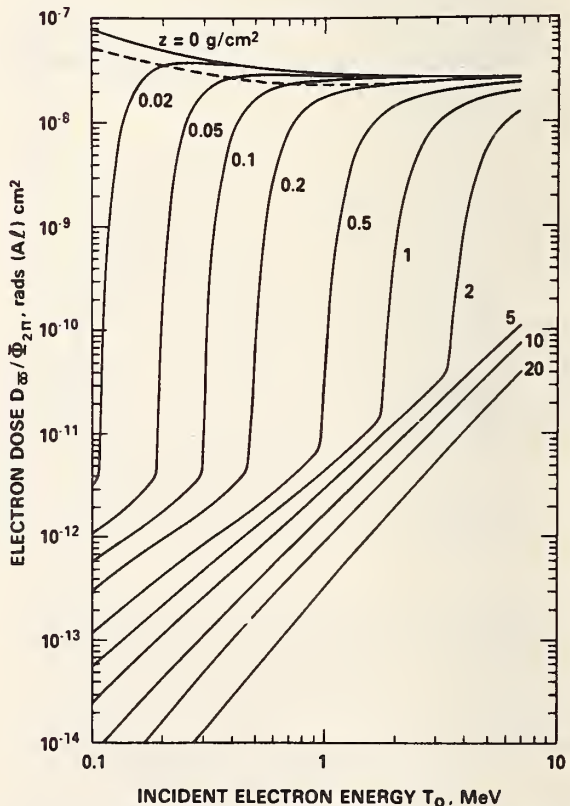


FIG. 4. Electron dose for fixed depths  $z$  in a semi-infinite aluminum medium, plotted as a function of incident energy  $T_0$ . The calculated results  $D_{\bar{\infty}}$  are given in terms of the dose per unit  $2\pi$  isotropic incident fluence. The dashed curve is the zero-depth dose based only on the stopping power and neglects backscattering from greater depths.

In Fig. 5, the electron dose as a function of  $T_0$ , at  $z = 0, 0.5$  and  $5 \text{ g/cm}^2$ , is compared for the cases of the aluminum dose in a semi-infinite aluminum medium, the aluminum dose at the edge of finite aluminum slabs, and the tissue dose in a semi-infinite aluminum medium. For very thin slabs the dose is less than the stopping power because of the escape of energy in the form of energetic knock-on electrons. We find that except for the region where the bremsstrahlung dominates, the tissue dose is roughly a factor 1.3\* larger than the aluminum dose and that the dose for finite slabs is roughly 0.7 of that for a semi-infinite medium (there are variations with  $z$  and  $T_0$  of as much as  $\sim \pm 20\%$  from this approximate value for the  $D_{\infty}/D_0$  ratio). However, for the bremsstrahlung component, the situation is more complicated because of the strong variation with photon energy and detector material of the mass energy-absorption coefficient.

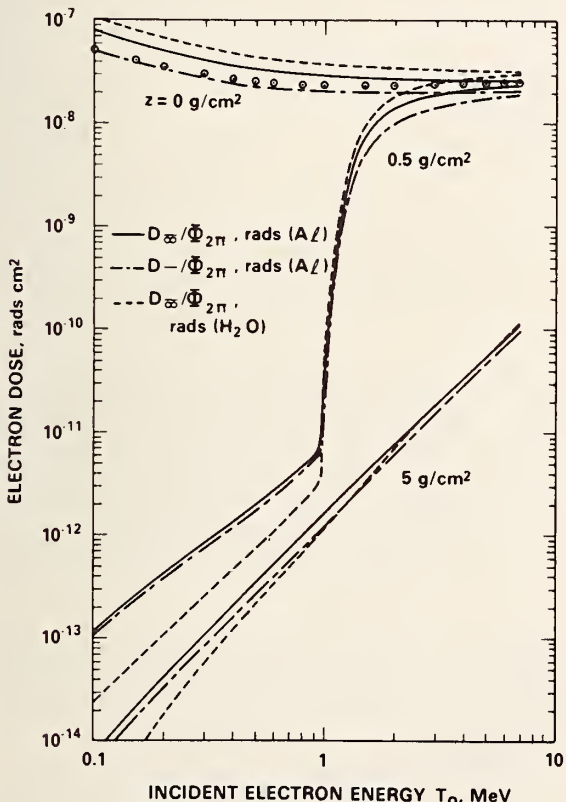


FIG. 5. Comparison of electron dose distributions in semi-infinite aluminum media and at the edge of finite aluminum slabs, for both aluminum and tissue-equivalent detectors. Solid curves pertain to the aluminum dose  $D_{\infty}$  at depths  $z$  in a semi-infinite aluminum medium; dot-dashed curves pertain to the aluminum dose  $D_0$  at the edge of aluminum slabs of thickness  $z$ ; dashed curves pertain to the tissue dose  $D_{\infty}$  at depths  $z$  in a semi-infinite aluminum medium. The points for  $z = 0$  are based only on the stopping power.

\* This factor can be estimated simply from stopping power tables. Based on the calculated fluence spectra, we find values from about 1.24 to 1.34.

Measurements were made by Van Gunten<sup>15</sup> of the aluminum dose in hollow aluminum cubes, one face of which was irradiated by monoenergetic, isotropic electron beams. Those measurements made directly behind and at the center of the irradiated face would seem to closely correspond to  $D_0$ , except possibly for a small additional contribution backscattered from the other sides of the cube. The calculated results are compared in Table I to the properly normalized<sup>16</sup> data of Van Gunten. For  $T_0 = 1, 2$  and  $3 \text{ MeV}$ , the agreement is good, within the stated uncertainty of 10% for the experimental data. However, there is a discrepancy at  $4 \text{ MeV}$  where the measured doses are consistently lower than the calculated ones. We can find no ready explanation for this discrepancy.

TABLE I. Comparison of calculated and measured dose behind aluminum slab shields irradiated by monoenergetic, isotropic electron beams. The experimental results of Van Gunten<sup>15</sup> and the calculated results are given in units of  $10^{-7} \text{ rads (Al)}$ , and are normalized to a unit  $2\pi$  isotropic incident fluence. Results are given for various incident electron energies  $T_0$  and shield thickness  $z$ .

$T_0(\text{MeV})$	$z(\text{mils}^{\text{a}})$	Exptl. Dose	Calc. Dose
1	30	$0.110 \pm 0.011$	0.115
1	60	$0.00781 \pm 0.0078$	0.00701
2	30	$0.164 \pm 0.016$	0.167
2	60	$0.118 \pm 0.012$	0.120
2	125	$0.0163 \pm 0.0016$	0.0153
3	30	$0.169 \pm 0.017$	0.181
3	60	$0.155 \pm 0.016$	0.153
3	125	$0.0812 \pm 0.0081$	0.0859
4	30	$0.149 \pm 0.015$	0.189
4	60	$0.136 \pm 0.014$	0.168
4	125	$0.0915 \pm 0.0092$	0.122
4	250	$0.0146 \pm 0.0015$	0.0252

<sup>a</sup> 1 mil =  $0.00686 \text{ g/cm}^2$  of aluminum

#### Calculations for Arbitrary Incident Spectra

The monoenergetic-source results have been incorporated into a computer code SHIELOOSE\*\* which rapidly performs the necessary interpolation and integration for any incident spectrum.

#### Slab Shields

The results from the approximate proton calculations are compared in Fig. 6 with those calculated by Burrell<sup>17</sup> and by Alsmiller<sup>18</sup> for aluminum slabs. The SHIELOOSE results are no more than 10-20% higher than these other results which include the effects of nuclear interactions. Such a discrepancy is consistent with the findings of Santoro et al<sup>19</sup> who tested the effects of nuclear collisions and secondary particles in proton space-shielding calculations.

Electron results for simple exponential incident spectra  $\phi(T_0) = (1/2\pi\alpha) \exp(-T_0/\alpha)$  are given in Fig. 7 and are compared to those of Watts and Burrell<sup>20</sup>. When the bremsstrahlung component is omitted the curves are generally in good agreement as should be expected, since both calculations are based on data obtained (independently) using ETRAN. In order to indicate the effect of bremsstrahlung on the depth-dose distribution, curves including this component are given also in Fig. 7.

\*\* This code will be available from the Radiation Shielding Information Center, Oak Ridge National Laboratory, and from the National Space Science Data Center, Goddard Space Flight Center.

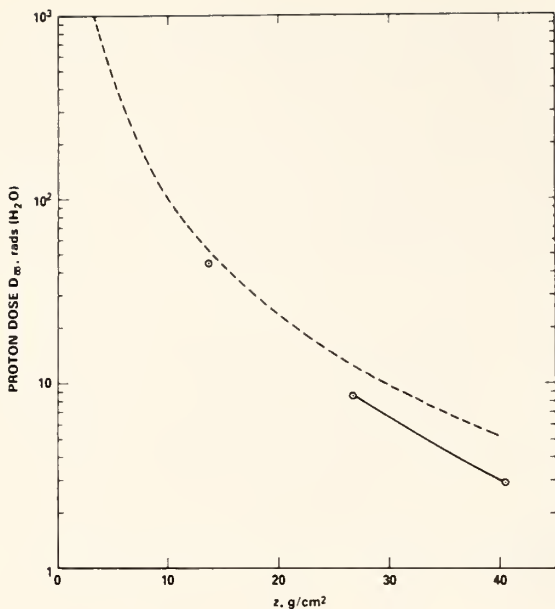


FIG. 6. Comparison of proton depth-dose distributions  $D_{\infty}$  in aluminum slab shields. The dashed curve is from the present calculations, the solid curve from Alsmiller<sup>18</sup>, and the points from Burrell<sup>17</sup>. All results were calculated for an incident, isotropic proton fluence (in  $\text{cm}^{-2}\text{Mev}^{-1}\text{sr}^{-1}$ ) of  $\varphi(T_0) = 2.5 \times 10^{11} T_0^{-2.07}$  for  $5 \leq T_0 \leq 60 \text{ MeV}$  and  $\varphi(T_0) = 5.486 \times 10^{14} T_0^{-3.95}$  for  $60 < T_0 \leq 1000 \text{ MeV}$ , and pertain to irradiation from one side only.

Previous bremsstrahlung calculations in space-shielding problems have been done in various ways, but generally have been based on the straight-ahead approximation. As an example, we compare in Fig. 8 our results with those of Watts and Burrell<sup>20</sup> for exponential incident electron spectra. These authors considered a number of models describing the energy and angular distributions of the emitted bremsstrahlung and give various results ranging from those from their most elaborate treatment to a simple order-of-magnitude estimate (based in part on our older Monte Carlo data<sup>4</sup> pertaining to the energy content of bremsstrahlung beams emerging from aluminum targets). As seen in Fig. 8, these results disagree with the SHIELDOSE results by as much as a factor of two; however, it turns out that their more approximate results fortuitously agree to within  $\sim 30\%$ .

#### Spherical Shields

In application to spacecraft there is usually interest in geometries other than those of simple slab targets. Calculations for complicated geometries are beyond the scope of this work. However, results have been obtained for the dose at the center of uniform solid spheres using slab depth-dose distributions. This is accomplished using the relation

$$D_c(z) \approx 2 D_{\infty}(z) \left\{ 1 - \frac{d \log D_{\infty}(z')}{d \log z'} \Big|_{z' = z} \right\}, \quad (10)$$

where  $D_c(z)$  is the dose at the center of a sphere of radius  $z$ . This relationship, which has been suggested by Jordan<sup>12</sup> and references cited by him, is exact for

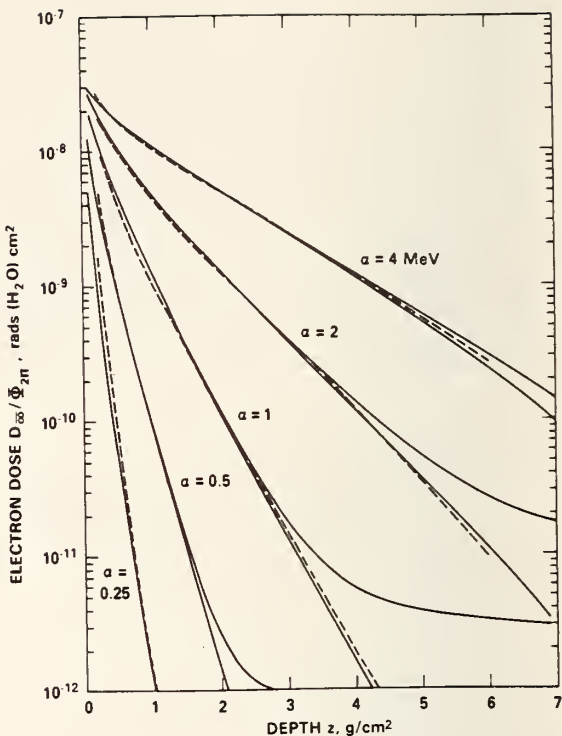


FIG. 7. Electron dose  $D_{\infty}$  as a function of depth  $z$  in a semi-infinite aluminum medium. Results are for exponential incident spectra,  $\varphi(T_0) = \text{const. } x \exp(-T_0/\alpha)$ , and are given in terms of the dose per unit  $2\pi$  isotropic incident fluence. Dashed curves are from calculations of Watts and Burrell<sup>20</sup> based on ETRAN depth-dose data; solid curves are from present calculations (upper curves include bremsstrahlung component, lower curves do not).

an isotropic fluence of particles in the straight-ahead approximation. The factor of  $2 = \Phi_{4\pi}/\Phi_{2\pi}$  in Eq. 10 merely takes into account that a sphere is irradiated from all directions while the semi-infinite medium is irradiated only from one side.

Proton doses at centers of spheres are shown in Fig. 9, where our results are compared with those calculated by Burrell<sup>17</sup> and Hill<sup>21</sup>. The overestimate by  $\sim 10\text{-}20\%$  for large radius  $z$  of our results, is -- as in the slab case -- attributable to our neglect of attenuation due to nuclear interactions.

In the case of electrons and bremsstrahlung, the use of Eq. 10 is, because of multiple scattering effects, more approximate. Jordan<sup>12</sup> has made Monte Carlo calculations specifically for the slab and spherical geometries in order to validate Eq. 10, at least up to depths where the bremsstrahlung contribution is still

\*Eq. 10 is given by Jordan<sup>12</sup> in terms of the dose  $D_z$  between two finite slab shields each of thickness  $z$ , rather than in terms of the dose  $D_{\infty}$  in a semi-infinite medium. For protons in the straight-ahead approximation,  $D_z = D_{\infty}$ ; for electrons, except for very small  $z$  where some differences in the backscattering becomes evident,  $D_z \approx D_{\infty}$ .

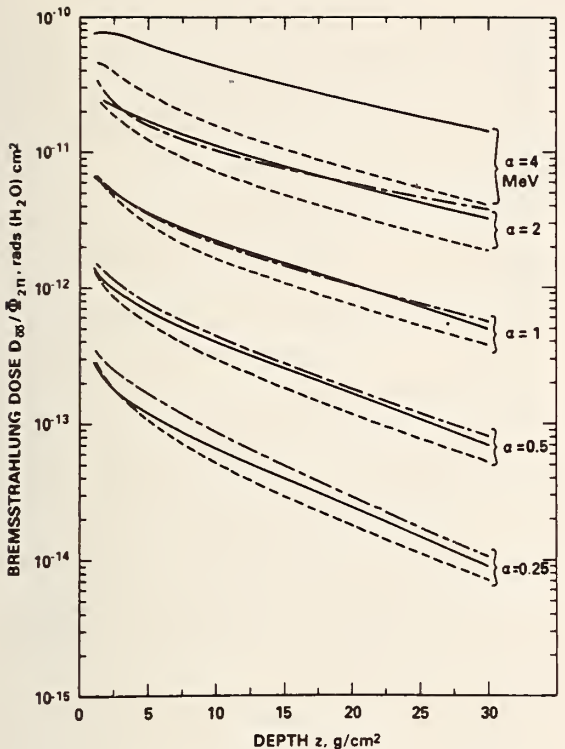


FIG. 8. Bremsstrahlung dose  $D_{\infty}$  as a function of depth  $z$  in a semi-infinite aluminum medium. Results are for exponential incident spectra with an e-folding energy  $\alpha$ , and are given in terms of the dose per unit  $2\pi$  isotropic incident fluence. Solid curves are from present calculations; broken curves are from the straight-ahead calculations of Watts and Burrell<sup>20</sup> (dashed curves from their most elaborate treatment, dot-dashed curves are their most approximate estimate).

small. Shown in Fig. 10 are his Monte Carlo results both for  $D_{\infty}$  and  $D_{\infty}$  for the fission spectrum,  $\varphi(T_0) = \text{const} \times \exp \{-0.575 T_0 - 0.055 T_0^2\}$ . Shown also are our results\* based on our Monte Carlo calculations for  $D_{\infty}$  and the use of Eq. 10 for  $D_{\infty}$ . The disagreement ( $\sim 10\%$ ) in  $D_{\infty}$  for small  $z$  is evidently due to our use of  $D_{\infty}$  rather than  $D_{\infty}$ , while the disagreement (again  $\sim 10\%$ ) at large  $z$  for both  $D_{\infty}$  and  $D_{\infty}$  apparently is the result of using different Monte Carlo calculations.

The ratio of the sphere dose to the slab dose is plotted in Fig. 11 for the fission spectrum and for an exponential spectrum with  $\alpha = 0.5$  MeV. Shown also is the ratio derived from Jordan's data for the fission spectrum. We make the following observations pertinent to space-shielding calculations: (a) Using Eq. 10 for electrons appears to be an approximation good to within  $\sim 10\text{-}20\%$ . This is not to say that the straight-ahead

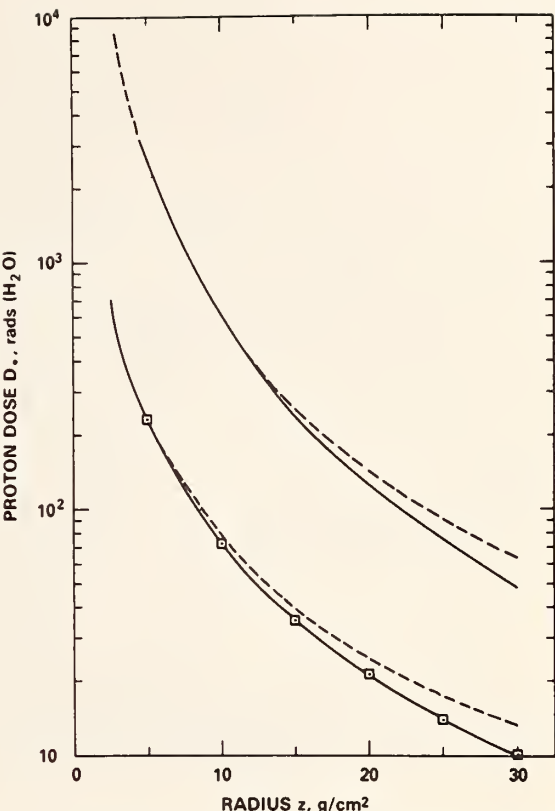


FIG. 9. Proton dose at the centers of aluminum spheres  $D_{\infty}$  as a function of sphere radius  $z$ . Dashed curves are from present calculations; solid curves are from those of Burrell<sup>17</sup>; and points are from Hill<sup>21</sup>. Upper set of results are for an incident, isotropic proton fluence (in  $\text{cm}^{-2}\text{MeV}^{-1}\text{sr}^{-1}$ ) of  $\varphi(T_0) = 5.486 \times 10^{14} T_0^{-3.95}$ ; the lower set are for  $\varphi(T_0) = 1.257 \times 10^{12} T_0^{3.12}$ . Irradiation of the sphere is assumed to be from all directions.

approximation per se, i.e., neglecting angular deflections, is accurate for describing electron penetration, but rather that, for the incident electron distributions of interest, electron penetration can be described by some functions (details of which we need not know) as if the electrons move along straight lines. (b) The argument in favor of using the results of Eq. 10 for the bremsstrahlung tail is the success of some form of the straight-ahead approximation in describing at least the shape of the depth-dose distribution as demonstrated, for example, in Fig. 8. (c) Whereas  $D_{\infty}/D_{\infty}$  is less than about 6 to 8 for protons, this ratio is as large as 13 for electrons and about 3 in the bremsstrahlung tail.

#### Realistic Spectra

Finally, we give an example of SHIELDOSE results for incident spectra kindly provided by E.G. Stassinopoulos of NASA/GSFC using the radiation-environment models and orbit-integration codes<sup>22</sup> developed at the National Space Science Data Center. Figure 12 shows the one-year aluminum dose, both  $D_{\infty}$  and  $D_{\infty}$ , for the omnidirectional, orbit-integrated, trapped electron fluence for a geostationary orbit with an altitude of 35790 km, an inclination of  $0^\circ$ , and for a parking longitude of  $160^\circ\text{W}$ . The spectrum, shown in the insert of Fig. 12,

\* Our dose in silicon was estimated from the dose in aluminum by multiplying by 1.03, which takes into account the electron stopping-power ratio. For the bremsstrahlung component also included in the results, this factor should actually be somewhat larger but has little effect on the comparison.

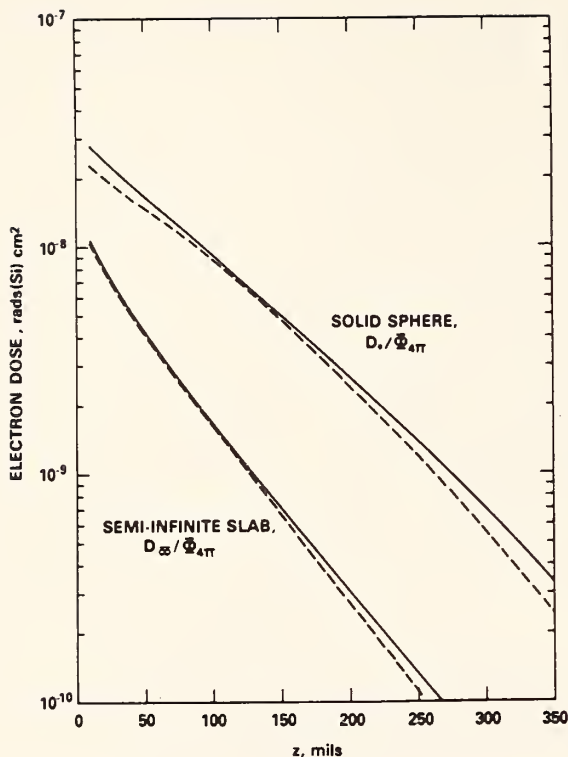


FIG. 10. Comparison of the electron dose in a semi-infinite medium (at depth  $z$ ) and at the centers of spheres (radius  $z$ ). Results are for aluminum targets (100 mils =  $0.686 \text{ g/cm}^2$ ) irradiated by an isotropic electron fluence having a fission spectrum,  $\psi(T_0) = 0.057 \exp(-0.575 T_0 - 0.055 T_0^2) \text{ cm}^{-2} \text{ MeV}^{-1} \text{ sr}^{-1}$ . Dashed curves are Jordan's<sup>12</sup> results from Monte Carlo calculations for each geometry. Solid curves are the present results based on Monte Carlo calculations for the semi-infinite medium and on the use of Eq. 10 for the spheres.

was calculated for the epoch 1979.0 using the AEI7-HI model. The solar proton fluence for this orbit and period is  $\psi(T_0) = 9.25 \times 10^8 \exp(-T_0/26.5 \text{ MeV}) \text{ cm}^{-2} \text{ MeV}^{-1} \text{ sr}^{-1}$ , and corresponds to one anomalously large event predicted at the 95% confidence level.

#### Acknowledgements

The author would like to thank E.G. Stassinopoulos, who suggested this work, and Martin Berger for many helpful discussions and suggestions.

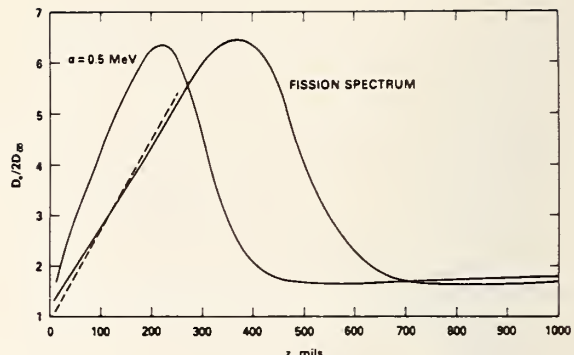


FIG. 11. Ratio of the electron dose  $D_s$  at centers of aluminum spheres (radius  $z$ ) to twice the dose  $D_\infty$  in a semi-infinite aluminum medium (at depth  $z$ ). The results, pertaining to aluminum detectors, are plotted out to large  $z$  where the bremsstrahlung dominates. Solid curves are our results based on Eq. 10 and are given both for incident electrons with a fission spectrum and for electrons with an e-folding energy  $\alpha = 0.5 \text{ MeV}$ . Dashed curve is the fission-spectrum results of Jordan<sup>12</sup> who considered explicitly the two geometries.

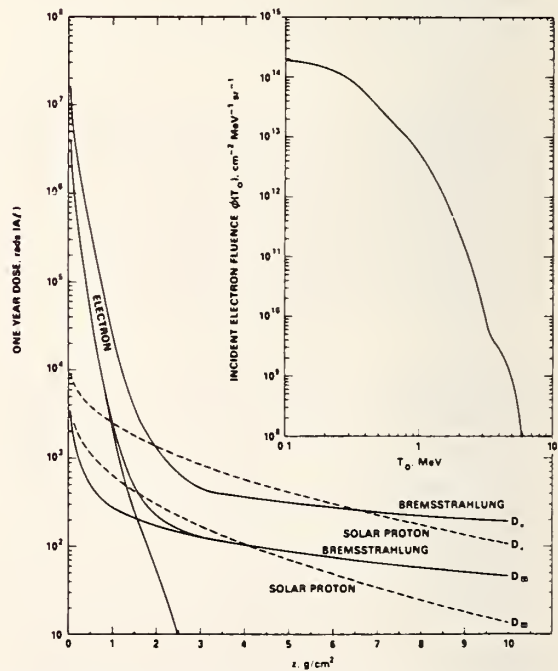


FIG. 12. Depth-dose distributions in aluminum targets for the radiation encountered during one year in a geostationary orbit. The orbit parameters and incident radiation spectra, are described in the text; the incident electron fluence is given in the insert. Results are given both for the dose  $D_\infty$  at depth  $z$  in a semi-infinite medium and for the dose  $D_s$  at the center of a sphere of radius  $z$ . The solar-proton dose, for 1 anomalously-large event, is given by the dashed curves.

References

1. A. Holmes-Siedle and R.F.A. Freeman, IEEE Trans. Nucl. Sci. NS-24, 2259 (1977).
2. H.M. Colbert, Sandia Laboratory Report SLL-74-0012 (1973).
3. H.S. Davis and T.M. Jordan, NASA Jet Propulsion Laboratory Technical Memorandum 33-765 (1976).
4. M.J. Berger and S.M. Seltzer, NASA Publ. SP-169 (1968).
5. M.J. Berger and S.M. Seltzer, Computer Code Collection 107, Oak Ridge Shielding Information Center (1968).
6. M.J. Berger and S.M. Seltzer, Phys. Rev C2, 621 (1970).
7. S.M. Seltzer, National Bureau of Standards Publ. NBS-IR 74457 (1974); S.M. Seltzer and M.J. Berger, Nucl. Instr. and Meth. 119, 157 (1974).
8. R.H. Pratt, H.K. Tseng, C.M. Lee and L. Kissel, At. Data and Nucl. Data Tables 20, 175 (1977).
9. W.H. Barkas and M.J. Berger, NASA Publ. SP-3013 (1964).
10. R.G. Alsmiller, J. Barish and W.W. Scott, Nucl. Sci. and Engr. 35, 405 (1969).
11. M.J. Berger and S.M. Seltzer, NASA Publ. SP-3012 (1964).
12. T.M. Jordan, Exptl. and Math. Phys. Consultants Report EMP.L77.023 (1977).
13. L.V. Spencer and F.H. Attix, Rad. Res. 3, 239 (1955).
14. J.H. Hubbell, National Bureau of Standards Publ. NSRDS-NBS 29 (1969).
15. O.O. Van Gunten, Thesis, Univ. of Maryland (1974).
16. O.O. Van Gunten, private communication.
17. M.O. Burrell, NASA Technical Memorandum X-53063 1964).
18. R.G. Alsmiller, Oak Ridge National Laboratory Report ORNL 62-10-29 (1962).
19. R.T. Santoro, R.G. Alsmiller and J. Barish, Nucl. Sci. and Engr. 49, 375 (1972).
20. J.W. Watts and M.O. Burrell, NASA Publ. TN D-6385 (1971).
21. C.W. Hill, Lockheed-Georgia Co. Report ER-6643 (1964).
22. E.G. Stassinopoulos and C.Z. Gregory, NASA-GSFC Report X-601-74-330 (Nov. 1974) and E.G. Stassinopoulos, J.J. Hebert and E.L. Butler, NASA-GSFC Report X-601-77-114 (May 1977).

## Appendix B. Monoenergetic depth-dose data.

Scaled, monoenergetic depth-dose distributions are given in the following tables. The results are normalized to a unit incident current ( $1 \text{ cm}^{-2}$ ) of particles crossing into the plane aluminum medium, and pertain to particles with an isotropic angular distribution incident from one side only. The dose, absorbed in thin detectors of various materials of interest as given both as a function of depth  $z$  in a semi-infinite medium,  $D_{\infty}^{\text{det}}(z)$ , and as a function of thickness  $z$  at the transmission surface of a finite thickness slab,  $D_{-}^{\text{det}}(z)$ . Reference can be made to figure 1 for a further indication of irradiation and target geometry. The scaling is done in terms of the mean (c.s.d.a.) range  $r_0(T_0)$  in  $\text{g/cm}^2$  (given in tables 1 and 2 of the main text) and incident energy,  $T_0$  in MeV. The tables are organized as follows:

Table B.1.  $(r_0/T_0) D_{\infty}^{Al}(z/r_0) = (r_0/T_0) D_{-}^{Al}(z/r_0)$  for protons.  
 Units: dimensionless.

Table B.2.  $(r_0/T_0) D_{\infty}^{H_2O}(z/r_0) = (r_0/T_0) D_{-}^{H_2O}(z/r_0)$  for protons.  
 Units: dimensionless.

Table B.3.  $(r_0/T_0) D_{\infty}^{Si}(z/r_0) = (r_0/T_0) D_{-}^{Si}(z/r_0)$  for protons.  
 Units: dimensionless.

Table B.4.  $(r_0/T_0) D_{\infty}^{SiO_2}(z/r_0) = (r_0/T_0) D_{-}^{SiO_2}(z/r_0)$  for protons.  
 Units: dimensionless.

Table B.5.  $(r_0/T_0) D_{\infty}^{Al}(z/r_0)$  for electrons. Units: dimensionless.

Table B.6.  $(r_0/T_0) D_{-}^{Al}(z/r_0)$  for electrons. Units: dimensionless.

Table B.7.  $(r_0/T_0) D_{\infty}^{H_2^0}(z/r_0)$  for electrons. Units: dimensionless.

Table B.8.  $(r_0/T_0) D_{-}^{H_2^0}(z/r_0)$  for electrons. Units: dimensionless.

Table B.9.  $(r_0/T_0) D_{\infty}^{Si}(z/r_0)$  for electrons. Units: dimensionless.

Table B.10.  $(r_0/T_0) D_{-}^{Si}(z/r_0)$  for electrons. Units: dimensionless.

Table B.11.  $(r_0/T_0) D_{\infty}^{SiO_2}(z/r_0)$  for electrons. Units: dimensionless.

Table B.12.  $(r_0/T_0) D_{-}^{SiO_2}(z/r_0)$  for electrons. Units: dimensionless.

Table B.13.  $(1/T_0) D_{\infty}^{Al}(z/T_0)$  for bremsstrahlung. Units:  $\text{cm}^2/\text{g.}$

Table B.14.  $(1/T_0) D_{-}^{Al}(z/T_0)$  for bremsstrahlung. Units:  $\text{cm}^2/\text{g.}$

Table B.15.  $(1/T_0) D_{\infty}^{H_2^0}(z/T_0)$  for bremsstrahlung. Units:  $\text{cm}^2/\text{g.}$

Table B.16.  $(1/T_0) D_{-}^{H_2^0}(z/T_0)$  for bremsstrahlung. Units:  $\text{cm}^2/\text{g.}$

Table B.17.  $(1/T_0) D_{\infty}^{Si}(z/T_0)$  for bremsstrahlung. Units:  $\text{cm}^2/\text{g.}$

Table B.18.  $(1/T_0) D_{-}^{Si}(z/T_0)$  for bremsstrahlung. Units:  $\text{cm}^2/\text{g.}$

Table B.19.  $(1/T_0) D_{\infty}^{SiO_2}(z/T_0)$  for bremsstrahlung. Units:  $\text{cm}^2/\text{g.}$

Table B.20.  $(1/T_0) D_{-}^{SiO_2}(z/T_0)$  for bremsstrahlung. Units:  $\text{cm}^2/\text{g.}$

Table B.1.  $(r_0/T_0) D_{\infty}^{\alpha}(z/r_0) = (r_0/T_0) D_{\infty}^{\alpha}(z/r_0)$  for protons. Units: dimensionless.

$r_0/r_0$	$T_0 = 2$	$3$	$4$	$5$	$6$	$8$	$10$	$15$	$20$	$30$	$40$	$50$	$60$	$80$
0.0	1.290	1.237	1.172	1.153	1.141	1.151	1.139	1.133	1.126	1.124	1.124	1.125	1.125	1.130
0.02	1.268	1.206	1.233	1.257	1.212	1.194	1.171	1.169	1.163	1.156	1.153	1.154	1.154	1.158
0.04	1.290	1.257	1.231	1.274	1.249	1.231	1.212	1.213	1.209	1.202	1.195	1.192	1.192	1.179
0.06	1.354	1.306	1.318	1.287	1.262	1.245	1.225	1.225	1.221	1.214	1.214	1.204	1.204	1.206
0.08	1.364	1.364	1.326	1.296	1.273	1.255	1.236	1.233	1.231	1.224	1.217	1.214	1.213	1.215
0.10	1.371	1.375	1.336	1.332	1.303	1.280	1.264	1.244	1.239	1.231	1.225	1.221	1.220	1.221
0.12	1.378	1.378	1.336	1.336	1.308	1.286	1.271	1.251	1.245	1.244	1.237	1.231	1.226	1.227
0.14	1.380	1.380	1.338	1.329	1.312	1.291	1.276	1.257	1.251	1.248	1.242	1.237	1.231	1.231
0.16	1.379	1.379	1.339	1.339	1.314	1.294	1.280	1.261	1.251	1.251	1.245	1.235	1.233	1.233
0.18	1.379	1.379	1.338	1.338	1.314	1.295	1.281	1.263	1.252	1.252	1.246	1.240	1.236	1.234
0.20	1.377	1.377	1.336	1.336	1.313	1.295	1.282	1.264	1.252	1.252	1.246	1.240	1.236	1.234
0.22	1.374	1.374	1.337	1.304	1.304	1.286	1.272	1.263	1.249	1.234	1.227	1.219	1.217	1.233
0.24	1.369	1.369	1.326	1.294	1.294	1.277	1.264	1.255	1.250	1.250	1.244	1.238	1.233	1.232
0.26	1.362	1.355	1.326	1.283	1.283	1.267	1.255	1.242	1.227	1.224	1.219	1.215	1.212	1.229
0.28	1.301	1.287	1.257	1.257	1.274	1.285	1.274	1.258	1.244	1.243	1.238	1.231	1.229	1.226
0.30	1.346	1.313	1.294	1.279	1.279	1.269	1.254	1.239	1.238	1.231	1.227	1.222	1.221	1.220
0.32	1.337	1.304	1.286	1.272	1.272	1.263	1.249	1.234	1.231	1.227	1.222	1.219	1.217	1.215
0.34	1.326	1.294	1.284	1.277	1.277	1.264	1.255	1.242	1.227	1.224	1.219	1.212	1.210	1.208
0.36	1.314	1.295	1.271	1.271	1.271	1.255	1.242	1.234	1.221	1.215	1.211	1.207	1.204	1.200
0.38	1.301	1.271	1.255	1.255	1.271	1.250	1.244	1.226	1.211	1.205	1.202	1.198	1.193	1.191
0.40	1.287	1.257	1.243	1.243	1.257	1.233	1.226	1.216	1.211	1.201	1.194	1.188	1.185	1.181
0.42	1.272	1.243	1.230	1.220	1.243	1.220	1.214	1.205	1.191	1.183	1.181	1.176	1.174	1.168
0.44	1.256	1.227	1.215	1.207	1.227	1.215	1.201	1.193	1.179	1.170	1.168	1.160	1.158	1.156
0.46	1.238	1.211	1.199	1.199	1.211	1.192	1.187	1.179	1.166	1.156	1.155	1.151	1.149	1.143
0.48	1.220	1.193	1.183	1.175	1.175	1.171	1.171	1.165	1.152	1.141	1.141	1.137	1.134	1.128
0.50	1.201	1.175	1.165	1.158	1.158	1.155	1.155	1.149	1.137	1.125	1.125	1.122	1.119	1.116
0.52	1.180	1.155	1.146	1.140	1.140	1.137	1.137	1.133	1.121	1.108	1.108	1.105	1.103	1.100
0.54	1.159	1.134	1.125	1.125	1.125	1.118	1.118	1.115	1.115	1.104	1.104	1.091	1.088	1.097
0.56	1.136	1.112	1.104	1.104	1.104	1.100	1.098	1.095	1.095	1.086	1.072	1.069	1.066	1.061
0.58	1.112	1.089	1.081	1.078	1.078	1.076	1.076	1.075	1.075	1.066	1.052	1.052	1.049	1.045
0.60	1.087	1.064	1.057	1.054	1.054	1.053	1.053	1.053	1.053	1.050	1.031	1.030	1.028	1.025
0.62	1.061	1.038	1.032	1.030	1.030	1.030	1.030	1.030	1.023	1.023	1.008	1.008	1.006	1.005
0.64	1.033	1.012	1.006	1.004	1.004	1.004	1.004	1.004	1.006	1.006	0.985	0.985	0.983	0.979
0.66	1.004	0.983	0.978	0.976	0.976	0.977	0.977	0.980	0.974	0.961	0.958	0.958	0.957	0.955
0.68	0.974	0.953	0.948	0.947	0.947	0.949	0.949	0.947	0.947	0.935	0.932	0.932	0.929	0.928
0.70	0.942	0.922	0.917	0.917	0.917	0.917	0.917	0.917	0.919	0.919	0.907	0.903	0.903	0.902
0.72	0.908	0.889	0.885	0.885	0.885	0.885	0.885	0.885	0.887	0.887	0.874	0.874	0.873	0.869
0.74	0.873	0.855	0.851	0.851	0.851	0.851	0.851	0.851	0.859	0.857	0.848	0.843	0.843	0.841
0.76	0.837	0.819	0.815	0.815	0.815	0.816	0.816	0.816	0.823	0.816	0.810	0.810	0.809	0.806
0.78	0.798	0.781	0.777	0.777	0.777	0.778	0.778	0.778	0.781	0.776	0.776	0.775	0.774	0.771
0.80	0.756	0.737	0.737	0.737	0.737	0.737	0.737	0.737	0.748	0.748	0.744	0.738	0.737	0.734
0.82	0.712	0.696	0.693	0.694	0.694	0.694	0.694	0.694	0.705	0.705	0.703	0.699	0.697	0.696
0.84	0.665	0.647	0.648	0.651	0.651	0.659	0.661	0.661	0.660	0.660	0.656	0.653	0.654	0.651
0.86	0.615	0.602	0.599	0.600	0.603	0.611	0.613	0.613	0.611	0.611	0.607	0.608	0.608	0.606
0.88	0.563	0.550	0.547	0.548	0.551	0.559	0.562	0.562	0.560	0.560	0.559	0.559	0.559	0.558
0.90	0.506	0.494	0.492	0.492	0.495	0.495	0.495	0.495	0.502	0.502	0.509	0.506	0.506	0.505
0.92	0.442	0.432	0.429	0.430	0.432	0.432	0.432	0.432	0.442	0.442	0.447	0.448	0.446	0.444
0.94	0.369	0.360	0.358	0.358	0.360	0.360	0.360	0.360	0.369	0.369	0.374	0.375	0.375	0.374
0.96	0.283	0.276	0.274	0.274	0.276	0.276	0.276	0.276	0.283	0.283	0.290	0.292	0.291	0.290
0.98	0.180	0.175	0.174	0.174	0.175	0.175	0.175	0.175	0.179	0.179	0.185	0.188	0.189	0.188
1.00	0.0	0.0	0.0	0.0	0.0	0.0	0.0	0.0	0.0	0.0	0.0	0.0	0.0	0.0

Table B.1.  $(r_o/T_o) D_{\infty}^{A\ell}(z/r_o) = (r_o/T_o) D_{\infty}^{\ell}(z/r_o)$  for protons. Units: dimensionless. (Continued)

$r_o/T_o$	$z/r_o$	100	200	300	400	500	600	800	1000	1500	2000	3000	4000	5000
0.0	0.0	1.137	1.155	1.175	1.195	1.215	1.235	1.255	1.289	1.325	1.361	1.445	1.557	1.642
0.02	0.02	1.164	1.180	1.198	1.215	1.235	1.251	1.271	1.291	1.333	1.370	1.441	1.542	1.619
0.04	0.04	1.184	1.199	1.212	1.227	1.249	1.267	1.287	1.309	1.337	1.352	1.436	1.527	1.619
0.06	0.06	1.199	1.212	1.222	1.222	1.241	1.249	1.265	1.285	1.313	1.338	1.386	1.428	1.511
0.08	0.08	1.210	1.218	1.229	1.235	1.241	1.248	1.256	1.276	1.290	1.315	1.353	1.380	1.418
0.10	0.10	1.224	1.234	1.245	1.245	1.245	1.245	1.257	1.269	1.290	1.311	1.329	1.356	1.408
0.12	0.12	1.229	1.234	1.239	1.239	1.241	1.241	1.245	1.251	1.262	1.272	1.281	1.291	1.310
0.14	0.14	1.229	1.238	1.238	1.236	1.236	1.236	1.245	1.253	1.262	1.270	1.281	1.297	1.312
0.16	0.16	1.233	1.233	1.229	1.227	1.230	1.237	1.244	1.252	1.265	1.275	1.283	1.296	1.312
0.18	0.18	1.235	1.235	1.235	1.235	1.241	1.248	1.256	1.265	1.273	1.281	1.289	1.309	1.337
0.20	0.20	1.218	1.218	1.219	1.219	1.221	1.223	1.229	1.234	1.240	1.246	1.254	1.278	1.309
0.22	0.22	1.224	1.234	1.239	1.239	1.241	1.245	1.257	1.269	1.276	1.282	1.291	1.297	1.323
0.24	0.24	1.232	1.236	1.236	1.236	1.236	1.236	1.241	1.251	1.259	1.262	1.272	1.281	1.297
0.26	0.26	1.229	1.229	1.225	1.227	1.230	1.237	1.244	1.253	1.262	1.270	1.279	1.296	1.312
0.28	0.28	1.225	1.225	1.225	1.225	1.225	1.225	1.234	1.244	1.252	1.260	1.279	1.297	1.316
0.30	0.30	1.219	1.219	1.219	1.219	1.221	1.223	1.229	1.234	1.240	1.246	1.254	1.278	1.299
0.32	0.32	1.213	1.213	1.214	1.214	1.215	1.215	1.224	1.234	1.240	1.246	1.254	1.278	1.297
0.34	0.34	1.206	1.206	1.205	1.205	1.207	1.207	1.209	1.212	1.215	1.218	1.222	1.234	1.250
0.36	0.36	1.196	1.196	1.197	1.197	1.198	1.198	1.199	1.201	1.203	1.205	1.207	1.212	1.225
0.38	0.38	1.188	1.188	1.186	1.186	1.186	1.186	1.186	1.186	1.186	1.187	1.187	1.189	1.192
0.40	0.40	1.178	1.178	1.175	1.175	1.175	1.175	1.175	1.175	1.175	1.175	1.175	1.175	1.194
0.42	0.42	1.166	1.166	1.163	1.163	1.162	1.162	1.162	1.162	1.162	1.162	1.162	1.162	1.160
0.44	0.44	1.154	1.154	1.150	1.150	1.150	1.150	1.150	1.150	1.150	1.150	1.150	1.150	1.150
0.46	0.46	1.141	1.141	1.137	1.137	1.134	1.134	1.134	1.134	1.134	1.134	1.134	1.134	1.134
0.48	0.48	1.126	1.126	1.122	1.122	1.118	1.118	1.118	1.118	1.118	1.118	1.118	1.118	1.118
0.50	0.50	1.111	1.106	1.106	1.106	1.102	1.102	1.102	1.102	1.102	1.102	1.102	1.102	1.102
0.52	0.52	1.094	1.094	1.094	1.094	1.094	1.094	1.094	1.094	1.094	1.094	1.094	1.094	1.094
0.54	0.54	1.077	1.077	1.077	1.077	1.077	1.077	1.077	1.077	1.077	1.077	1.077	1.077	1.077
0.56	0.56	1.058	1.058	1.058	1.058	1.058	1.058	1.058	1.058	1.058	1.058	1.058	1.058	1.058
0.58	0.58	1.053	1.053	1.053	1.053	1.053	1.053	1.053	1.053	1.053	1.053	1.053	1.053	1.053
0.60	0.60	1.018	1.018	1.012	1.012	1.005	1.005	1.005	1.005	1.005	1.005	1.005	1.005	1.005
0.62	0.62	0.996	0.996	0.989	0.989	0.983	0.983	0.983	0.983	0.983	0.983	0.983	0.983	0.983
0.64	0.64	0.973	0.973	0.966	0.966	0.959	0.959	0.947	0.947	0.947	0.947	0.947	0.947	0.947
0.66	0.66	0.948	0.948	0.941	0.941	0.934	0.934	0.922	0.922	0.922	0.922	0.922	0.922	0.922
0.68	0.68	0.922	0.922	0.915	0.915	0.908	0.908	0.895	0.895	0.883	0.883	0.871	0.871	0.871
0.70	0.70	0.895	0.887	0.887	0.887	0.887	0.887	0.887	0.887	0.887	0.887	0.887	0.887	0.887
0.72	0.72	0.866	0.858	0.855	0.855	0.852	0.852	0.852	0.852	0.852	0.852	0.852	0.852	0.852
0.74	0.74	0.835	0.828	0.820	0.820	0.817	0.817	0.817	0.817	0.817	0.817	0.817	0.817	0.817
0.76	0.76	0.803	0.796	0.788	0.788	0.781	0.781	0.779	0.779	0.779	0.779	0.779	0.779	0.779
0.78	0.78	0.769	0.761	0.754	0.754	0.740	0.740	0.727	0.727	0.714	0.702	0.682	0.663	0.643
0.80	0.80	0.732	0.692	0.724	0.717	0.703	0.690	0.677	0.677	0.666	0.645	0.627	0.590	0.559
0.82	0.82	0.695	0.677	0.667	0.667	0.654	0.654	0.638	0.638	0.627	0.606	0.588	0.559	0.524
0.84	0.84	0.649	0.642	0.635	0.635	0.622	0.622	0.609	0.609	0.597	0.586	0.565	0.548	0.512
0.86	0.86	0.604	0.597	0.590	0.590	0.578	0.578	0.565	0.565	0.553	0.543	0.523	0.506	0.471
0.88	0.88	0.556	0.556	0.543	0.543	0.531	0.531	0.519	0.519	0.508	0.497	0.478	0.462	0.429
0.90	0.90	0.503	0.497	0.491	0.491	0.480	0.480	0.469	0.469	0.458	0.448	0.430	0.383	0.344
0.92	0.92	0.443	0.438	0.432	0.432	0.422	0.422	0.412	0.412	0.402	0.393	0.376	0.360	0.326
0.94	0.94	0.375	0.369	0.364	0.364	0.355	0.355	0.346	0.346	0.338	0.330	0.315	0.303	0.281
0.96	0.96	0.289	0.286	0.283	0.283	0.275	0.275	0.268	0.268	0.255	0.243	0.233	0.213	0.176
0.98	0.98	0.188	0.186	0.183	0.183	0.174	0.174	0.169	0.169	0.165	0.157	0.150	0.136	0.111
1.00	1.00	0.0	0.0	0.0	0.0	0.0	0.0	0.0	0.0	0.0	0.0	0.0	0.0	0.0

Table B.2.  $(r_o/T_o) D_{\infty}^-(z/r_o) = (r_o/T_o) D_{\infty}^0(z/r_o)$  for protons. Units: dimensionless.

$r_o/T_o$	2	3	4	5	6	8	10	15	20	30	40	50	60	80
0.0	1.952	1.826	1.698	1.751	1.660	1.613	1.594	1.553	1.529	1.490	1.479	1.478	1.479	1.478
0.02	2.009	1.881	1.805	1.752	1.713	1.663	1.640	1.599	1.546	1.532	1.524	1.516	1.516	1.516
0.04	2.052	1.923	1.846	1.793	1.755	1.703	1.676	1.634	1.604	1.579	1.555	1.550	1.546	1.546
0.06	2.085	1.955	1.878	1.825	1.786	1.734	1.704	1.661	1.634	1.588	1.579	1.573	1.568	1.568
0.08	2.110	1.980	1.903	1.850	1.811	1.758	1.726	1.683	1.655	1.624	1.607	1.591	1.585	1.585
0.10	2.130	2.000	1.923	1.870	1.832	1.778	1.744	1.700	1.672	1.640	1.622	1.612	1.608	1.608
0.12	2.146	2.016	1.939	1.886	1.848	1.795	1.759	1.714	1.685	1.653	1.635	1.623	1.616	1.617
0.14	2.159	2.029	1.952	1.900	1.862	1.809	1.772	1.726	1.697	1.663	1.645	1.633	1.626	1.617
0.16	2.170	2.040	1.964	1.911	1.874	1.822	1.783	1.736	1.706	1.672	1.653	1.641	1.633	1.623
0.18	2.179	2.048	1.973	1.921	1.884	1.832	1.791	1.744	1.713	1.679	1.660	1.647	1.639	1.628
0.20	2.184	2.054	1.979	1.927	1.889	1.839	1.798	1.750	1.719	1.684	1.664	1.651	1.642	1.631
0.22	2.186	2.057	1.982	1.931	1.895	1.844	1.802	1.754	1.721	1.686	1.666	1.653	1.644	1.632
0.24	2.186	2.058	1.983	1.933	1.897	1.847	1.804	1.754	1.722	1.687	1.666	1.653	1.644	1.631
0.26	2.184	2.056	1.983	1.932	1.897	1.848	1.805	1.753	1.722	1.686	1.665	1.651	1.642	1.629
0.28	2.180	2.055	1.980	1.930	1.896	1.847	1.804	1.751	1.720	1.684	1.663	1.649	1.639	1.625
0.30	2.174	2.048	1.976	1.921	1.890	1.844	1.801	1.748	1.716	1.680	1.658	1.644	1.634	1.620
0.32	2.166	2.041	1.969	1.921	1.887	1.840	1.797	1.742	1.711	1.674	1.653	1.638	1.628	1.614
0.34	2.156	2.032	1.961	1.913	1.880	1.834	1.791	1.736	1.704	1.667	1.646	1.631	1.620	1.606
0.36	2.144	2.021	1.951	1.904	1.872	1.826	1.784	1.736	1.704	1.669	1.649	1.637	1.622	1.611
0.38	2.131	2.008	1.960	1.893	1.861	1.817	1.775	1.727	1.696	1.659	1.637	1.622	1.611	1.596
0.40	2.115	1.994	1.926	1.876	1.849	1.806	1.764	1.716	1.686	1.649	1.627	1.611	1.601	1.586
0.42	2.098	1.978	1.911	1.866	1.835	1.793	1.752	1.693	1.662	1.625	1.603	1.588	1.576	1.560
0.44	2.078	1.960	1.894	1.850	1.820	1.778	1.738	1.679	1.648	1.611	1.589	1.573	1.562	1.556
0.46	2.057	1.940	1.875	1.837	1.802	1.762	1.723	1.663	1.632	1.595	1.573	1.558	1.546	1.530
0.48	2.034	1.918	1.855	1.812	1.783	1.744	1.706	1.666	1.635	1.578	1.556	1.540	1.529	1.512
0.50	2.009	1.895	1.832	1.791	1.763	1.724	1.687	1.647	1.617	1.559	1.537	1.522	1.510	1.493
0.52	1.982	1.870	1.808	1.768	1.740	1.703	1.666	1.626	1.597	1.539	1.517	1.502	1.490	1.473
0.54	1.953	1.842	1.782	1.743	1.716	1.680	1.644	1.604	1.576	1.518	1.496	1.480	1.469	1.451
0.56	1.922	1.813	1.754	1.716	1.690	1.655	1.620	1.581	1.551	1.495	1.473	1.456	1.446	1.428
0.58	1.889	1.782	1.724	1.687	1.661	1.628	1.594	1.556	1.526	1.470	1.448	1.435	1.421	1.404
0.60	1.854	1.749	1.693	1.656	1.631	1.599	1.566	1.529	1.499	1.443	1.422	1.406	1.395	1.377
0.62	1.816	1.713	1.658	1.623	1.599	1.568	1.536	1.498	1.461	1.415	1.394	1.378	1.367	1.350
0.64	1.776	1.676	1.622	1.588	1.565	1.535	1.505	1.465	1.420	1.385	1.364	1.349	1.337	1.320
0.66	1.734	1.635	1.584	1.550	1.528	1.499	1.460	1.420	1.387	1.353	1.332	1.317	1.306	1.289
0.68	1.689	1.593	1.542	1.510	1.489	1.462	1.434	1.383	1.352	1.319	1.298	1.283	1.272	1.255
0.70	1.641	1.548	1.499	1.468	1.432	1.395	1.366	1.324	1.315	1.283	1.262	1.248	1.237	1.220
0.72	1.590	1.500	1.453	1.425	1.403	1.378	1.343	1.307	1.276	1.244	1.224	1.210	1.199	1.182
0.74	1.536	1.469	1.404	1.375	1.357	1.333	1.309	1.265	1.235	1.203	1.184	1.170	1.159	1.143
0.76	1.480	1.396	1.352	1.324	1.307	1.285	1.262	1.220	1.191	1.160	1.141	1.127	1.117	1.101
0.78	1.419	1.338	1.296	1.270	1.253	1.233	1.211	1.172	1.144	1.114	1.095	1.072	1.056	1.046
0.80	1.353	1.236	1.236	1.211	1.195	1.176	1.156	1.120	1.093	1.063	1.045	1.033	1.023	1.007
0.82	1.281	1.208	1.170	1.147	1.132	1.106	1.096	1.063	1.038	1.008	0.991	0.979	0.969	0.954
0.84	1.205	1.136	1.100	1.078	1.065	1.048	1.031	1.001	0.978	0.949	0.933	0.921	0.912	0.898
0.86	1.123	1.059	1.026	1.005	0.993	0.978	0.963	0.935	0.915	0.887	0.871	0.860	0.852	0.838
0.88	1.037	0.977	0.947	0.928	0.916	0.903	0.889	0.864	0.847	0.821	0.806	0.795	0.787	0.774
0.90	0.941	0.889	0.859	0.842	0.831	0.820	0.807	0.786	0.771	0.748	0.733	0.723	0.715	0.704
0.92	0.832	0.784	0.759	0.744	0.735	0.724	0.714	0.696	0.683	0.664	0.650	0.641	0.634	0.623
0.94	0.704	0.664	0.643	0.630	0.622	0.613	0.604	0.590	0.580	0.565	0.553	0.544	0.538	0.528
0.96	0.550	0.518	0.502	0.491	0.485	0.478	0.472	0.461	0.454	0.443	0.434	0.422	0.414	0.404
0.98	0.361	0.340	0.329	0.322	0.318	0.313	0.309	0.302	0.298	0.284	0.280	0.274	0.274	0.274
1.00	0.0	0.0	0.0	0.0	0.0	0.0	0.0	0.0	0.0	0.0	0.0	0.0	0.0	0.0

Table B.2.  $(r_o/\tau_o) D_{-}^{H_2^0}(z/r_o) = (r_o/\tau_o) D_{-}^{H_2^0}(z/r_o)$  for protons. Units: dimensionless. (Continued)

T <sub>0</sub> =100		T <sub>0</sub> /r <sub>0</sub>		500		600		800		1000		1500		2000		3000		4000		5000	
0.0	1.481	0.0	1.518	1.651	1.607	1.693	1.769	1.835	1.969	2.068	2.204	2.292	2.353	2.399	2.449	2.533	2.628	2.724	2.824	2.924	2.999
0.04	1.496	0.04	1.530	1.651	1.628	1.667	1.705	1.773	1.826	1.953	2.042	2.127	2.199	2.249	2.299	2.349	2.420	2.515	2.614	2.715	2.815
0.08	1.517	0.08	1.548	1.574	1.587	1.618	1.642	1.682	1.695	1.711	1.733	1.773	1.826	1.887	1.915	1.989	2.053	2.114	2.172	2.201	2.249
0.12	1.530	0.12	1.556	1.567	1.583	1.588	1.599	1.627	1.655	1.684	1.712	1.763	1.806	1.845	1.895	1.962	2.017	2.072	2.110	2.155	2.201
0.16	1.544	0.16	1.569	1.579	1.583	1.599	1.608	1.632	1.658	1.683	1.708	1.754	1.794	1.847	1.934	2.017	2.072	2.110	2.155	2.201	2.249
0.20	1.558	0.20	1.582	1.599	1.605	1.614	1.614	1.635	1.657	1.681	1.703	1.744	1.780	1.845	1.907	1.982	2.031	2.066	2.110	2.155	2.201
0.24	1.571	0.24	1.613	1.613	1.618	1.636	1.636	1.653	1.671	1.689	1.703	1.733	1.765	1.830	1.878	1.946	2.021	2.066	2.110	2.155	2.201
0.28	1.585	0.28	1.625	1.625	1.625	1.634	1.634	1.649	1.664	1.680	1.708	1.733	1.783	1.821	1.874	1.949	2.021	2.066	2.110	2.155	2.201
0.32	1.599	0.32	1.632	1.625	1.625	1.631	1.631	1.643	1.656	1.669	1.694	1.715	1.759	1.792	1.838	1.888	1.949	2.017	2.072	2.110	2.155
0.36	1.612	0.36	1.641	1.641	1.641	1.651	1.651	1.661	1.676	1.697	1.734	1.762	1.802	1.847	1.887	1.927	1.982	2.031	2.066	2.110	2.155
0.40	1.625	0.40	1.651	1.651	1.651	1.660	1.660	1.673	1.684	1.697	1.721	1.754	1.792	1.838	1.888	1.934	2.017	2.072	2.110	2.155	2.201
0.44	1.638	0.44	1.664	1.664	1.664	1.671	1.671	1.684	1.697	1.711	1.733	1.765	1.802	1.847	1.887	1.934	2.017	2.072	2.110	2.155	2.201
0.48	1.651	0.48	1.681	1.681	1.681	1.687	1.687	1.697	1.711	1.724	1.744	1.773	1.806	1.847	1.887	1.934	2.017	2.072	2.110	2.155	2.201
0.52	1.664	0.52	1.691	1.691	1.691	1.698	1.698	1.711	1.724	1.737	1.754	1.782	1.811	1.852	1.891	1.934	2.017	2.072	2.110	2.155	2.201
0.56	1.677	0.56	1.711	1.711	1.711	1.718	1.718	1.731	1.744	1.757	1.774	1.802	1.831	1.871	1.910	1.949	2.021	2.066	2.110	2.155	2.201
0.60	1.690	0.60	1.725	1.725	1.725	1.732	1.732	1.745	1.758	1.771	1.788	1.816	1.844	1.883	1.922	1.961	2.031	2.066	2.110	2.155	2.201
0.64	1.703	0.64	1.738	1.738	1.738	1.745	1.745	1.758	1.771	1.784	1.797	1.825	1.853	1.892	1.931	1.969	2.031	2.066	2.110	2.155	2.201
0.68	1.716	0.68	1.751	1.751	1.751	1.758	1.758	1.771	1.784	1.797	1.810	1.838	1.866	1.905	1.943	1.982	2.031	2.066	2.110	2.155	2.201
0.72	1.729	0.72	1.764	1.764	1.764	1.771	1.771	1.784	1.797	1.810	1.823	1.851	1.879	1.918	1.956	1.994	2.031	2.066	2.110	2.155	2.201
0.76	1.742	0.76	1.777	1.777	1.777	1.784	1.784	1.797	1.810	1.823	1.836	1.864	1.892	1.930	1.968	2.007	2.031	2.066	2.110	2.155	2.201
0.80	1.755	0.80	1.791	1.791	1.791	1.798	1.798	1.811	1.824	1.837	1.850	1.878	1.906	1.944	1.982	2.021	2.031	2.066	2.110	2.155	2.201
0.84	1.768	0.84	1.804	1.804	1.804	1.811	1.811	1.824	1.837	1.850	1.863	1.891	1.919	1.957	1.995	2.031	2.066	2.110	2.155	2.201	2.249
0.88	1.781	0.88	1.817	1.817	1.817	1.824	1.824	1.837	1.850	1.863	1.876	1.904	1.932	1.970	2.008	2.031	2.066	2.110	2.155	2.201	2.249
0.92	1.794	0.92	1.830	1.830	1.830	1.837	1.837	1.850	1.863	1.876	1.889	1.917	1.945	1.983	2.021	2.031	2.066	2.110	2.155	2.201	2.249
0.96	1.807	0.96	1.843	1.843	1.843	1.850	1.850	1.863	1.876	1.889	1.902	1.930	1.958	1.996	2.031	2.066	2.110	2.155	2.201	2.249	2.249
1.00	1.820	1.00	1.856	1.856	1.856	1.863	1.863	1.876	1.889	1.902	1.915	1.943	1.971	2.009	2.031	2.066	2.110	2.155	2.201	2.249	2.249

Table B.3.  $(r_0/T_0) D_{\infty}^{Si}(z/r_0) = (r_0/T_0) D_{-}^{Si}(z/r_0)$  for protons. Units: dimensionless.

$r_0/T_0 =$	2	3	4	5	6	8	10	15	20	30	40	50	60	80
$z/r_0$	0.02	0.04	0.06	0.08	0.10	0.12	0.14	0.16	0.18	0.20	0.22	0.24	0.26	0.28
$T_0 =$	1.309	1.259	1.229	1.194	1.175	1.165	1.165	1.165	1.165	1.160	1.160	1.154	1.152	1.153
$r_0/T_0$	0.02	0.04	0.06	0.08	0.10	0.12	0.14	0.16	0.18	0.20	0.22	0.24	0.26	0.28
$D_{\infty}^{Si}(z/r_0)$	1.195	1.218	1.224	1.224	1.224	1.224	1.224	1.224	1.224	1.224	1.224	1.224	1.224	1.224
$D_{-}^{Si}(z/r_0)$	1.209	1.235	1.255	1.255	1.255	1.255	1.255	1.255	1.255	1.255	1.255	1.255	1.255	1.255
$D_{\infty}^{Si}(z/r_0) - D_{-}^{Si}(z/r_0)$	-0.014	-0.019	-0.024	-0.024	-0.024	-0.024	-0.024	-0.024	-0.024	-0.024	-0.024	-0.024	-0.024	-0.024
$D_{\infty}^{Si}(z/r_0) + D_{-}^{Si}(z/r_0)$	1.184	1.184	1.184	1.184	1.184	1.184	1.184	1.184	1.184	1.184	1.184	1.184	1.184	1.184
$D_{\infty}^{Si}(z/r_0) \cdot D_{-}^{Si}(z/r_0)$	0.000	0.000	0.000	0.000	0.000	0.000	0.000	0.000	0.000	0.000	0.000	0.000	0.000	0.000
$D_{\infty}^{Si}(z/r_0) / D_{-}^{Si}(z/r_0)$	1.000	1.000	1.000	1.000	1.000	1.000	1.000	1.000	1.000	1.000	1.000	1.000	1.000	1.000
$D_{\infty}^{Si}(z/r_0) - D_{-}^{Si}(z/r_0)$	0.000	0.000	0.000	0.000	0.000	0.000	0.000	0.000	0.000	0.000	0.000	0.000	0.000	0.000

Table B.3.  $(r_0/T_0) D_{\frac{z}{\infty}}^{Si}(z/r_0) = (r_0/T_0) D_{-}^{Si}(z/r_0)$  for protons. Units: dimensionless. (Continued)

$z/r_0$	$T_0=100$	0.0	1.167	1.186	1.207	1.231	1.269	1.290	1.329	1.362	1.430	1.489	1.607	1.696	1.821	1.904	1.963	
0.02	1.194	1.212	1.231	1.251	1.270	1.283	1.292	1.301	1.316	1.334	1.371	1.432	1.485	1.592	1.672	1.786	1.861	1.915
0.04	1.215	1.230	1.245	1.260	1.273	1.282	1.297	1.301	1.316	1.334	1.376	1.430	1.478	1.576	1.649	1.752	1.870	1.877
0.06	1.230	1.242	1.254	1.269	1.274	1.282	1.297	1.301	1.316	1.334	1.376	1.426	1.470	1.570	1.626	1.720	1.784	1.829
0.08	1.242	1.250	1.262	1.274	1.281	1.288	1.297	1.301	1.316	1.333	1.373	1.420	1.460	1.523	1.579	1.688	1.747	1.789
0.10	1.250	1.256	1.267	1.274	1.281	1.288	1.297	1.301	1.316	1.332	1.373	1.413	1.449	1.523	1.579	1.677	1.711	1.750
0.12	1.256	1.266	1.270	1.273	1.274	1.278	1.282	1.288	1.297	1.302	1.334	1.369	1.404	1.437	1.504	1.555	1.627	1.676
0.14	1.264	1.264	1.266	1.269	1.273	1.278	1.282	1.288	1.297	1.302	1.334	1.363	1.394	1.424	1.485	1.531	1.596	1.641
0.16	1.264	1.266	1.266	1.269	1.273	1.278	1.282	1.288	1.297	1.302	1.334	1.363	1.394	1.411	1.465	1.507	1.565	1.605
0.18	1.266	1.266	1.274	1.274	1.274	1.278	1.282	1.299	1.316	1.320	1.332	1.347	1.373	1.397	1.445	1.482	1.535	1.570
0.20	1.267	1.267	1.274	1.274	1.274	1.278	1.281	1.296	1.310	1.325	1.338	1.361	1.382	1.425	1.457	1.504	1.536	1.559
0.22	1.266	1.266	1.268	1.274	1.274	1.278	1.281	1.295	1.306	1.320	1.334	1.366	1.394	1.425	1.457	1.501	1.522	1.559
0.24	1.264	1.264	1.266	1.268	1.274	1.274	1.278	1.288	1.296	1.302	1.317	1.334	1.350	1.383	1.407	1.443	1.467	1.486
0.26	1.260	1.264	1.264	1.266	1.269	1.273	1.278	1.282	1.290	1.297	1.316	1.333	1.351	1.382	1.412	1.453	1.493	1.513
0.28	1.256	1.256	1.259	1.263	1.269	1.270	1.274	1.278	1.286	1.293	1.305	1.320	1.339	1.356	1.382	1.399	1.413	1.435
0.30	1.250	1.250	1.252	1.255	1.255	1.257	1.262	1.266	1.274	1.280	1.289	1.298	1.317	1.331	1.351	1.365	1.376	1.386
0.32	1.244	1.244	1.245	1.245	1.247	1.247	1.252	1.257	1.261	1.266	1.273	1.279	1.294	1.305	1.321	1.332	1.340	1.349
0.34	1.236	1.236	1.237	1.237	1.238	1.241	1.245	1.248	1.251	1.254	1.257	1.261	1.271	1.278	1.290	1.298	1.304	1.313
0.36	1.227	1.227	1.227	1.227	1.228	1.230	1.232	1.234	1.236	1.239	1.241	1.244	1.247	1.252	1.259	1.264	1.269	1.273
0.38	1.218	1.218	1.217	1.217	1.217	1.217	1.218	1.219	1.220	1.220	1.221	1.221	1.222	1.223	1.228	1.231	1.233	1.237
0.40	1.207	1.207	1.205	1.205	1.205	1.204	1.204	1.205	1.205	1.205	1.205	1.205	1.205	1.205	1.205	1.207	1.207	1.208
0.42	1.195	1.195	1.193	1.193	1.193	1.190	1.190	1.188	1.186	1.186	1.185	1.185	1.183	1.179	1.174	1.171	1.166	1.162
0.44	1.183	1.183	1.180	1.180	1.178	1.175	1.175	1.178	1.172	1.172	1.167	1.167	1.158	1.149	1.144	1.135	1.130	1.127
0.46	1.169	1.169	1.166	1.166	1.163	1.163	1.159	1.159	1.151	1.151	1.148	1.148	1.142	1.135	1.124	1.116	1.104	1.097
0.48	1.154	1.154	1.150	1.150	1.148	1.148	1.142	1.142	1.137	1.137	1.132	1.128	1.120	1.113	1.098	1.088	1.073	1.063
0.50	1.138	1.138	1.134	1.134	1.131	1.131	1.124	1.124	1.118	1.118	1.113	1.113	1.108	1.098	1.072	1.059	1.042	1.030
0.52	1.122	1.122	1.117	1.117	1.113	1.113	1.106	1.106	1.099	1.099	1.092	1.092	1.086	1.075	1.065	1.045	1.031	1.010
0.54	1.104	1.104	1.099	1.099	1.094	1.094	1.086	1.086	1.078	1.078	1.071	1.064	1.052	1.041	1.018	1.002	0.978	0.951
0.56	1.085	1.085	1.079	1.079	1.074	1.074	1.065	1.065	1.056	1.056	1.048	1.041	1.027	1.015	0.990	0.972	0.946	0.916
0.58	1.064	1.064	1.059	1.059	1.053	1.053	1.044	1.044	1.034	1.034	1.025	1.017	1.012	1.002	0.989	0.942	0.914	0.881
0.60	1.043	1.043	1.037	1.037	1.031	1.031	1.021	1.021	1.010	1.010	1.001	1.001	0.976	0.963	0.933	0.912	0.882	0.846
0.62	1.020	1.020	1.014	1.014	1.008	1.008	0.997	0.997	0.986	0.986	0.976	0.972	0.950	0.935	0.904	0.881	0.849	0.811
0.64	0.996	0.996	0.990	0.990	0.984	0.984	0.972	0.972	0.961	0.961	0.950	0.940	0.922	0.907	0.874	0.850	0.816	0.776
0.66	0.971	0.965	0.958	0.958	0.946	0.946	0.934	0.934	0.923	0.923	0.912	0.908	0.894	0.877	0.844	0.818	0.783	0.741
0.68	0.945	0.938	0.931	0.931	0.918	0.918	0.906	0.906	0.894	0.894	0.884	0.864	0.854	0.834	0.812	0.786	0.749	0.706
0.70	0.916	0.909	0.902	0.902	0.890	0.890	0.877	0.877	0.865	0.865	0.854	0.846	0.834	0.816	0.780	0.753	0.715	0.689
0.72	0.887	0.880	0.872	0.872	0.866	0.866	0.859	0.859	0.846	0.846	0.834	0.823	0.802	0.784	0.748	0.720	0.681	0.635
0.74	0.855	0.848	0.841	0.841	0.828	0.828	0.814	0.814	0.802	0.802	0.790	0.769	0.735	0.717	0.679	0.646	0.619	0.599
0.76	0.822	0.815	0.808	0.808	0.794	0.794	0.781	0.781	0.768	0.768	0.757	0.735	0.717	0.699	0.661	0.630	0.583	0.563
0.78	0.787	0.780	0.773	0.773	0.759	0.759	0.745	0.745	0.733	0.733	0.721	0.700	0.681	0.664	0.644	0.615	0.574	0.526
0.80	0.749	0.742	0.735	0.735	0.721	0.721	0.703	0.703	0.695	0.695	0.683	0.662	0.643	0.626	0.606	0.578	0.537	0.489
0.82	0.708	0.701	0.694	0.694	0.681	0.681	0.667	0.667	0.655	0.655	0.643	0.622	0.604	0.567	0.539	0.499	0.472	0.451
0.84	0.664	0.658	0.651	0.651	0.645	0.645	0.625	0.625	0.612	0.612	0.601	0.580	0.558	0.537	0.519	0.484	0.420	0.394
0.86	0.617	0.611	0.605	0.605	0.592	0.592	0.578	0.578	0.568	0.568	0.557	0.532	0.510	0.491	0.474	0.440	0.415	0.354
0.88	0.568	0.563	0.556	0.556	0.544	0.544	0.522	0.522	0.510	0.510	0.491	0.469	0.449	0.426	0.394	0.370	0.336	0.312
0.90	0.514	0.509	0.503	0.503	0.491	0.491	0.470	0.470	0.459	0.459	0.441	0.422	0.403	0.386	0.351	0.321	0.289	0.252
0.92	0.453	0.448	0.443	0.443	0.432	0.432	0.412	0.412	0.403	0.403	0.384	0.358	0.331	0.311	0.285	0.266	0.238	0.205
0.94	0.381	0.377	0.373	0.373	0.364	0.364	0.344	0.344	0.335	0.335	0.323	0.302	0.281	0.261	0.249	0.218	0.180	0.154
0.96	0.296	0.293	0.289	0.289	0.282	0.282	0.262	0.262	0.255	0.255	0.241	0.221	0.203	0.180	0.153	0.129	0.103	0.095
0.98	0.191	0.190	0.187	0.187	0.182	0.182	0.173	0.173	0.169	0.169	0.161	0.154	0.141	0.129	0.113	0.095	0.070	0.050
1.00	0.0	0.0	0.0	0.0	0.0	0.0	0.0	0.0	0.0	0.0	0.0	0.0	0.0	0.0	0.0	0.0	0.0	0.0

Table B.4.  $(r_0/T_0) D_{\infty}(z/r_0) = (r_0/T_0) D_{\infty}^{\text{SiO}_2}(z/r_0)$  for protons. Units: dimensionless.

$z/r_0$	$T_0 =$	2	3	4	5	6	8	10	15	20	30	40	50	60	80
0.0	1.409	1.345	1.302	1.269	1.247	1.228	1.209	1.196	1.194	1.195	1.195	1.194	1.195	1.199	1.199
0.02	1.443	1.380	1.338	1.306	1.284	1.265	1.242	1.227	1.225	1.226	1.226	1.225	1.226	1.226	1.229
0.04	1.467	1.406	1.424	1.435	1.354	1.333	1.308	1.295	1.274	1.269	1.269	1.267	1.266	1.268	1.251
0.06	1.483	1.496	1.447	1.504	1.406	1.370	1.323	1.305	1.295	1.288	1.288	1.274	1.267	1.249	1.229
0.08	1.493	1.406	1.424	1.438	1.399	1.357	1.323	1.305	1.299	1.283	1.283	1.274	1.267	1.251	1.229
0.10	1.504	1.501	1.447	1.504	1.382	1.361	1.328	1.309	1.299	1.283	1.283	1.274	1.267	1.251	1.229
0.12	1.510	1.454	1.418	1.454	1.391	1.371	1.345	1.336	1.328	1.309	1.309	1.299	1.299	1.297	1.297
0.14	1.514	1.425	1.460	1.425	1.398	1.379	1.354	1.342	1.335	1.325	1.325	1.314	1.305	1.303	1.303
0.16	1.516	1.456	1.463	1.463	1.404	1.404	1.385	1.365	1.357	1.347	1.347	1.330	1.322	1.312	1.309
0.18	1.517	1.465	1.465	1.465	1.408	1.408	1.390	1.370	1.359	1.349	1.349	1.330	1.322	1.312	1.309
0.20	1.516	1.465	1.465	1.465	1.410	1.410	1.392	1.378	1.358	1.346	1.346	1.335	1.325	1.314	1.307
0.22	1.512	1.463	1.463	1.463	1.410	1.410	1.393	1.370	1.355	1.346	1.346	1.336	1.325	1.313	1.311
0.24	1.508	1.450	1.459	1.459	1.408	1.408	1.392	1.369	1.350	1.352	1.352	1.344	1.335	1.324	1.312
0.26	1.502	1.452	1.454	1.454	1.405	1.405	1.390	1.368	1.350	1.349	1.349	1.342	1.332	1.322	1.312
0.28	1.494	1.494	1.421	1.421	1.401	1.401	1.386	1.365	1.346	1.338	1.338	1.328	1.318	1.312	1.309
0.30	1.486	1.440	1.415	1.395	1.381	1.361	1.356	1.342	1.333	1.323	1.323	1.314	1.304	1.301	1.298
0.32	1.476	1.432	1.407	1.388	1.375	1.356	1.337	1.326	1.318	1.308	1.308	1.298	1.295	1.291	1.291
0.34	1.465	1.421	1.398	1.380	1.363	1.349	1.330	1.319	1.309	1.301	1.301	1.295	1.288	1.284	1.284
0.36	1.452	1.410	1.387	1.370	1.359	1.349	1.332	1.310	1.302	1.293	1.293	1.283	1.276	1.276	1.276
0.38	1.439	1.397	1.375	1.363	1.348	1.337	1.322	1.303	1.293	1.283	1.283	1.273	1.270	1.266	1.266
0.40	1.424	1.424	1.383	1.363	1.348	1.337	1.322	1.303	1.289	1.282	1.282	1.273	1.267	1.260	1.255
0.42	1.408	1.408	1.368	1.348	1.325	1.311	1.292	1.277	1.261	1.256	1.256	1.252	1.248	1.244	1.244
0.44	1.391	1.352	1.335	1.316	1.304	1.284	1.260	1.248	1.234	1.229	1.229	1.225	1.222	1.217	1.217
0.46	1.372	1.335	1.316	1.316	1.304	1.296	1.284	1.264	1.254	1.249	1.249	1.244	1.235	1.222	1.222
0.48	1.353	1.316	1.296	1.296	1.280	1.280	1.269	1.252	1.234	1.229	1.229	1.220	1.215	1.211	1.203
0.50	1.332	1.296	1.275	1.275	1.259	1.259	1.243	1.232	1.217	1.213	1.213	1.204	1.199	1.195	1.187
0.52	1.310	1.275	1.252	1.252	1.235	1.235	1.223	1.215	1.200	1.200	1.200	1.187	1.182	1.178	1.170
0.54	1.287	1.252	1.238	1.238	1.223	1.223	1.215	1.201	1.191	1.181	1.177	1.168	1.164	1.160	1.156
0.56	1.262	1.229	1.215	1.215	1.202	1.202	1.195	1.182	1.161	1.161	1.157	1.149	1.140	1.137	1.132
0.58	1.236	1.204	1.204	1.204	1.183	1.179	1.173	1.161	1.140	1.140	1.135	1.128	1.123	1.117	1.111
0.60	1.209	1.177	1.177	1.177	1.158	1.155	1.150	1.145	1.133	1.133	1.130	1.126	1.120	1.117	1.111
0.62	1.181	1.150	1.150	1.150	1.132	1.132	1.129	1.125	1.115	1.115	1.106	1.103	1.098	1.095	1.090
0.64	1.151	1.120	1.104	1.104	1.092	1.092	1.089	1.089	1.079	1.079	1.078	1.078	1.075	1.072	1.066
0.66	1.119	1.090	1.079	1.079	1.073	1.073	1.071	1.062	1.062	1.062	1.058	1.058	1.050	1.047	1.042
0.68	1.086	1.057	1.047	1.047	1.043	1.043	1.042	1.042	1.034	1.034	1.031	1.031	1.027	1.024	1.016
0.70	1.051	1.023	1.023	1.023	1.014	1.014	1.010	1.010	1.007	1.007	1.006	1.006	1.004	1.004	1.004
0.72	1.015	0.938	0.938	0.938	0.979	0.976	0.976	0.976	0.971	0.971	0.966	0.966	0.979	0.979	0.970
0.74	0.976	0.950	0.942	0.942	0.939	0.939	0.939	0.939	0.937	0.937	0.937	0.937	0.936	0.936	0.936
0.76	0.936	0.911	0.903	0.903	0.901	0.901	0.904	0.904	0.900	0.888	0.888	0.875	0.872	0.867	0.862
0.78	0.893	0.869	0.869	0.869	0.861	0.861	0.864	0.864	0.851	0.851	0.842	0.838	0.832	0.830	0.826
0.80	0.848	0.825	0.825	0.825	0.817	0.816	0.817	0.822	0.811	0.811	0.802	0.802	0.798	0.795	0.786
0.82	0.799	0.777	0.777	0.777	0.770	0.770	0.770	0.775	0.774	0.774	0.767	0.767	0.754	0.750	0.748
0.84	0.747	0.726	0.726	0.726	0.720	0.718	0.720	0.725	0.725	0.725	0.720	0.714	0.707	0.706	0.698
0.86	0.692	0.667	0.667	0.667	0.665	0.665	0.667	0.673	0.673	0.673	0.670	0.665	0.658	0.655	0.650
0.88	0.634	0.616	0.616	0.616	0.609	0.609	0.611	0.613	0.613	0.613	0.613	0.606	0.602	0.599	0.599
0.90	0.570	0.554	0.554	0.554	0.549	0.549	0.550	0.555	0.557	0.557	0.555	0.550	0.545	0.542	0.542
0.92	0.499	0.485	0.485	0.485	0.479	0.479	0.481	0.481	0.483	0.483	0.483	0.480	0.478	0.478	0.478
0.94	0.418	0.406	0.406	0.406	0.402	0.402	0.402	0.402	0.402	0.402	0.402	0.402	0.402	0.402	0.402
0.96	0.321	0.312	0.312	0.312	0.309	0.309	0.308	0.312	0.312	0.312	0.312	0.312	0.312	0.312	0.312
0.98	0.205	0.199	0.199	0.199	0.197	0.197	0.196	0.196	0.196	0.196	0.196	0.196	0.196	0.196	0.196
1.00	0.0	0.0	0.0	0.0	0.0	0.0	0.0	0.0	0.0	0.0	0.0	0.0	0.0	0.0	0.0

Table B.4.  $(r_0/T_0) D_{-\infty}^2(z/r_0) = (r_0/T_0) D_{-\infty}^2(z/r_0)$  for protons. Units: dimensionless. (Continued)

$r_0/r$	$T_0=100$	150	200	300	400	500	600	800	1000	1500	2000	3000	4000	5000
0.0	1.205	1.223	1.243	1.262	1.285	1.326	1.365	1.398	1.466	1.526	1.645	1.734	1.861	1.944
0.02	1.234	1.250	1.268	1.286	1.305	1.342	1.377	1.403	1.469	1.522	1.630	1.711	1.825	1.901
0.04	1.255	1.269	1.286	1.302	1.320	1.353	1.385	1.415	1.467	1.516	1.613	1.687	1.791	1.861
0.06	1.271	1.284	1.299	1.308	1.329	1.359	1.389	1.414	1.464	1.507	1.597	1.664	1.759	1.822
0.08	1.283	1.294	1.308	1.335	1.351	1.363	1.389	1.414	1.457	1.498	1.579	1.640	1.726	1.785
0.10	1.292	1.299	1.308	1.318	1.341	1.363	1.388	1.411	1.450	1.487	1.561	1.616	1.699	1.749
0.12	1.304	1.312	1.321	1.334	1.351	1.376	1.381	1.406	1.450	1.474	1.542	1.592	1.663	1.713
0.14	1.308	1.315	1.323	1.340	1.358	1.376	1.393	1.414	1.453	1.482	1.568	1.622	1.693	1.748
0.16	1.311	1.316	1.323	1.339	1.354	1.377	1.395	1.414	1.453	1.488	1.579	1.640	1.726	1.787
0.18	1.311	1.316	1.321	1.335	1.349	1.363	1.373	1.390	1.410	1.433	1.482	1.550	1.621	1.697
0.20	1.311	1.316	1.321	1.335	1.349	1.363	1.376	1.390	1.418	1.441	1.493	1.559	1.625	1.694
0.22	1.311	1.314	1.319	1.330	1.342	1.354	1.366	1.384	1.402	1.410	1.468	1.507	1.570	1.635
0.24	1.309	1.311	1.315	1.324	1.334	1.345	1.355	1.371	1.386	1.418	1.442	1.476	1.501	1.519
0.26	1.306	1.306	1.310	1.318	1.326	1.334	1.343	1.356	1.369	1.416	1.445	1.466	1.481	1.494
0.28	1.301	1.302	1.304	1.310	1.316	1.323	1.330	1.341	1.351	1.374	1.414	1.431	1.444	1.457
0.30	1.296	1.295	1.295	1.297	1.301	1.306	1.311	1.317	1.325	1.333	1.351	1.383	1.397	1.407
0.32	1.289	1.288	1.288	1.288	1.291	1.295	1.298	1.302	1.309	1.314	1.328	1.338	1.352	1.371
0.34	1.282	1.279	1.279	1.279	1.280	1.282	1.285	1.288	1.292	1.295	1.304	1.311	1.321	1.334
0.36	1.273	1.270	1.270	1.270	1.270	1.270	1.270	1.274	1.277	1.280	1.284	1.290	1.294	1.298
0.38	1.263	1.259	1.259	1.258	1.256	1.255	1.255	1.255	1.255	1.255	1.256	1.258	1.260	1.262
0.40	1.252	1.248	1.248	1.246	1.246	1.249	1.249	1.250	1.253	1.256	1.256	1.258	1.260	1.262
0.42	1.241	1.235	1.235	1.233	1.233	1.228	1.228	1.229	1.229	1.229	1.231	1.233	1.235	1.237
0.44	1.228	1.222	1.222	1.221	1.221	1.218	1.218	1.220	1.220	1.220	1.221	1.222	1.224	1.226
0.46	1.214	1.207	1.207	1.207	1.207	1.203	1.203	1.205	1.205	1.205	1.206	1.207	1.208	1.209
0.48	1.199	1.192	1.192	1.192	1.192	1.196	1.196	1.196	1.196	1.196	1.197	1.197	1.198	1.199
0.50	1.183	1.175	1.175	1.175	1.175	1.170	1.170	1.169	1.169	1.169	1.170	1.170	1.171	1.172
0.52	1.165	1.158	1.158	1.158	1.158	1.152	1.152	1.152	1.152	1.152	1.153	1.153	1.154	1.155
0.54	1.147	1.139	1.139	1.139	1.139	1.132	1.132	1.132	1.132	1.132	1.132	1.132	1.132	1.133
0.56	1.128	1.119	1.119	1.119	1.119	1.112	1.112	1.112	1.112	1.112	1.112	1.112	1.112	1.113
0.58	1.107	1.098	1.098	1.098	1.098	1.091	1.091	1.091	1.091	1.091	1.091	1.091	1.091	1.092
0.60	1.085	1.076	1.076	1.076	1.076	1.055	1.055	1.055	1.055	1.055	1.055	1.055	1.055	1.056
0.62	1.062	1.052	1.052	1.052	1.052	1.044	1.044	1.044	1.044	1.044	1.044	1.044	1.044	1.045
0.64	1.037	1.028	1.028	1.028	1.028	1.019	1.019	1.019	1.019	1.019	1.019	1.019	1.019	1.020
0.66	1.011	1.002	1.002	1.002	1.002	0.993	0.993	0.993	0.993	0.993	0.993	0.993	0.993	0.994
0.68	0.984	0.974	0.974	0.974	0.974	0.965	0.965	0.965	0.965	0.965	0.965	0.965	0.965	0.966
0.70	0.955	0.945	0.945	0.945	0.945	0.936	0.936	0.936	0.936	0.936	0.936	0.936	0.936	0.937
0.72	0.924	0.914	0.914	0.914	0.914	0.905	0.889	0.889	0.889	0.889	0.889	0.889	0.889	0.890
0.74	0.892	0.882	0.882	0.882	0.882	0.873	0.857	0.857	0.857	0.857	0.857	0.857	0.857	0.858
0.76	0.858	0.848	0.848	0.848	0.848	0.839	0.822	0.822	0.822	0.822	0.822	0.822	0.822	0.823
0.78	0.821	0.812	0.812	0.812	0.812	0.802	0.786	0.777	0.777	0.777	0.777	0.777	0.777	0.778
0.80	0.782	0.772	0.772	0.772	0.772	0.763	0.747	0.732	0.732	0.732	0.732	0.732	0.732	0.733
0.82	0.740	0.730	0.730	0.730	0.730	0.721	0.705	0.691	0.691	0.691	0.691	0.691	0.691	0.692
0.84	0.694	0.685	0.685	0.685	0.685	0.676	0.661	0.647	0.647	0.647	0.647	0.647	0.647	0.648
0.86	0.646	0.638	0.638	0.638	0.638	0.629	0.614	0.600	0.587	0.587	0.587	0.587	0.587	0.588
0.88	0.595	0.587	0.587	0.587	0.587	0.579	0.565	0.551	0.551	0.551	0.551	0.551	0.551	0.552
0.90	0.539	0.531	0.531	0.531	0.531	0.524	0.510	0.498	0.498	0.498	0.498	0.498	0.498	0.499
0.92	0.475	0.468	0.468	0.468	0.468	0.462	0.448	0.435	0.435	0.435	0.435	0.435	0.435	0.436
0.94	0.401	0.395	0.395	0.395	0.395	0.389	0.378	0.369	0.369	0.369	0.369	0.369	0.369	0.370
0.96	0.312	0.307	0.307	0.307	0.307	0.302	0.294	0.286	0.286	0.286	0.286	0.286	0.286	0.287
0.98	0.203	0.200	0.200	0.200	0.200	0.196	0.191	0.186	0.186	0.186	0.186	0.186	0.186	0.187
1.00	0.0	0.0	0.0	0.0	0.0	0.0	0.0	0.0	0.0	0.0	0.0	0.0	0.0	0.0

Table B.5.  $(r_0/T_0) D_{\infty}^{A\alpha}(z/r_0)$  for electrons. Units: dimensionless.

$z/r_0$	$T_0 = 0.1$	$0.2$	$0.5$	$1.0$	$2.0$	$3.0$	$5.0$	$7.0$	$10.0$
0.0	1.722	1.771	1.892	2.019	2.082	2.055	2.041	1.961	1.898
0.025	1.779	1.817	1.910	2.009	2.062	2.044	2.028	1.959	1.887
0.050	1.809	1.838	1.909	1.986	2.023	2.014	1.994	1.936	1.859
0.075	1.814	1.837	1.892	1.952	1.951	1.933	1.969	1.944	1.816
0.100	1.801	1.819	1.861	1.906	1.928	1.913	1.881	1.839	1.764
0.125	1.774	1.787	1.820	1.854	1.868	1.849	1.812	1.775	1.704
0.150	1.736	1.746	1.771	1.796	1.805	1.783	1.739	1.707	1.641
0.175	1.691	1.698	1.717	1.735	1.737	1.716	1.669	1.640	1.578
0.200	1.642	1.647	1.659	1.670	1.670	1.651	1.602	1.575	1.516
0.225	1.589	1.591	1.597	1.603	1.603	1.588	1.540	1.513	1.457
0.250	1.531	1.531	1.532	1.534	1.535	1.525	1.479	1.454	1.399
0.275	1.468	1.468	1.464	1.464	1.467	1.462	1.421	1.395	1.343
0.300	1.401	1.398	1.392	1.392	1.390	1.398	1.363	1.338	1.288
0.325	1.327	1.324	1.317	1.315	1.325	1.321	1.304	1.281	1.234
0.350	1.247	1.245	1.239	1.238	1.251	1.262	1.244	1.224	1.181
0.375	1.163	1.161	1.158	1.159	1.176	1.190	1.183	1.167	1.128
0.400	1.075	1.074	1.074	1.074	1.079	1.098	1.116	1.120	1.075
0.425	0.985	0.985	0.985	0.988	0.996	1.020	1.041	1.056	1.049
0.450	0.892	0.892	0.893	0.900	0.912	0.939	0.964	0.939	0.965
0.475	0.796	0.796	0.799	0.809	0.826	0.857	0.885	0.921	0.925
0.500	0.699	0.699	0.703	0.717	0.738	0.775	0.806	0.850	0.849
0.525	0.604	0.604	0.609	0.625	0.649	0.727	0.778	0.792	0.789
0.550	0.514	0.514	0.520	0.536	0.562	0.609	0.649	0.705	0.724
0.575	0.433	0.433	0.438	0.453	0.478	0.528	0.572	0.632	0.656
0.600	0.361	0.361	0.364	0.376	0.393	0.449	0.496	0.558	0.606
0.625	0.297	0.297	0.299	0.326	0.355	0.424	0.486	0.520	0.547
0.650	0.240	0.240	0.244	0.258	0.305	0.354	0.414	0.453	0.490
0.675	0.189	0.188	0.189	0.199	0.243	0.289	0.346	0.388	0.435
0.700	0.144	0.142	0.141	0.149	0.187	0.228	0.281	0.326	0.381
0.725	0.103	0.103	0.102	0.101	0.107	0.138	0.173	0.222	0.268
0.750	0.068	0.068	0.068	0.074	0.098	0.125	0.169	0.214	0.277
0.775	0.041	0.041	0.043	0.048	0.066	0.086	0.124	0.164	0.227
0.800	0.024	0.024	0.025	0.029	0.041	0.056	0.088	0.121	0.177
0.825	0.013	0.013	0.014	0.017	0.024	0.035	0.059	0.086	0.133
0.850	0.006	0.006	0.007	0.007	0.013	0.020	0.038	0.057	0.096
0.875	0.003	0.003	0.003	0.004	0.007	0.010	0.022	0.036	0.066
0.900	0.001	0.001	0.001	0.002	0.003	0.005	0.011	0.020	0.041
0.925	0.000	0.000	0.000	0.000	0.001	0.002	0.005	0.010	0.022
0.950	0.000	0.000	0.000	0.000	0.000	0.000	0.001	0.003	0.010
0.975	0.000	0.000	0.000	0.000	0.000	0.000	0.001	0.002	0.000
1.000	0.000	0.000	0.000	0.000	0.000	0.000	0.000	0.000	0.000

Table B.6.  $(r_0/T_0) D_{-}^{A\ell}(z/r_0)$  for electrons. Units: dimensionless.

$z/r_0$	$T_0=0.1$	$0.2$	$0.5$	$1$	$2$	$3$	$5$	$7$	$7.0$	$10.0$
0.0	1.122	1.164	1.272	1.399	1.510	1.538	1.573	1.565	1.561	1.561
0.025	1.148	1.185	1.280	1.392	1.492	1.520	1.558	1.554	1.544	1.544
0.050	1.160	1.193	1.277	1.375	1.465	1.492	1.529	1.528	1.516	1.516
0.075	1.162	1.190	1.263	1.350	1.431	1.456	1.489	1.491	1.478	1.478
0.100	1.155	1.179	1.242	1.318	1.390	1.414	1.442	1.446	1.434	1.434
0.125	1.159	1.160	1.214	1.280	1.345	1.367	1.389	1.395	1.384	1.384
0.150	1.150	1.135	1.182	1.238	1.297	1.317	1.335	1.342	1.333	1.333
0.175	1.091	1.106	1.145	1.194	1.247	1.267	1.281	1.289	1.281	1.281
0.200	1.060	1.073	1.106	1.148	1.197	1.218	1.230	1.238	1.231	1.231
0.225	1.026	1.036	1.064	1.100	1.147	1.168	1.180	1.188	1.182	1.182
0.250	0.988	0.996	1.019	1.051	1.095	1.119	1.132	1.139	1.133	1.133
0.275	0.946	0.953	0.973	1.001	1.044	1.069	1.084	1.092	1.086	1.086
0.300	0.901	0.907	0.924	0.950	0.991	1.018	1.037	1.044	1.039	1.039
0.325	0.853	0.858	0.873	0.897	0.938	0.966	0.989	0.997	0.993	0.993
0.350	0.800	0.805	0.820	0.843	0.884	0.913	0.941	0.950	0.947	0.947
0.375	0.746	0.751	0.766	0.789	0.828	0.859	0.892	0.902	0.901	0.901
0.400	0.689	0.695	0.710	0.733	0.772	0.803	0.841	0.854	0.855	0.855
0.425	0.632	0.637	0.653	0.676	0.715	0.747	0.790	0.805	0.809	0.809
0.450	0.573	0.573	0.578	0.594	0.618	0.657	0.690	0.737	0.755	0.762
0.475	0.513	0.518	0.534	0.558	0.599	0.632	0.684	0.704	0.714	0.714
0.500	0.451	0.457	0.473	0.498	0.539	0.575	0.629	0.652	0.666	0.666
0.525	0.391	0.396	0.412	0.437	0.480	0.517	0.573	0.598	0.616	0.616
0.550	0.334	0.339	0.354	0.377	0.422	0.460	0.517	0.545	0.567	0.567
0.575	0.281	0.286	0.298	0.320	0.364	0.404	0.461	0.491	0.517	0.517
0.600	0.234	0.237	0.247	0.266	0.310	0.350	0.405	0.438	0.469	0.469
0.625	0.191	0.193	0.201	0.217	0.258	0.298	0.351	0.385	0.421	0.421
0.650	0.152	0.154	0.159	0.172	0.210	0.248	0.299	0.334	0.375	0.375
0.675	0.118	0.119	0.122	0.133	0.167	0.201	0.248	0.285	0.330	0.330
0.700	0.088	0.089	0.091	0.100	0.128	0.158	0.201	0.237	0.287	0.287
0.725	0.064	0.064	0.065	0.071	0.094	0.120	0.158	0.193	0.245	0.245
0.750	0.044	0.044	0.044	0.049	0.066	0.087	0.120	0.153	0.205	0.205
0.775	0.029	0.029	0.028	0.031	0.044	0.059	0.087	0.117	0.166	0.166
0.800	0.018	0.017	0.017	0.019	0.027	0.039	0.061	0.086	0.128	0.128
0.825	0.010	0.010	0.009	0.010	0.016	0.024	0.041	0.060	0.096	0.096
0.850	0.005	0.005	0.005	0.005	0.009	0.014	0.026	0.040	0.069	0.069
0.875	0.002	0.002	0.002	0.002	0.004	0.007	0.015	0.025	0.046	0.046
0.900	0.001	0.001	0.001	0.001	0.002	0.003	0.008	0.014	0.023	0.023
0.925	0.000	0.000	0.000	0.000	0.001	0.001	0.003	0.006	0.015	0.015
0.950	0.000	0.000	0.000	0.000	0.000	0.000	0.001	0.002	0.006	0.006
0.975	0.000	0.000	0.000	0.000	0.000	0.000	0.000	0.000	0.001	0.001
1.000	0.000	0.000	0.000	0.000	0.000	0.000	0.000	0.000	0.000	0.000

Table B.7.  $(r_0/T_0) D_{\infty}^{H_2^0}(z/r_0)$  for electrons. Units: dimensionless.

$r_0/z$	$T_0=0.1$	$H_2^0$	$D_{\infty}^{H_2^0}(z/r_0)$	for electrons.	Units:	dimensionless.
0.0	2.296	2.345	2.466	2.590	2.645	2.605
0.025	2.372	2.405	2.489	2.577	2.618	2.590
0.050	2.410	2.433	2.488	2.546	2.574	2.552
0.075	2.418	2.432	2.465	2.501	2.516	2.496
0.100	2.402	2.409	2.422	2.443	2.447	2.426
0.125	2.366	2.368	2.372	2.376	2.370	2.346
0.150	2.316	2.314	2.309	2.302	2.288	2.263
0.175	2.257	2.252	2.238	2.222	2.204	2.179
0.200	2.192	2.184	2.163	2.140	2.119	2.098
0.225	2.121	2.110	2.083	2.054	2.034	2.018
0.250	2.044	2.031	1.998	1.965	1.948	1.938
0.275	1.960	1.945	1.909	1.874	1.861	1.858
0.300	1.870	1.854	1.816	1.780	1.772	1.766
0.325	1.771	1.756	1.718	1.684	1.681	1.692
0.350	1.666	1.651	1.616	1.585	1.587	1.604
0.375	1.553	1.540	1.510	1.484	1.491	1.512
0.400	1.436	1.426	1.401	1.381	1.393	1.418
0.425	1.316	1.307	1.289	1.276	1.293	1.322
0.450	1.192	1.186	1.173	1.168	1.191	1.224
0.475	1.064	1.061	1.055	1.057	1.087	1.124
0.500	0.934	0.934	0.934	0.944	0.944	0.982
0.525	0.807	0.808	0.814	0.831	0.877	0.923
0.550	0.688	0.690	0.699	0.719	0.771	0.823
0.575	0.579	0.581	0.590	0.611	0.668	0.725
0.600	0.483	0.484	0.490	0.509	0.569	0.629
0.625	0.397	0.396	0.396	0.415	0.474	0.537
0.650	0.321	0.319	0.317	0.329	0.386	0.449
0.675	0.253	0.250	0.246	0.254	0.307	0.365
0.700	0.193	0.189	0.184	0.190	0.235	0.289
0.725	0.138	0.135	0.132	0.137	0.174	0.219
0.750	0.091	0.090	0.089	0.094	0.124	0.158
0.775	0.055	0.055	0.055	0.062	0.083	0.108
0.800	0.032	0.032	0.032	0.033	0.052	0.071
0.825	0.017	0.017	0.019	0.022	0.031	0.044
0.850	0.008	0.008	0.009	0.009	0.011	0.017
0.875	0.004	0.004	0.004	0.004	0.005	0.008
0.900	0.001	0.001	0.001	0.002	0.002	0.004
0.925	0.000	0.000	0.000	0.001	0.001	0.002
0.950	0.000	0.000	0.000	0.000	0.000	0.000
0.975	0.000	0.000	0.000	0.000	0.000	0.000
1.000	0.000	0.000	0.000	0.000	0.000	0.000

Table B.8.  $(r_0/T_0) D_{-}^{H2^0}(z/r_0)$  for electrons. Units: dimensionless.

$z/r_0$	$T_0=0.1$	0.0	0.2	0.5	1.0	2.0	3.0	5.0	7.0	10.0
0.0	1.497	1.543	1.660	1.798	1.921	1.950	1.973	1.950	1.950	1.932
0.025	1.531	1.570	1.670	1.789	1.898	1.928	1.955	1.938	1.913	1.913
0.050	1.549	1.582	1.666	1.768	1.864	1.894	1.919	1.908	1.880	1.880
0.075	1.552	1.579	1.649	1.735	1.821	1.849	1.871	1.864	1.864	1.835
0.100	1.542	1.564	1.622	1.694	1.769	1.797	1.813	1.809	1.782	1.782
0.125	1.523	1.540	1.586	1.646	1.712	1.738	1.768	1.747	1.722	1.722
0.150	1.494	1.508	1.544	1.592	1.651	1.676	1.681	1.681	1.659	1.659
0.175	1.459	1.469	1.496	1.535	1.589	1.614	1.614	1.616	1.596	1.596
0.200	1.419	1.426	1.445	1.476	1.525	1.551	1.551	1.553	1.534	1.534
0.225	1.373	1.377	1.325	1.391	1.415	1.461	1.489	1.489	1.474	1.474
0.250	1.322	1.325	1.333	1.352	1.396	1.426	1.429	1.431	1.415	1.415
0.275	1.267	1.268	1.272	1.287	1.330	1.363	1.369	1.372	1.356	1.356
0.300	1.207	1.206	1.209	1.221	1.263	1.298	1.310	1.313	1.299	1.299
0.325	1.142	1.141	1.142	1.153	1.195	1.232	1.250	1.254	1.242	1.242
0.350	1.072	1.072	1.073	1.084	1.126	1.164	1.189	1.195	1.185	1.185
0.375	0.999	0.999	0.995	1.002	1.014	1.056	1.095	1.127	1.136	1.128
0.400	0.924	0.924	0.925	0.929	0.942	0.984	1.025	1.064	1.075	1.075
0.425	0.847	0.847	0.849	0.854	0.869	0.912	0.953	0.999	1.014	1.014
0.450	0.769	0.771	0.778	0.794	0.838	0.880	0.933	0.952	0.956	0.956
0.475	0.688	0.691	0.700	0.718	0.763	0.807	0.865	0.888	0.888	0.888
0.500	0.606	0.609	0.620	0.640	0.688	0.733	0.796	0.822	0.836	0.836
0.525	0.525	0.529	0.540	0.562	0.612	0.660	0.725	0.755	0.774	0.774
0.550	0.448	0.452	0.463	0.485	0.538	0.587	0.654	0.688	0.712	0.712
0.575	0.378	0.381	0.391	0.412	0.465	0.516	0.584	0.620	0.651	0.651
0.600	0.315	0.316	0.324	0.342	0.395	0.446	0.513	0.553	0.590	0.590
0.625	0.257	0.258	0.262	0.279	0.328	0.379	0.445	0.487	0.530	0.530
0.650	0.205	0.205	0.208	0.221	0.268	0.316	0.378	0.422	0.472	0.472
0.675	0.159	0.158	0.160	0.171	0.212	0.256	0.314	0.360	0.416	0.416
0.700	0.119	0.118	0.119	0.128	0.163	0.201	0.255	0.300	0.362	0.362
0.725	0.086	0.085	0.085	0.092	0.120	0.153	0.200	0.245	0.309	0.309
0.750	0.059	0.058	0.058	0.063	0.084	0.110	0.152	0.194	0.258	0.258
0.775	0.039	0.038	0.037	0.040	0.056	0.076	0.111	0.148	0.210	0.210
0.800	0.024	0.023	0.022	0.024	0.035	0.050	0.078	0.109	0.163	0.163
0.825	0.014	0.013	0.013	0.014	0.021	0.031	0.052	0.077	0.122	0.122
0.850	0.007	0.007	0.006	0.007	0.011	0.018	0.033	0.051	0.087	0.087
0.875	0.003	0.003	0.003	0.003	0.006	0.009	0.019	0.032	0.059	0.059
0.900	0.001	0.001	0.001	0.001	0.002	0.004	0.010	0.018	0.037	0.037
0.925	0.000	0.000	0.000	0.000	0.001	0.002	0.008	0.020	0.050	0.050
0.950	0.000	0.000	0.000	0.000	0.000	0.001	0.003	0.003	0.008	0.008
0.975	0.000	0.000	0.000	0.000	0.000	0.000	0.000	0.000	0.002	0.002
1.000	0.000	0.000	0.000	0.000	0.000	0.000	0.000	0.000	0.000	0.000

Table B.9.  $(r_0/T_0) D_{\infty}^{Si}(z/r_0)$  for electrons. Units: dimensionless.

$z/r_0$	$T_0=0.1$	0.2	0.5	1.0	2.0	3.0	5.0	7.0	10.0
0.0	1.761	1.808	1.921	2.031	2.047	1.969	1.857	1.680	1.474
0.025	1.818	1.854	1.942	2.029	2.047	1.989	1.897	1.752	1.570
0.050	1.847	1.875	1.944	2.012	2.029	1.985	1.907	1.788	1.628
0.075	1.852	1.874	1.928	1.982	1.996	1.960	1.891	1.796	1.654
0.100	1.839	1.856	1.898	1.941	1.951	1.920	1.856	1.779	1.655
0.125	1.811	1.825	1.858	1.891	1.897	1.868	1.807	1.746	1.635
0.150	1.772	1.783	1.809	1.834	1.837	1.809	1.749	1.700	1.601
0.175	1.727	1.735	1.754	1.773	1.773	1.748	1.689	1.648	1.560
0.200	1.677	1.682	1.695	1.708	1.708	1.686	1.629	1.593	1.515
0.225	1.622	1.625	1.633	1.641	1.641	1.624	1.569	1.537	1.467
0.250	1.563	1.564	1.567	1.570	1.572	1.561	1.510	1.480	1.416
0.275	1.499	1.498	1.497	1.497	1.502	1.496	1.451	1.421	1.364
0.300	1.430	1.428	1.424	1.422	1.430	1.430	1.391	1.363	1.311
0.325	1.355	1.352	1.347	1.345	1.356	1.361	1.331	1.305	1.258
0.350	1.273	1.271	1.271	1.267	1.267	1.280	1.290	1.270	1.205
0.375	1.187	1.186	1.184	1.186	1.186	1.203	1.217	1.208	1.151
0.400	1.098	1.097	1.098	1.098	1.104	1.124	1.141	1.144	1.107
0.425	1.005	1.006	1.010	1.010	1.019	1.043	1.064	1.072	1.042
0.450	0.910	0.912	0.919	0.933	0.961	0.985	1.012	1.011	0.986
0.475	0.812	0.816	0.827	0.844	0.877	0.905	0.942	0.947	0.928
0.500	0.713	0.718	0.732	0.754	0.792	0.825	0.871	0.881	0.869
0.525	0.616	0.622	0.638	0.664	0.707	0.743	0.797	0.813	0.809
0.550	0.525	0.530	0.548	0.574	0.623	0.663	0.722	0.743	0.747
0.575	0.442	0.447	0.462	0.488	0.539	0.584	0.646	0.672	0.686
0.600	0.368	0.372	0.384	0.407	0.458	0.507	0.571	0.602	0.625
0.625	0.303	0.304	0.312	0.331	0.382	0.432	0.496	0.532	0.565
0.650	0.245	0.245	0.248	0.263	0.311	0.361	0.423	0.464	0.506
0.675	0.193	0.192	0.192	0.203	0.247	0.294	0.353	0.397	0.449
0.700	0.147	0.145	0.144	0.151	0.189	0.232	0.287	0.334	0.394
0.725	0.105	0.104	0.103	0.109	0.140	0.175	0.226	0.274	0.340
0.750	0.069	0.069	0.069	0.075	0.098	0.126	0.172	0.219	0.286
0.775	0.042	0.042	0.043	0.048	0.065	0.086	0.126	0.168	0.234
0.800	0.024	0.024	0.026	0.029	0.041	0.056	0.089	0.124	0.183
0.825	0.013	0.013	0.014	0.016	0.024	0.034	0.059	0.088	0.139
0.850	0.006	0.006	0.007	0.008	0.013	0.019	0.038	0.059	0.101
0.875	0.003	0.003	0.003	0.004	0.006	0.010	0.022	0.037	0.069
0.900	0.001	0.001	0.001	0.001	0.002	0.004	0.011	0.021	0.044
0.925	0.000	0.000	0.000	0.000	0.001	0.001	0.005	0.010	0.024
0.950	0.000	0.000	0.000	0.000	0.000	0.000	0.003	0.010	0.022
0.975	0.000	0.000	0.000	0.000	0.000	0.000	0.000	0.001	0.000
1.000	0.000	0.000	0.000	0.000	0.000	0.000	0.000	0.000	0.000

Table B.10.  $(r_0/T_0) D_{-}^{Si}(z/r_0)$  for electrons. Units: dimensionless.

$z/r_0$	$T_0=0.1$	0.2	0.5	1.0	2.0	3.0	5.0	7.0	10.0
0.0	1.149	1.191	1.299	1.423	1.522	1.533	1.529	1.478	1.438
0.025	1.173	1.211	1.305	1.413	1.496	1.504	1.500	1.454	1.391
0.050	1.186	1.218	1.300	1.394	1.467	1.473	1.469	1.429	1.356
0.075	1.187	1.215	1.215	1.368	1.433	1.440	1.436	1.402	1.329
0.100	1.179	1.203	1.203	1.337	1.396	1.404	1.400	1.374	1.307
0.125	1.164	1.184	1.238	1.301	1.356	1.366	1.363	1.343	1.287
0.150	1.142	1.159	1.205	1.260	1.313	1.326	1.324	1.310	1.266
0.175	1.115	1.129	1.169	1.217	1.268	1.283	1.284	1.275	1.242
0.200	1.083	1.096	1.129	1.172	1.221	1.239	1.241	1.236	1.213
0.225	1.048	1.059	1.087	1.125	1.172	1.192	1.198	1.196	1.180
0.250	1.009	1.018	1.042	1.076	1.121	1.143	1.152	1.154	1.142
0.275	0.966	0.974	0.995	1.025	1.068	1.093	1.106	1.110	1.101
0.300	0.920	0.927	0.945	0.973	1.015	1.041	1.058	1.064	1.058
0.325	0.871	0.876	0.893	0.919	0.960	0.987	1.009	1.017	1.013
0.350	0.817	0.823	0.839	0.864	0.904	0.932	0.960	0.969	0.966
0.375	0.762	0.767	0.783	0.807	0.847	0.876	0.909	0.919	0.918
0.400	0.704	0.710	0.726	0.750	0.789	0.820	0.857	0.869	0.869
0.425	0.645	0.651	0.667	0.691	0.730	0.762	0.805	0.818	0.821
0.450	0.585	0.591	0.607	0.631	0.671	0.703	0.751	0.767	0.771
0.475	0.524	0.529	0.545	0.570	0.610	0.645	0.696	0.715	0.722
0.500	0.461	0.467	0.483	0.508	0.550	0.586	0.640	0.662	0.674
0.525	0.399	0.405	0.421	0.446	0.489	0.527	0.584	0.609	0.625
0.550	0.341	0.346	0.361	0.385	0.430	0.469	0.527	0.555	0.577
0.575	0.287	0.291	0.304	0.327	0.372	0.412	0.470	0.502	0.530
0.600	0.239	0.242	0.252	0.272	0.316	0.356	0.414	0.448	0.482
0.625	0.195	0.197	0.205	0.221	0.263	0.303	0.358	0.395	0.435
0.650	0.155	0.157	0.162	0.176	0.214	0.252	0.304	0.342	0.388
0.675	0.120	0.121	0.125	0.136	0.169	0.204	0.252	0.291	0.341
0.700	0.090	0.090	0.093	0.101	0.130	0.160	0.204	0.242	0.296
0.725	0.065	0.065	0.066	0.072	0.095	0.120	0.160	0.196	0.252
0.750	0.045	0.044	0.045	0.049	0.066	0.086	0.120	0.154	0.209
0.775	0.029	0.029	0.028	0.030	0.043	0.058	0.087	0.117	0.169
0.800	0.018	0.017	0.017	0.018	0.026	0.037	0.060	0.086	0.131
0.825	0.010	0.010	0.009	0.010	0.015	0.022	0.040	0.061	0.098
0.850	0.005	0.005	0.005	0.005	0.008	0.012	0.025	0.041	0.071
0.875	0.003	0.002	0.002	0.002	0.003	0.006	0.014	0.025	0.048
0.900	0.001	0.001	0.001	0.001	0.001	0.003	0.007	0.014	0.030
0.925	0.000	0.000	0.000	0.000	0.000	0.001	0.003	0.007	0.016
0.950	0.000	0.000	0.000	0.000	0.000	0.001	0.002	0.007	0.011
0.975	0.000	0.000	0.000	0.000	0.000	0.000	0.000	0.000	0.000
1.000	0.000	0.000	0.000	0.000	0.000	0.000	0.000	0.000	0.000

Table B.11.  $(r_0/T_0) D_{\frac{SiO_2}{\infty}}(z/r_0)$  for electrons. Units: dimensionless.

$z/r_0$	$T_0=0.1$	0.2	0.5	1.0	2.0	3.0	5.0	7.0	10.0
0.0	1.833	1.880	1.992	2.102	2.130	2.069	1.993	1.855	1.704
0.025	1.893	1.928	2.012	2.097	2.121	2.076	2.011	1.894	1.757
0.050	1.923	1.949	2.013	2.077	2.096	2.060	2.001	1.905	1.779
0.075	1.929	1.949	2.013	2.044	2.056	2.026	1.970	1.890	1.775
0.100	1.915	1.930	2.013	2.000	2.006	1.978	1.922	1.857	1.752
0.125	1.886	1.897	1.923	1.948	1.948	1.920	1.863	1.810	1.713
0.150	1.846	1.854	1.872	1.889	1.884	1.856	1.798	1.754	1.666
0.175	1.799	1.803	1.815	1.825	1.818	1.791	1.732	1.695	1.614
0.200	1.747	1.749	1.754	1.758	1.750	1.727	1.668	1.635	1.561
0.225	1.690	1.690	1.690	1.689	1.681	1.663	1.606	1.575	1.508
0.250	1.628	1.626	1.621	1.616	1.611	1.593	1.539	1.484	1.455
0.275	1.562	1.558	1.549	1.541	1.539	1.533	1.465	1.424	1.347
0.300	1.490	1.485	1.474	1.464	1.466	1.465	1.395	1.363	1.293
0.325	1.411	1.406	1.394	1.385	1.391	1.395	1.323	1.301	1.238
0.350	1.327	1.322	1.311	1.304	1.313	1.313	1.248	1.237	1.183
0.375	1.237	1.233	1.225	1.222	1.234	1.234	1.171	1.172	1.127
0.400	1.144	1.141	1.137	1.137	1.154	1.154	1.092	1.106	1.060
0.425	1.047	1.046	1.046	1.050	1.071	1.071	1.012	1.037	1.070
0.450	0.948	0.949	0.952	0.961	0.987	0.987	0.92	1.016	1.012
0.475	0.847	0.849	0.856	0.870	0.901	0.930	0.930	0.966	0.953
0.500	0.743	0.747	0.758	0.777	0.814	0.847	0.847	0.892	0.892
0.525	0.642	0.647	0.661	0.684	0.727	0.764	0.741	0.833	0.830
0.550	0.547	0.552	0.567	0.592	0.640	0.682	0.741	0.762	0.768
0.575	0.461	0.465	0.479	0.504	0.554	0.601	0.664	0.691	0.705
0.600	0.384	0.387	0.398	0.420	0.472	0.522	0.587	0.619	0.643
0.625	0.316	0.317	0.324	0.342	0.394	0.445	0.511	0.548	0.582
0.650	0.255	0.255	0.258	0.272	0.321	0.372	0.436	0.478	0.523
0.675	0.201	0.200	0.200	0.210	0.255	0.304	0.364	0.416	0.465
0.700	0.153	0.151	0.149	0.157	0.196	0.240	0.297	0.346	0.408
0.725	0.109	0.108	0.107	0.113	0.145	0.182	0.234	0.285	0.353
0.750	0.072	0.072	0.072	0.078	0.103	0.132	0.179	0.228	0.299
0.775	0.044	0.044	0.045	0.050	0.069	0.090	0.132	0.177	0.245
0.800	0.025	0.026	0.027	0.031	0.043	0.059	0.094	0.131	0.193
0.825	0.014	0.014	0.015	0.017	0.026	0.037	0.064	0.094	0.148
0.850	0.007	0.007	0.008	0.009	0.014	0.021	0.041	0.064	0.108
0.875	0.003	0.003	0.003	0.004	0.007	0.011	0.024	0.040	0.075
0.900	0.001	0.001	0.001	0.002	0.003	0.005	0.013	0.023	0.048
0.925	0.000	0.000	0.000	0.000	0.001	0.002	0.006	0.011	0.027
0.950	0.000	0.000	0.000	0.000	0.000	0.002	0.004	0.012	0.033
0.975	0.000	0.000	0.000	0.000	0.000	0.000	0.000	0.001	0.000
1.000	0.000	0.000	0.000	0.000	0.000	0.000	0.000	0.000	0.000

Table B.12.  $(r_0/T_0) D_{-} \text{SiO}_2(z/r_0)$  for electrons. Units: dimensionless.

$z/r_0$	$T_0=0.1$	0.0	0.2	0.5	1.0	2.0	3.0	5.0	7.0	10.0
0.0	1.195	1.237	1.342	1.464	1.566	1.583	1.595	1.564	1.525	1.493
0.025	1.221	1.258	1.350	1.456	1.542	1.556	1.566	1.537	1.493	1.462
0.050	1.234	1.266	1.346	1.439	1.513	1.524	1.533	1.508	1.462	1.432
0.075	1.236	1.263	1.333	1.413	1.478	1.489	1.497	1.476	1.441	1.401
0.100	1.228	1.251	1.311	1.380	1.439	1.451	1.458	1.441	1.405	1.368
0.125	1.212	1.232	1.282	1.342	1.396	1.410	1.415	1.405	1.371	1.334
0.150	1.189	1.206	1.248	1.300	1.350	1.366	1.371	1.365	1.323	1.298
0.175	1.161	1.175	1.210	1.254	1.303	1.320	1.325	1.323	1.279	1.259
0.200	1.129	1.140	1.169	1.207	1.253	1.272	1.278	1.279	1.233	1.218
0.225	1.092	1.101	1.125	1.158	1.202	1.223	1.230	1.230	1.185	1.175
0.250	1.052	1.059	1.079	1.108	1.149	1.172	1.181	1.181	1.137	1.130
0.275	1.007	1.013	1.030	1.055	1.095	1.119	1.131	1.131	1.088	1.085
0.300	0.959	0.964	0.979	1.001	1.040	1.066	1.081	1.081	1.039	1.038
0.325	0.907	0.912	0.925	0.946	0.984	1.011	1.031	1.031	0.990	0.991
0.350	0.852	0.856	0.869	0.890	0.927	0.955	0.981	0.981	0.930	0.943
0.375	0.794	0.798	0.811	0.832	0.869	0.898	0.930	0.930	0.878	0.891
0.400	0.734	0.738	0.752	0.773	0.811	0.841	0.878	0.878	0.825	0.840
0.425	0.673	0.677	0.691	0.713	0.751	0.782	0.825	0.825	0.771	0.796
0.450	0.610	0.615	0.629	0.651	0.690	0.723	0.771	0.771	0.737	0.747
0.475	0.546	0.551	0.566	0.583	0.628	0.664	0.716	0.716	0.659	0.697
0.500	0.481	0.486	0.501	0.524	0.567	0.603	0.659	0.659	0.601	0.647
0.525	0.416	0.422	0.437	0.461	0.504	0.543	0.601	0.601	0.553	0.597
0.550	0.355	0.360	0.374	0.398	0.443	0.484	0.543	0.543	0.517	0.547
0.575	0.300	0.304	0.316	0.338	0.383	0.425	0.484	0.484	0.426	0.462
0.600	0.249	0.252	0.262	0.281	0.325	0.368	0.426	0.426	0.369	0.449
0.625	0.204	0.205	0.212	0.229	0.271	0.313	0.371	0.371	0.314	0.353
0.650	0.162	0.163	0.168	0.182	0.221	0.260	0.321	0.321	0.261	0.301
0.675	0.126	0.126	0.129	0.142	0.175	0.211	0.271	0.271	0.212	0.252
0.700	0.094	0.094	0.096	0.105	0.134	0.166	0.212	0.212	0.167	0.206
0.725	0.068	0.068	0.069	0.075	0.099	0.126	0.171	0.171	0.127	0.163
0.750	0.047	0.046	0.047	0.051	0.069	0.091	0.141	0.141	0.093	0.126
0.775	0.031	0.030	0.030	0.032	0.046	0.062	0.093	0.093	0.065	0.141
0.800	0.019	0.018	0.018	0.019	0.028	0.041	0.064	0.064	0.044	0.066
0.825	0.011	0.010	0.010	0.011	0.017	0.025	0.044	0.044	0.028	0.045
0.850	0.006	0.005	0.005	0.005	0.005	0.009	0.014	0.014	0.016	0.028
0.875	0.003	0.002	0.002	0.002	0.002	0.004	0.007	0.007	0.008	0.016
0.900	0.001	0.001	0.001	0.001	0.001	0.002	0.003	0.003	0.004	0.018
0.925	0.000	0.000	0.000	0.000	0.000	0.001	0.001	0.001	0.001	0.008
0.950	0.000	0.000	0.000	0.000	0.000	0.000	0.000	0.000	0.000	0.002
0.975	0.000	0.000	0.000	0.000	0.000	0.000	0.000	0.000	0.000	0.000
1.000	0.000	0.000	0.000	0.000	0.000	0.000	0.000	0.000	0.000	0.000

Table B.13.  $(1/T_0) \bar{\alpha}^{A\&}(z/T_0)$  for bremsstrahlung.

$z/T_0$	$T_0 = 0.02$	0.05	0.10	0.20	0.50	1.00	2.00	5.00	10.00	20.00
$(g/cm^2/\text{MeV})$										
1.0E-03	5.74E-02	1.71E-02	8.39E-03	3.55E-03	2.20E-03	1.63E-03	1.39E-03	1.61E-03	1.90E-03	1.90E-03
1.5E-03	5.89E-02	1.78E-02	8.75E-03	3.71E-03	2.27E-03	1.64E-03	1.43E-03	1.63E-03	1.93E-03	1.93E-03
2.0E-03	5.99E-02	1.84E-02	9.04E-03	3.83E-03	2.33E-03	1.73E-03	1.47E-03	1.64E-03	1.98E-03	1.98E-03
3.0E-03	6.14E-02	1.93E-02	9.49E-03	4.05E-03	2.43E-03	1.80E-03	1.51E-03	1.66E-03	2.09E-03	2.09E-03
4.0E-03	6.25E-02	3.76E-02	2.01E-02	9.96E-03	4.21E-03	2.51E-03	1.85E-03	1.58E-03	2.10E-03	2.10E-03
5.0E-03	6.45E-02	4.08E-02	2.08E-02	1.02E-02	4.36E-03	2.58E-03	1.89E-03	1.62E-03	2.11E-03	2.11E-03
6.0E-03	6.70E-02	4.34E-02	2.13E-02	1.05E-02	4.47E-03	2.64E-03	1.93E-03	1.66E-03	2.12E-03	2.12E-03
8.0E-03	7.12E-02	4.73E-02	2.23E-02	1.09E-02	4.67E-03	2.74E-03	2.00E-03	1.73E-03	2.18E-03	2.18E-03
1.0E-02	7.32E-02	4.95E-02	2.28E-02	1.13E-02	4.81E-03	2.83E-03	2.05E-03	1.78E-03	2.12E-03	2.27E-03
1.5E-02	6.95E-02	5.04E-02	2.37E-02	1.17E-02	5.05E-03	3.00E-03	2.15E-03	1.90E-03	2.22E-03	2.57E-03
2.0E-02	6.05E-02	4.78E-02	2.42E-02	1.20E-02	5.20E-03	3.12E-03	2.22E-03	2.00E-03	2.31E-03	2.85E-03
3.0E-02	4.44E-02	3.94E-02	2.44E-02	1.24E-02	5.38E-03	3.26E-03	2.32E-03	2.17E-03	2.53E-03	3.28E-03
4.0E-02	3.36E-02	3.14E-02	2.41E-02	1.28E-02	5.46E-03	3.33E-03	2.39E-03	2.30E-03	2.74E-03	3.61E-03
5.0E-02	2.64E-02	2.53E-02	2.28E-02	1.29E-02	5.50E-03	3.36E-03	2.44E-03	2.39E-03	2.92E-03	3.86E-03
6.0E-02	2.15E-02	2.07E-02	2.10E-02	1.27E-02	5.51E-03	3.38E-03	2.47E-03	2.47E-03	3.07E-03	4.08E-03
8.0E-02	1.54E-02	1.47E-02	1.60E-02	1.15E-02	5.49E-03	3.39E-03	2.53E-03	2.59E-03	3.28E-03	4.42E-03
1.0E-01	1.20E-02	1.11E-02	1.17E-02	9.68E-03	5.39E-03	3.41E-03	2.57E-03	2.68E-03	3.40E-03	4.68E-03
1.5E-01	7.44E-03	6.62E-03	5.97E-03	6.00E-03	4.58E-03	3.24E-03	2.59E-03	2.79E-03	3.55E-03	5.04E-03
2.0E-01	5.29E-03	4.64E-03	3.87E-03	3.90E-03	3.45E-03	2.45E-03	2.44E-03	2.77E-03	3.64E-03	5.15E-03
3.0E-01	3.30E-03	2.87E-03	2.10E-03	2.33E-03	2.04E-03	1.91E-03	1.85E-03	1.89E-03	2.54E-03	4.98E-03
4.0E-01	2.39E-03	2.187E-03	1.66E-03	1.35E-03	1.35E-03	1.24E-03	1.27E-03	1.45E-03	2.20E-03	4.56E-03
5.0E-01	1.87E-03	1.53E-03	1.38E-03	1.13E-03	8.85E-04	9.26E-04	9.51E-04	1.18E-03	1.93E-03	4.05E-03
6.0E-01	1.53E-03	1.38E-03	1.13E-03	8.85E-04	7.53E-04	6.79E-04	6.10E-03	1.75E-03	2.60E-03	3.60E-03
8.0E-01	1.11E-03	1.03E-03	8.58E-04	7.03E-04	5.69E-04	6.13E-04	8.29E-04	1.51E-03	2.19E-03	2.93E-03
1.0E+00	8.45E-04	8.21E-04	6.96E-04	5.92E-04	5.92E-04	5.74E-04	5.44E-04	7.49E-04	1.36E-03	2.43E-03
1.5E+00	5.06E-04	5.50E-04	4.77E-04	4.17E-04	4.57E-04	4.57E-04	6.26E-04	6.26E-04	1.07E-03	1.43E-03
2.0E+00	3.35E-04	4.07E-04	3.62E-04	3.20E-04	2.95E-04	3.51E-04	5.37E-04	8.80E-04	1.09E-03	1.52E-03
3.0E+00	1.77E-04	2.57E-04	2.42E-04	2.16E-04	2.20E-04	2.73E-04	4.13E-04	6.25E-04	6.31E-04	
4.0E+00	1.10E-04	1.83E-04	1.79E-04	1.64E-04	1.77E-04	2.27E-04	3.30E-04	4.49E-04		
5.0E+00	7.58E-05	1.40E-04	1.42E-04	1.32E-04	1.49E-04	1.49E-04	2.72E-04	3.19E-04		
6.0E+00	5.55E-05	1.11E-04	1.17E-04	1.11E-04	1.29E-04	1.29E-04	1.69E-04	2.30E-04		
8.0E+00	3.22E-05	7.85E-05	8.55E-05	8.38E-05	1.03E-04	1.30E-04	1.65E-04	1.95E-04		
1.0E+01	1.98E-05	5.98E-05	6.68E-05	6.76E-05	8.59E-05	1.05E-04	1.19E-04			
1.5E+01	6.67E-06	3.53E-05	4.23E-05	4.53E-05	4.96E-05	5.96E-05	6.54E-05			
2.0E+01	2.64E-06	2.28E-05	2.99E-05	3.36E-05	3.36E-05	4.33E-05	4.04E-05			
3.0E+01	5.92E-07	1.27E-05	1.73E-05	2.11E-05	2.11E-05	2.35E-05	1.37E-05			
4.0E+01	2.01E-07	5.97E-06	1.10E-05	1.43E-05	1.43E-05	1.30E-05	1.30E-05			
5.0E+01	9.35E-08	3.88E-06	7.50E-06	1.01E-05	7.22E-06					
6.0E+01	5.44E-08	2.74E-06	5.29E-06	7.26E-06						
8.0E+01	3.00E-08	1.43E-06	2.86E-06	3.92E-06						
1.0E+02	1.66E-08	6.75E-07	1.15E-06	2.20E-06						
1.5E+02	3.75E-09	8.77E-08	5.44E-07	5.81E-07						
2.0E+02	8.53E-10	4.34E-08	2.15E-07							
3.0E+02	4.35E-11	2.34E-08								
4.0E+02	2.23E-12	1.48E-09								
5.0E+02	1.15E-13	9.34E-11								
6.0E+02	5.87E-15									
8.0E+02	4.05E-20									
1.0E+03	1.43E-26									

Table B.14.  $(1/T_0) D_{-}^{A\alpha}(z/T_0)$  for bremsstrahlung. Units:  $\text{cm}^2/\text{g} \cdot$ 

$z/T_0$ ( $\text{g}/\text{cm}^2/\text{MeV}$ )	$T_0=0.02$	$0.05$	$0.10$	$0.20$	$0.50$	$1.00$	$2.00$	$5.00$	$10.00$	$20.00$
1.0E-03	7.67E-03	3.64E-03	1.97E-03	1.16E-03	5.29E-04	4.09E-04	1.33E-04	3.00E-04	1.73E-04	2.57E-04
1.5E-03	9.92E-03	5.23E-03	2.62E-03	1.50E-03	6.71E-04	5.00E-04	1.73E-04	3.60E-04	1.42E-04	4.14E-04
2.0E-03	1.19E-02	6.53E-03	3.18E-03	1.80E-03	7.97E-04	5.66E-04	4.07E-04	2.08E-04	1.84E-04	5.34E-04
3.0E-03	1.53E-02	8.61E-03	4.15E-03	2.30E-03	1.01E-03	6.65E-04	4.75E-04	2.68E-04	2.61E-04	6.72E-04
4.0E-03	1.81E-02	1.03E-02	5.75E-03	2.73E-03	1.18E-03	7.43E-04	5.28E-04	3.21E-04	3.41E-04	7.30E-04
5.0E-03	2.16E-02	1.17E-02	5.75E-03	2.73E-03	1.32E-03	8.08E-04	5.69E-04	3.69E-04	4.28E-04	7.54E-04
6.0E-03	2.52E-02	1.30E-02	6.45E-03	3.38E-03	1.45E-03	8.67E-04	6.06E-04	4.15E-04	5.18E-04	7.70E-04
8.0E-03	3.20E-02	1.53E-02	7.65E-03	3.89E-03	1.66E-03	9.74E-04	6.68E-04	4.99E-04	6.69E-04	8.13E-04
1.0E-02	3.76E-02	1.73E-02	8.64E-03	4.30E-03	1.82E-03	1.07E-03	7.22E-04	5.78E-04	7.82E-04	8.94E-04
1.5E-02	4.41E-02	2.11E-02	1.04E-02	5.03E-03	2.13E-03	1.26E-03	8.39E-04	7.48E-04	9.60E-04	1.22E-03
2.0E-02	4.37E-02	2.38E-02	1.44E-02	5.52E-03	2.34E-03	1.41E-03	9.42E-04	8.85E-04	1.09E-03	1.58E-03
3.0E-02	3.71E-02	2.57E-02	1.28E-02	6.21E-03	2.62E-03	1.63E-03	1.10E-03	1.35E-03	2.12E-03	2.12E-03
4.0E-02	3.03E-02	2.48E-02	1.38E-02	6.77E-03	2.80E-03	1.75E-03	1.26E-03	1.26E-03	1.60E-03	2.49E-03
5.0E-02	2.50E-02	2.25E-02	1.41E-02	7.18E-03	2.95E-03	1.85E-03	1.36E-03	1.39E-03	1.81E-03	2.80E-03
6.0E-02	2.10E-02	1.97E-02	1.38E-02	7.39E-03	3.05E-03	1.92E-03	1.44E-03	1.50E-03	1.99E-03	3.07E-03
8.0E-02	1.54E-02	1.42E-02	1.19E-02	6.72E-03	2.33E-03	2.04E-03	1.55E-03	1.69E-03	2.28E-03	3.54E-03
1.0E-01	1.20E-02	1.04E-02	9.57E-03	6.67E-03	2.33E-03	2.13E-03	1.64E-03	1.83E-03	2.49E-03	3.88E-03
1.5E-01	7.44E-03	5.93E-03	5.67E-03	4.86E-03	3.15E-03	2.19E-03	1.78E-03	2.06E-03	2.80E-03	4.32E-03
2.0E-01	5.29E-03	4.24E-03	3.84E-03	3.47E-03	2.60E-03	2.02E-03	1.77E-03	2.15E-03	2.97E-03	4.50E-03
3.0E-01	3.29E-03	2.81E-03	2.29E-03	1.96E-03	1.64E-03	1.50E-03	1.49E-03	2.09E-03	3.02E-03	4.49E-03
4.0E-01	2.37E-03	2.10E-03	1.65E-03	1.33E-03	1.12E-03	1.10E-03	1.21E-03	1.87E-03	2.80E-03	4.14E-03
5.0E-01	1.85E-03	1.66E-03	1.32E-03	1.03E-03	8.54E-04	8.33E-04	8.33E-04	9.90E-04	1.66E-03	3.71E-03
6.0E-01	1.52E-03	1.33E-03	1.10E-03	8.61E-04	6.91E-04	6.70E-04	8.48E-04	1.49E-03	2.29E-03	3.31E-03
8.0E-01	1.10E-03	1.03E-03	8.45E-04	6.69E-04	5.12E-04	5.18E-04	6.38E-04	1.28E-03	1.95E-03	2.71E-03
1.0E+00	8.45E-04	8.21E-04	6.84E-04	5.54E-04	4.18E-04	4.49E-04	6.16E-04	1.15E-03	1.70E-03	2.26E-03
1.5E+00	5.06E-04	5.36E-04	4.59E-04	3.83E-04	3.04E-04	3.42E-04	5.05E-04	9.16E-04	1.27E-03	1.49E-03
2.0E+00	3.35E-04	3.92E-04	3.42E-04	2.90E-04	2.46E-04	2.82E-04	4.29E-04	7.52E-04	9.85E-04	6.09E-04
3.0E+00	1.76E-05	2.49E-04	2.24E-04	1.93E-04	1.79E-04	2.16E-04	3.32E-04	5.34E-04	5.34E-04	6.09E-04
4.0E+00	1.09E-04	1.78E-04	1.65E-04	1.43E-04	1.41E-04	1.76E-04	2.67E-04	3.90E-04	4.94E-05	4.41E-05
5.0E+00	7.52E-05	1.36E-04	1.30E-04	1.14E-04	1.18E-04	1.51E-04	2.21E-04	3.06E-05	3.06E-05	4.41E-05
6.0E+00	5.50E-05	1.09E-04	1.07E-04	9.40E-05	1.02E-04	1.31E-04	1.84E-04	1.24E-05	1.73E-05	2.87E-04
8.0E+00	3.21E-05	7.65E-05	7.83E-05	7.00E-05	7.97E-05	9.00E-05	1.03E-04	1.32E-04	1.32E-04	1.32E-04
1.0E+01	1.98E-05	5.80E-05	6.9E-05	5.96E-05	7.09E-05	8.05E-05	9.56E-05	8.22E-05	9.56E-05	9.56E-05
1.5E+01	6.67E-06	3.90E-05	3.76E-05	3.63E-05	3.63E-05	4.45E-05	4.94E-05	4.94E-05	4.94E-05	4.94E-05
2.0E+01	2.64E-06	2.17E-05	2.59E-05	2.65E-05	3.20E-05	3.06E-05	3.27E-06	3.27E-06	3.27E-06	3.27E-06
3.0E+01	5.92E-07	1.01E-05	1.45E-05	1.64E-05	1.73E-05	1.73E-05	1.73E-05	1.73E-05	1.73E-05	1.73E-05
4.0E+01	2.01E-07	5.76E-06	9.20E-06	1.10E-05	9.70E-06	9.70E-06	9.70E-06	9.70E-06	9.70E-06	9.70E-06
5.0E+01	3.55E-08	3.77E-06	6.25E-06	7.74E-06	6.57E-05	7.74E-05	7.74E-05	7.74E-05	7.74E-05	7.74E-05
6.0E+01	5.44E-08	2.68E-06	4.43E-06	5.56E-06	4.45E-05	5.56E-05	5.56E-05	5.56E-05	5.56E-05	5.56E-05
8.0E+01	3.00E-08	1.37E-06	2.44E-06	3.01E-06	3.01E-06	4.50E-07	4.50E-07	4.50E-07	4.50E-07	4.50E-07
1.0E+02	1.66E-08	6.27E-07	1.43E-06	1.69E-06	1.69E-06	2.41E-07	2.41E-07	2.41E-07	2.41E-07	2.41E-07
1.5E+02	3.75E-09	8.37E-08	4.43E-07	4.43E-07	4.43E-07	8.37E-08	8.37E-08	8.37E-08	8.37E-08	8.37E-08
2.0E+02	5.33E-10	4.30E-08	1.55E-07	1.55E-07	1.55E-07	4.30E-08	4.30E-08	4.30E-08	4.30E-08	4.30E-08
3.0E+02	4.35E-11	2.23E-12	1.48E-09	1.34E-09	1.34E-09	2.23E-12	2.23E-12	2.23E-12	2.23E-12	2.23E-12
4.0E+02	4.00E-12	1.15E-13	9.34E-11	9.34E-11	9.34E-11	4.00E-12	4.00E-12	4.00E-12	4.00E-12	4.00E-12
5.0E+02	4.00E-12	1.15E-13	9.34E-11	9.34E-11	9.34E-11	4.00E-12	4.00E-12	4.00E-12	4.00E-12	4.00E-12
6.0E+02	5.87E-15	1.54E-17	8.0E+02	8.0E+02	8.0E+02	5.87E-15	5.87E-15	5.87E-15	5.87E-15	5.87E-15
8.0E+02	1.54E-17	4.05E-20	1.0E+03	1.0E+03	1.0E+03	1.54E-17	1.54E-17	1.54E-17	1.54E-17	1.54E-17
1.0E+03	4.43E-20	1.43E-26	1.5E+03	1.5E+03	1.5E+03	4.43E-20	4.43E-20	4.43E-20	4.43E-20	4.43E-20

Table B.15.  $(1/T_0) D_{\infty}^2(z/T_0)$  for bremsstrahlung. Units:  $\text{cm}^2/\text{g}$ .

$z/T_0$	$T_0 = 0.02$	$0.05$	$0.10$	$0.20$	$0.50$	$1.00$	$2.00$	$5.00$	$10.00$	$20.00$
$(\text{g}/\text{cm}^2/\text{MeV})$										
$1.0E-03$	$1.33E-02$	$6.66E-03$	$3.74E-03$	$1.80E-03$	$4.47E-04$	$6.59E-04$	$8.09E-04$	$1.11E-04$	$1.50E-03$	$1.85E-03$
$1.5E-03$	$1.37E-02$	$6.92E-03$	$3.88E-03$	$1.88E-03$	$4.78E-04$	$6.76E-04$	$8.25E-04$	$1.12E-04$	$1.53E-03$	$1.95E-03$
$2.0E-03$	$1.40E-02$	$6.97E-03$	$4.02E-03$	$1.95E-03$	$4.90E-04$	$6.90E-04$	$8.37E-04$	$1.14E-04$	$1.54E-03$	$1.96E-03$
$3.0E-03$	$1.44E-02$	$7.69E-03$	$4.43E-03$	$2.13E-03$	$5.05E-03$	$7.13E-04$	$8.71E-04$	$1.18E-04$	$1.56E-03$	$2.04E-03$
$4.0E-03$	$1.48E-02$	$8.54E-03$	$4.58E-03$	$2.21E-03$	$5.24E-03$	$7.32E-04$	$8.91E-04$	$1.21E-04$	$1.62E-03$	$2.06E-03$
$5.0E-03$	$1.53E-02$	$9.34E-03$	$4.71E-03$	$2.27E-03$	$5.42E-03$	$7.50E-04$	$8.84E-04$	$1.24E-04$	$1.64E-03$	$2.08E-03$
$6.0E-03$	$1.59E-02$	$9.97E-03$	$4.71E-03$	$2.27E-03$	$5.42E-03$	$7.64E-04$	$8.96E-04$	$1.27E-04$	$1.79E-03$	$2.11E-03$
$8.0E-03$	$1.70E-02$	$1.09E-02$	$4.90E-03$	$2.36E-03$	$5.86E-03$	$7.90E-04$	$9.16E-04$	$1.32E-04$	$1.93E-03$	$2.18E-03$
$1.0E-02$	$1.75E-02$	$1.15E-02$	$5.05E-03$	$2.43E-03$	$6.01E-03$	$8.11E-04$	$9.33E-04$	$1.37E-04$	$2.00E-03$	$2.27E-03$
$1.5E-02$	$1.66E-02$	$1.17E-02$	$5.24E-03$	$2.53E-03$	$6.16E-03$	$8.55E-04$	$9.70E-04$	$1.47E-04$	$2.08E-03$	$2.53E-03$
$2.0E-02$	$1.44E-02$	$1.10E-02$	$5.32E-03$	$2.58E-03$	$6.20E-03$	$8.89E-04$	$9.90E-04$	$1.55E-03$	$1.66E-03$	$2.78E-03$
$3.0E-02$	$1.04E-02$	$8.90E-03$	$5.35E-03$	$2.66E-03$	$6.24E-03$	$9.35E-04$	$1.05E-03$	$1.69E-03$	$2.38E-03$	$3.21E-03$
$4.0E-02$	$7.77E-03$	$7.01E-03$	$5.28E-03$	$2.74E-03$	$6.26E-03$	$9.61E-04$	$1.09E-03$	$1.80E-03$	$2.60E-03$	$3.57E-03$
$5.0E-02$	$6.03E-03$	$5.55E-03$	$5.00E-03$	$2.76E-03$	$6.27E-03$	$9.76E-04$	$1.13E-03$	$1.89E-03$	$2.76E-03$	$3.85E-03$
$6.0E-02$	$4.85E-03$	$4.49E-03$	$4.55E-03$	$2.72E-03$	$6.16E-03$	$9.80E-04$	$1.15E-03$	$1.96E-03$	$2.90E-03$	$4.07E-03$
$8.0E-02$	$3.42E-03$	$3.11E-03$	$3.41E-03$	$2.43E-03$	$5.25E-03$	$9.90E-04$	$1.19E-03$	$2.08E-03$	$3.11E-03$	$4.41E-03$
$1.0E-01$	$2.61E-03$	$2.31E-03$	$2.44E-03$	$2.03E-03$	$5.03E-03$	$1.00E-03$	$1.21E-03$	$2.17E-03$	$3.25E-03$	$4.66E-03$
$1.5E-01$	$1.57E-03$	$1.33E-03$	$1.20E-03$	$1.22E-03$	$1.05E-03$	$9.64E-04$	$1.24E-03$	$2.28E-03$	$3.45E-03$	$5.05E-03$
$2.0E-01$	$1.10E-03$	$9.08E-04$	$7.46E-04$	$7.83E-04$	$8.18E-04$	$8.73E-04$	$1.20E-03$	$2.28E-03$	$3.52E-03$	$5.19E-03$
$3.0E-01$	$6.70E-04$	$5.47E-04$	$4.31E-04$	$4.11E-04$	$5.02E-04$	$6.65E-04$	$1.06E-03$	$2.17E-03$	$3.47E-03$	$5.04E-03$
$4.0E-01$	$4.78E-04$	$3.93E-04$	$3.12E-04$	$2.75E-04$	$3.56E-04$	$5.28E-04$	$9.24E-04$	$2.01E-03$	$3.24E-03$	$4.63E-03$
$5.0E-01$	$3.70E-04$	$3.09E-04$	$2.49E-04$	$2.16E-04$	$2.87E-04$	$4.47E-04$	$8.24E-04$	$1.86E-03$	$2.95E-03$	$4.18E-03$
$6.0E-01$	$2.99E-04$	$2.54E-04$	$2.11E-04$	$1.84E-04$	$2.48E-04$	$3.98E-04$	$7.59E-04$	$1.73E-03$	$2.70E-03$	$3.76E-03$
$8.0E-01$	$2.13E-04$	$1.88E-04$	$1.49E-04$	$1.63E-04$	$2.05E-04$	$3.49E-04$	$6.74E-04$	$1.52E-03$	$2.30E-03$	$3.05E-03$
$1.0E+00$	$1.62E-04$	$1.49E-04$	$1.33E-04$	$1.30E-04$	$1.82E-04$	$3.21E-04$	$6.24E-04$	$1.36E-03$	$2.02E-03$	$2.50E-03$
$1.5E+00$	$9.51E-05$	$8.88E-05$	$9.13E-05$	$9.68E-05$	$9.51E-04$	$2.71E-04$	$5.38E-04$	$1.09E-03$	$1.50E-03$	$1.63E-03$
$2.0E+00$	$6.26E-05$	$7.28E-05$	$6.96E-05$	$7.80E-05$	$1.33E-04$	$2.37E-04$	$4.72E-04$	$9.00E-04$	$1.15E-03$	$1.86E-04$
$3.0E+00$	$3.26E-05$	$4.58E-05$	$4.74E-05$	$5.69E-05$	$1.08E-04$	$1.95E-04$	$3.70E-04$	$6.40E-04$	$6.86E-04$	$6.86E-04$
$4.0E+00$	$2.01E-05$	$3.25E-05$	$3.60E-05$	$4.54E-05$	$2.05E-04$	$3.49E-04$	$6.74E-04$	$1.52E-03$	$2.30E-03$	$3.05E-03$
$5.0E+00$	$1.38E-05$	$2.47E-05$	$2.91E-05$	$3.84E-05$	$8.22E-05$	$1.46E-04$	$2.49E-04$	$6.24E-04$	$1.36E-03$	$2.02E-03$
$6.0E+00$	$1.01E-05$	$1.98E-05$	$2.43E-05$	$3.35E-05$	$7.39E-05$	$1.27E-04$	$2.11E-04$	$5.38E-04$	$1.09E-03$	$1.50E-03$
$8.0E+00$	$5.82E-06$	$1.40E-05$	$1.83E-05$	$2.72E-05$	$6.17E-05$	$1.00E-04$	$2.37E-04$	$4.72E-04$	$9.00E-04$	$1.15E-03$
$1.0E+01$	$3.56E-06$	$1.06E-05$	$1.46E-05$	$2.30E-05$	$5.29E-05$	$8.16E-05$	$1.72E-04$	$3.70E-04$	$6.40E-04$	$6.86E-04$
$1.5E+01$	$1.20E-06$	$6.32E-06$	$9.57E-06$	$1.69E-05$	$3.80E-05$	$5.29E-05$	$8.16E-05$	$1.66E-04$	$3.00E-04$	$4.63E-04$
$2.0E+01$	$4.71E-07$	$4.09E-06$	$6.97E-06$	$1.33E-05$	$2.81E-05$	$5.22E-05$	$8.16E-05$	$1.53E-04$	$2.30E-04$	$3.36E-04$
$3.0E+01$	$1.05E-07$	$1.94E-06$	$4.26E-06$	$8.82E-06$	$1.56E-05$	$3.00E-05$	$6.17E-05$	$1.00E-04$	$2.02E-04$	$3.00E-04$
$4.0E+01$	$3.55E-08$	$1.09E-06$	$2.86E-06$	$6.16E-06$	$8.85E-06$	$1.66E-05$	$3.00E-05$	$6.40E-04$	$1.15E-04$	$1.74E-05$
$6.0E+01$	$9.59E-09$	$5.05E-07$	$1.48E-06$	$3.23E-06$	$5.09E-06$	$8.63E-06$	$2.97E-06$	$5.09E-06$	$6.63E-06$	$8.00E-06$
$8.0E+01$	$5.28E-09$	$2.67E-07$	$8.42E-07$	$1.80E-06$	$3.23E-06$	$5.09E-06$	$8.63E-06$	$5.09E-06$	$6.63E-06$	$8.00E-06$
$1.0E+02$	$2.90E-09$	$1.28E-07$	$5.10E-07$	$1.05E-06$	$2.90E-06$	$5.09E-06$	$8.63E-06$	$5.09E-06$	$6.63E-06$	$8.00E-06$
$1.5E+02$	$6.54E-10$	$1.72E-08$	$1.70E-07$	$3.19E-07$	$6.63E-08$	$8.63E-07$	$1.44E-07$	$2.44E-08$	$3.23E-07$	$4.00E-07$
$2.0E+02$	$3.0E+02$	$7.42E-12$	$4.41E-09$	$9.49E-09$	$8.49E-06$	$2.97E-06$	$5.09E-06$	$6.63E-06$	$8.00E-06$	$8.00E-06$
$4.0E+02$	$4.0E+02$	$3.75E-13$	$2.73E-10$	$4.41E-09$	$4.41E-09$	$2.97E-06$	$5.09E-06$	$6.63E-06$	$8.00E-06$	$8.00E-06$
$5.0E+02$	$5.0E+02$	$1.89E-14$	$1.69E-11$	$1.69E-11$	$1.69E-11$	$2.97E-06$	$5.09E-06$	$6.63E-06$	$8.00E-06$	$8.00E-06$
$6.0E+02$	$6.0E+02$	$9.59E-16$	$2.44E-18$	$2.44E-18$	$2.44E-18$	$2.97E-06$	$5.09E-06$	$6.63E-06$	$8.00E-06$	$8.00E-06$
$8.0E+02$	$8.0E+02$	$1.0E+03$	$2.05E-27$	$2.05E-27$	$2.05E-27$	$2.97E-06$	$5.09E-06$	$6.63E-06$	$8.00E-06$	$8.00E-06$

Table B.16.  $(1/T_0) D_{-}^2(z/T_0)$  for bremsstrahlung. Units:  $\text{cm}^2/\text{g.}$

$z/T_0$ ( $\text{g}/\text{cm}^2/\text{MeV.}$ )	$T_0=0.02$	$0.05$	$0.10$	$0.20$	$0.50$	$1.00$	$2.00$	$5.00$	$10.00$	$20.00$
1.0E-03	1.87E-03	6.67E-04	4.69E-04	2.74E-04	1.24E-04	9.62E-04	1.56E-04	1.18E-04	7.52E-05	2.63E-05
1.5E-03	2.39E-03	1.25E-03	6.24E-04	3.53E-04	1.56E-04	1.18E-04	1.34E-04	1.34E-04	9.27E-05	3.85E-04
2.0E-03	2.86E-03	1.56E-03	7.53E-04	4.19E-04	1.83E-04	1.83E-04	2.30E-04	1.30E-04	8.82E-05	4.92E-04
3.0E-03	3.67E-03	2.04E-03	9.75E-04	5.30E-04	2.30E-04	1.59E-04	1.34E-04	1.24E-04	1.27E-04	6.17E-04
4.0E-03	4.32E-03	2.42E-03	1.32E-03	6.21E-04	2.69E-04	1.77E-04	1.48E-04	1.48E-04	1.97E-04	6.79E-04
5.0E-03	5.13E-03	2.76E-03	1.33E-03	6.98E-04	3.01E-04	1.95E-04	1.64E-04	1.64E-04	1.93E-04	6.62E-04
6.0E-03	5.99E-03	3.05E-03	1.49E-03	7.65E-04	3.29E-04	2.10E-04	1.78E-04	2.27E-04	4.47E-04	7.32E-04
8.0E-03	7.63E-03	3.56E-03	1.76E-03	8.75E-04	3.76E-04	2.38E-04	2.05E-04	2.92E-04	6.00E-04	7.88E-04
1.0E-02	8.94E-03	4.00E-03	1.97E-03	9.59E-04	4.14E-04	2.64E-04	2.29E-04	3.55E-04	7.09E-04	8.73E-04
1.5E-02	1.05E-02	4.88E-03	2.35E-03	1.12E-03	4.84E-04	3.19E-04	4.84E-04	4.84E-04	7.22E-04	1.19E-03
2.0E-02	1.03E-02	4.45E-03	2.56E-03	1.21E-03	5.33E-04	3.66E-04	3.37E-04	6.15E-04	9.74E-04	1.54E-04
3.0E-02	8.69E-03	5.83E-03	2.83E-03	1.35E-03	5.98E-04	4.35E-04	6.35E-04	8.02E-04	1.25E-03	2.07E-03
4.0E-02	6.99E-03	5.56E-03	3.02E-03	1.46E-03	6.41E-04	4.84E-04	5.17E-04	9.48E-04	1.49E-03	2.45E-03
5.0E-02	5.70E-03	4.98E-03	3.07E-03	1.54E-03	6.73E-04	5.17E-04	5.81E-04	1.07E-03	1.72E-03	2.76E-03
6.0E-02	4.72E-03	4.28E-03	2.97E-03	1.58E-03	6.99E-04	5.45E-04	6.32E-04	1.17E-03	1.90E-03	3.04E-03
8.0E-02	3.42E-03	3.01E-03	2.50E-03	1.53E-03	7.36E-04	5.86E-04	6.21E-04	7.68E-04	1.34E-03	2.19E-03
1.0E-01	2.61E-03	2.15E-03	1.97E-03	1.38E-03	7.57E-04	6.27E-04	6.64E-04	8.64E-04	1.49E-03	2.41E-03
1.5E-01	1.57E-03	1.17E-03	1.11E-03	9.87E-04	7.27E-04	6.64E-04	6.48E-04	9.04E-04	1.74E-03	2.77E-03
2.0E-01	1.10E-03	8.22E-04	7.35E-04	6.93E-04	6.20E-04	6.48E-04	6.48E-04	9.04E-04	1.86E-03	2.96E-03
3.0E-01	6.67E-04	5.34E-04	4.29E-04	3.90E-04	4.26E-04	5.43E-04	5.43E-04	8.81E-04	1.85E-03	3.05E-03
4.0E-01	4.72E-04	3.93E-04	3.06E-04	2.66E-04	3.18E-04	4.51E-04	4.51E-04	7.91E-04	1.74E-03	2.19E-03
5.0E-01	3.65E-04	3.09E-04	2.44E-04	2.09E-04	2.59E-04	3.86E-04	3.86E-04	6.50E-04	1.62E-03	2.66E-03
6.0E-01	2.96E-04	2.54E-04	2.05E-04	1.78E-04	2.23E-04	3.42E-04	3.42E-04	6.50E-04	1.50E-03	2.43E-03
8.0E-01	2.12E-04	1.88E-04	1.57E-04	1.42E-04	1.80E-04	2.95E-04	5.80E-04	5.80E-04	1.50E-03	2.43E-03
1.0E+00	1.62E-04	1.49E-04	1.28E-04	1.20E-04	1.57E-04	2.69E-04	5.35E-04	5.35E-04	1.20E-03	1.83E-03
1.5E+00	9.51E-05	9.61E-05	8.66E-05	8.78E-05	1.28E-04	2.26E-04	4.54E-04	4.54E-04	9.61E-04	1.37E-03
2.0E+00	6.26E-05	7.00E-05	6.52E-05	6.94E-05	1.11E-04	1.99E-04	3.96E-04	3.96E-04	7.93E-04	1.06E-03
3.0E+00	3.25E-05	4.42E-05	4.36E-05	4.99E-05	9.00E-05	1.62E-04	3.12E-04	3.12E-04	5.66E-04	6.66E-04
4.0E+00	1.99E-05	3.16E-05	3.28E-05	3.97E-05	7.67E-05	1.37E-04	2.54E-04	2.54E-04	4.15E-04	5.09E-04
5.0E+00	1.37E-05	2.42E-05	2.65E-05	3.33E-05	6.74E-05	1.20E-04	2.12E-04	2.12E-04	3.09E-04	1.58E-03
6.0E+00	1.00E-05	1.94E-05	2.23E-05	2.89E-05	6.04E-05	1.05E-04	1.79E-04	1.79E-04	2.23E-05	1.15E-05
8.0E+00	5.79E-06	1.36E-05	1.67E-05	2.30E-05	5.01E-05	8.39E-05	1.30E-04	1.30E-04	8.39E-05	1.30E-04
1.0E+01	3.55E-06	1.03E-05	1.34E-05	1.93E-05	3.04E-05	4.23E-05	6.83E-05	6.83E-05	9.46E-05	9.46E-05
1.5E+01	1.19E-06	6.06E-06	8.61E-06	1.38E-05	2.65E-06	4.16E-05	5.53E-06	5.53E-06	7.16E-06	7.16E-06
2.0E+01	4.71E-07	3.90E-06	6.13E-06	1.07E-05	2.23E-05	4.16E-05	7.27E-07	1.49E-06	2.53E-06	2.53E-06
3.0E+01	1.05E-07	1.85E-06	3.62E-06	7.09E-06	1.25E-05	2.41E-05	4.41E-06	4.41E-06	8.74E-07	8.74E-07
4.0E+01	3.55E-08	1.06E-06	2.40E-06	4.98E-06	8.60E-06	1.69E-06	3.60E-06	3.60E-06	5.16E-07	5.16E-07
5.0E+01	9.59E-09	4.95E-07	1.25E-06	2.65E-06	5.65E-06	1.49E-06	2.42E-06	2.42E-06	1.69E-11	1.69E-11
8.0E+01	5.28E-09	2.55E-07	7.27E-07	1.49E-06	2.73E-13	2.73E-13	4.41E-09	4.41E-09	2.05E-27	2.05E-27
1.0E+02	2.90E-09	1.19E-07	4.45E-07	8.41E-09	1.65E-08	1.45E-07	2.42E-08	2.42E-08	9.59E-16	9.59E-16
1.5E+02	6.54E-10	1.47E-10	8.41E-09	5.16E-08	1.41E-09	5.16E-08	2.43E-09	2.43E-09	2.44E-18	2.44E-18
2.0E+02	1.47E-10	8.41E-09	4.41E-09	2.42E-08	6.23E-21	6.23E-21	1.0E+03	1.0E+03	1.5E+03	1.5E+03

Table B.17.  $(1/\tau_0) D_{\infty}^{Si}(z/\tau_0)$  for bremsstrahlung. Units:  $\text{cm}^2/\text{g}$ .

$z/\tau_0$	$T_0 = 0.02$	$0.05$	$0.10$	$0.20$	$0.50$	$1.00$	$2.00$	$5.00$	$10.00$	$20.00$
$(\text{g}/\text{cm}^2/\text{MeV})$										
1.0E-03	7.15E-02	2.17E-02	1.07E-02	4.54E-03	2.77E-03	1.99E-03	1.58E-03	1.76E-03	2.05E-03	2.05E-03
1.5E-03	7.33E-02	2.25E-02	1.12E-02	4.73E-03	2.87E-03	2.06E-03	1.63E-03	1.78E-03	2.20E-03	2.20E-03
2.0E-03	7.46E-02	2.33E-02	1.16E-02	4.90E-03	2.95E-03	2.11E-03	1.67E-03	1.79E-03	2.26E-03	2.26E-03
3.0E-03	7.65E-02	4.27E-02	1.21E-02	5.17E-03	3.07E-03	2.20E-03	1.74E-03	1.81E-03	2.28E-03	2.28E-03
4.0E-03	7.78E-02	4.72E-02	2.55E-02	5.39E-03	3.18E-03	2.26E-03	1.80E-03	1.88E-03	2.27E-03	2.27E-03
5.0E-03	8.02E-02	5.12E-02	2.63E-02	5.57E-03	3.26E-03	2.32E-03	1.86E-03	1.98E-03	2.27E-03	2.27E-03
6.0E-03	8.36E-02	5.45E-02	2.70E-02	5.74E-03	3.34E-03	2.37E-03	1.90E-03	2.07E-03	2.28E-03	2.28E-03
8.0E-03	8.86E-02	5.92E-02	2.81E-02	5.95E-03	3.48E-03	2.45E-03	1.98E-03	2.22E-03	2.34E-03	2.34E-03
1.0E-02	9.10E-02	6.19E-02	2.89E-02	1.44E-02	6.13E-03	3.59E-03	2.50E-03	2.04E-03	2.31E-03	2.44E-03
1.5E-02	8.61E-02	6.30E-02	3.05E-02	1.49E-02	6.45E-03	3.80E-03	2.42E-03	2.42E-03	2.77E-03	2.77E-03
2.0E-02	7.53E-02	5.98E-02	3.08E-02	1.53E-02	6.65E-03	3.95E-03	2.72E-03	2.29E-03	2.53E-03	3.07E-03
3.0E-02	5.54E-02	4.95E-02	3.08E-02	1.59E-02	6.87E-03	4.14E-03	2.85E-03	2.47E-03	2.77E-03	3.54E-03
4.0E-02	4.20E-02	3.96E-02	3.05E-02	1.63E-02	6.99E-03	4.22E-03	2.93E-03	2.62E-03	2.99E-03	3.88E-03
5.0E-02	3.31E-02	3.20E-02	2.91E-02	1.64E-02	7.04E-03	4.26E-03	2.99E-03	2.73E-03	3.18E-03	4.15E-03
6.0E-02	2.70E-02	2.63E-02	2.66E-02	1.63E-02	7.06E-03	4.28E-03	3.03E-03	2.82E-03	3.34E-03	4.38E-03
8.0E-02	1.95E-02	1.87E-02	2.03E-02	1.47E-02	7.04E-03	4.31E-03	3.10E-03	2.95E-03	3.58E-03	4.76E-03
1.0E-01	1.52E-02	1.42E-02	1.49E-02	1.24E-02	6.90E-03	4.33E-03	3.15E-03	3.04E-03	3.71E-03	5.03E-03
1.5E-01	9.51E-03	8.53E-03	7.72E-03	7.74E-03	5.88E-03	4.13E-03	3.8E-03	3.15E-03	3.85E-03	5.40E-03
2.0E-01	6.77E-03	6.00E-03	5.03E-03	5.05E-03	4.43E-03	3.55E-03	2.97E-03	3.12E-03	3.95E-03	5.51E-03
3.0E-01	4.25E-03	3.74E-03	3.05E-03	2.66E-03	2.46E-03	2.33E-03	2.27E-03	2.84E-03	3.82E-03	5.32E-03
4.0E-01	3.09E-03	2.71E-03	2.30E-03	1.77E-03	1.58E-03	1.59E-03	1.59E-03	1.71E-03	2.43E-03	4.86E-03
5.0E-01	2.42E-03	2.15E-03	1.77E-03	1.37E-03	1.18E-03	1.18E-03	1.37E-03	1.37E-03	2.12E-03	4.31E-03
6.0E-01	1.98E-03	1.79E-03	1.48E-03	1.16E-03	9.58E-04	9.39E-04	1.16E-03	1.90E-03	2.76E-03	3.83E-03
8.0E-01	1.43E-03	1.34E-03	1.12E-03	9.17E-04	7.20E-04	7.41E-04	9.42E-04	1.63E-03	2.33E-03	3.12E-03
1.0E+00	1.10E-03	1.08E-03	9.12E-04	7.71E-04	5.98E-04	6.54E-04	8.48E-04	1.46E-03	2.04E-03	2.59E-03
1.5E+00	6.58E-04	7.26E-04	6.25E-04	5.43E-04	4.46E-04	5.02E-04	7.03E-04	1.15E-03	1.53E-03	1.61E-03
2.0E+00	4.37E-04	5.33E-04	4.75E-04	4.15E-04	3.66E-04	4.13E-04	6.00E-04	9.46E-04	1.16E-03	1.64E-04
3.0E+00	2.30E-04	3.37E-04	3.17E-04	2.80E-04	2.70E-04	3.18E-04	4.59E-04	6.71E-04	7.71E-04	8.0E-04
4.0E+00	1.43E-04	2.40E-04	2.36E-04	2.11E-04	2.15E-04	2.64E-04	3.65E-04	4.80E-04	5.13E-05	5.39E-04
5.0E+00	9.92E-05	1.83E-04	1.86E-04	1.70E-04	1.70E-04	1.80E-04	2.25E-04	3.02E-04	3.02E-04	3.02E-04
6.0E+00	7.26E-05	1.47E-04	1.53E-04	1.42E-04	1.56E-04	1.94E-04	2.53E-04	2.53E-04	2.53E-04	2.53E-04
8.0E+00	4.21E-05	1.03E-04	1.12E-04	1.07E-04	1.24E-04	1.50E-04	1.50E-04	1.83E-04	1.83E-04	1.83E-04
1.0E+01	2.58E-05	7.85E-05	8.75E-05	8.62E-05	1.03E-04	1.21E-04	1.21E-04	1.31E-04	1.31E-04	1.31E-04
1.5E+01	8.69E-06	6.65E-05	5.53E-05	5.75E-05	7.10E-05	7.48E-05	7.48E-05	7.48E-05	7.48E-05	7.48E-05
2.0E+01	3.45E-06	2.99E-05	3.90E-05	4.25E-05						
3.0E+01	7.74E-07	1.40E-05	2.25E-05							
4.0E+01	2.62E-07	7.87E-06	1.44E-05							
5.0E+01	1.22E-07	5.11E-06	9.75E-05	5.75E-05	7.10E-05	7.10E-05	7.10E-05	7.10E-05	7.10E-05	7.10E-05
6.0E+01	7.12E-08	3.60E-06	6.86E-06	9.05E-06	1.26E-05	8.46E-06	8.46E-06	8.46E-06	8.46E-06	8.46E-06
8.0E+01	3.93E-08	1.89E-06	3.70E-06	4.05E-06	5.05E-06	4.73E-06	4.73E-06	4.73E-06	4.73E-06	4.73E-06
1.0E+02	2.16E-08	8.90E-07	2.16E-06	4.87E-06	6.00E-06	4.87E-06	4.87E-06	4.87E-06	4.87E-06	4.87E-06
1.5E+02	4.90E-09	1.16E-07	7.00E-07							
2.0E+02	1.1E-09	5.72E-08	3.10E-08							
3.0E+02	5.67E-11	5.67E-11	5.67E-11	5.67E-11	5.67E-11	5.67E-11	5.67E-11	5.67E-11	5.67E-11	5.67E-11
4.0E+02	2.90E-12	1.95E-09								
5.0E+02	4.48E-13	1.48E-10								
6.0E+02	7.61E-15	1.99E-11								
8.0E+02	1.99E-17	1.99E-12								
1.0E+03	1.83E-20	5.22E-20								

Table B.18.  $(1/T_0) D_{-}^{31}(z/T_0)$  for bremsstrahlung. Units:  $\text{cm}^2/\text{g.}$ 

$z/T_0$ ( $\text{g}/\text{cm}^2/\text{MeV}$ )	$T_0=0.02$	$0.05$	$0.10$	$0.20$	$0.50$	$1.00$	$2.00$	$5.00$	$10.00$	$20.00$
1.0E-03	9.51E-03	6.56E-03	3.27E-03	1.88E-03	8.42E-03	3.77E-04	1.65E-04	1.14E-04	2.82E-04	
1.5E-03	1.23E-02	8.19E-03	3.97E-03	2.26E-03	9.98E-04	7.14E-04	5.53E-04	2.14E-04	4.57E-04	
2.0E-03	1.48E-02	1.08E-02	5.17E-03	2.90E-03	8.40E-04	5.12E-04	5.12E-04	2.56E-04	2.12E-04	
3.0E-03	1.90E-02	1.25E-02	6.24E-03	3.42E-03	1.49E-03	9.39E-04	6.63E-04	3.27E-04	2.97E-04	
4.0E-03	2.68E-02	1.46E-02	7.19E-03	3.87E-03	1.67E-03	1.02E-03	7.16E-04	4.46E-04	4.79E-04	
5.0E-03	3.13E-02	1.62E-02	8.07E-03	4.26E-03	1.83E-03	1.10E-03	7.61E-04	4.98E-04	5.72E-04	
6.0E-03	3.98E-02	1.90E-02	9.57E-03	5.41E-03	2.10E-03	1.23E-03	8.39E-04	5.96E-04	7.37E-04	
8.0E-03	4.66E-02	2.15E-02	1.09E-02	6.35E-03	2.31E-03	1.35E-03	9.06E-04	6.84E-04	8.60E-04	
1.0E-02	5.48E-02	2.65E-02	1.31E-02	7.71E-03	1.61E-03	1.05E-03	1.05E-03	8.75E-04	1.05E-03	
2.0E-02	5.44E-02	3.00E-02	1.44E-02	6.99E-03	2.98E-03	1.79E-03	1.18E-03	1.03E-03	1.20E-03	
3.0E-02	4.63E-02	3.23E-02	1.62E-02	7.90E-03	3.34E-03	2.06E-03	1.40E-03	1.26E-03	1.48E-03	
4.0E-02	3.80E-02	3.10E-02	1.75E-02	8.61E-03	3.58E-03	2.33E-03	1.55E-03	1.44E-03	1.75E-03	
5.0E-02	3.14E-02	2.79E-02	1.79E-02	9.15E-03	3.76E-03	2.35E-03	1.67E-03	1.59E-03	1.97E-03	
6.0E-02	2.64E-02	2.45E-02	1.76E-02	9.40E-03	3.91E-03	2.44E-03	1.77E-03	1.71E-03	2.17E-03	
8.0E-02	1.95E-02	1.81E-02	1.52E-02	9.30E-03	4.14E-03	2.59E-03	1.90E-03	1.91E-03	2.48E-03	
1.0E-01	1.52E-02	1.34E-02	1.22E-02	8.55E-03	4.27E-03	2.70E-03	2.01E-03	2.01E-03	2.70E-03	
1.5E-01	9.51E-03	7.81E-03	7.33E-03	6.27E-03	4.04E-03	2.76E-03	2.18E-03	2.31E-03	3.02E-03	
2.0E-01	6.77E-03	5.54E-03	4.98E-03	4.50E-03	3.34E-03	2.56E-03	2.16E-03	2.41E-03	3.19E-03	
3.0E-01	4.23E-03	3.60E-03	2.98E-03	2.57E-03	2.10E-03	1.88E-03	1.78E-03	2.32E-03	3.23E-03	
4.0E-01	3.06E-03	2.71E-03	2.15E-03	1.74E-03	1.45E-03	1.36E-03	1.36E-03	2.05E-03	2.99E-03	
5.0E-01	2.39E-03	2.15E-03	1.72E-03	1.34E-03	1.09E-03	1.03E-03	1.15E-03	1.80E-03	2.68E-03	
6.0E-01	1.96E-03	1.79E-03	1.44E-03	1.13E-03	8.81E-04	8.19E-04	9.72E-04	1.61E-03	2.42E-03	
8.0E-01	1.43E-03	1.34E-03	1.10E-03	8.73E-04	6.49E-04	6.26E-04	7.77E-04	1.37E-03	2.05E-03	
1.0E+00	1.10E-03	1.08E-03	8.95E-04	7.21E-04	5.27E-04	5.38E-04	6.91E-04	1.23E-03	1.79E-03	
1.5E+00	6.58E-04	7.07E-04	6.01E-04	4.97E-04	3.80E-04	4.04E-04	5.60E-04	9.75E-04	1.34E-03	
2.0E+00	4.37E-04	5.15E-04	4.48E-04	3.76E-04	3.05E-04	3.29E-04	4.73E-04	8.00E-04	1.04E-03	
3.0E+00	2.30E-04	3.26E-04	2.93E-04	2.49E-04	2.19E-04	2.49E-04	3.64E-04	5.67E-04	6.39E-04	
4.0E+00	1.43E-04	2.33E-04	2.16E-04	1.85E-04	1.72E-04	2.03E-04	2.92E-04	4.13E-04	4.13E-04	
5.0E+00	9.84E-05	7.78E-04	1.70E-04	1.47E-04	1.42E-04	1.72E-04	2.42E-04	3.04E-04	3.04E-04	
6.0E+00	7.20E-05	1.43E-04	1.40E-04	1.21E-04	1.22E-04	1.50E-04	2.01E-04	2.50E-04	2.50E-04	
8.0E+00	4.20E-05	1.01E-04	1.02E-04	8.97E-05	9.51E-05	1.17E-04	1.44E-04	1.44E-04	1.44E-04	
1.0E+01	2.57E-05	7.63E-05	7.98E-05	7.09E-05	7.80E-05	9.32E-05	1.04E-04	1.04E-04	1.04E-04	
1.5E+01	8.69E-06	4.47E-05	4.92E-05	4.60E-05	5.25E-05	5.56E-05	4.73E-05	4.73E-05	4.73E-05	
2.0E+01	3.45E-06	2.86E-05	3.39E-05	3.35E-05	3.74E-05	3.42E-05	3.42E-05	3.42E-05	3.42E-05	
3.0E+01	7.74E-07	1.33E-05	1.90E-04	1.22E-04	1.50E-04	1.72E-04	2.01E-04	2.38E-05	2.03E-05	
4.0E+01	2.62E-07	7.57E-06	1.20E-05	1.37E-05	1.37E-05	1.37E-05	1.37E-05	1.37E-05	1.37E-05	
5.0E+01	1.22E-07	4.98E-06	8.11E-06	9.59E-06	9.59E-06	9.59E-06	9.59E-06	9.59E-06	9.59E-06	
6.0E+01	7.12E-08	3.53E-06	5.75E-06	6.90E-06	3.77E-06	3.77E-06	3.77E-06	3.77E-06	3.77E-06	
8.0E+01	3.93E-08	1.81E-06	3.15E-06	3.71E-06	3.71E-06	3.71E-06	3.71E-06	3.71E-06	3.71E-06	
1.0E+02	2.16E-08	8.28E-07	1.28E-07	1.84E-06	2.08E-06	2.08E-06	2.08E-06	2.08E-06	2.08E-06	
1.5E+02	4.90E-09	1.10E-07	5.68E-07							
2.0E+02	7.61E-15	1.11E-09	5.67E-08	5.00E-07	2.00E-07	2.00E-07	2.00E-07	2.00E-07	2.00E-07	
3.0E+02	1.99E-17	1.99E-17	5.67E-11	3.10E-08	1.22E-08	1.22E-08	1.22E-08	1.22E-08	1.22E-08	
4.0E+02	5.22E-20	1.05E-09	5.67E-12	1.95E-09	1.23E-10	1.23E-10	1.23E-10	1.23E-10	1.23E-10	
5.0E+02	1.83E-26	1.83E-03	5.67E-12	1.95E-09	1.23E-10	1.23E-10	1.23E-10	1.23E-10	1.23E-10	

Table B.19.  $(1/T_0) D_{\infty}^{SiO_2}(z/T_0)$  for prestrahlung. Units:  $\text{cm}^2/\text{g.}$

$\frac{\omega}{\omega_0} / \text{eV}^2 / \text{MeV}$	$T_0 = 0.02$	$0.05$	$0.10$	$0.20$	$0.50$	$1.00$	$2.00$	$5.00$	$10.00$	$20.00$
$1.0E+03$	$1.0E+03$	$1.5E+03$	$2.0E+03$	$3.0E+03$	$4.0E+03$	$6.0E+03$	$1.0E+04$	$1.6E+04$	$2.6E+04$	$4.0E+04$
$1.5E+03$	$1.5E+03$	$2.3E+03$	$3.5E+03$	$5.0E+03$	$7.0E+03$	$1.1E+04$	$1.8E+04$	$2.8E+04$	$4.5E+04$	$7.0E+04$
$2.0E+03$	$2.0E+03$	$3.0E+03$	$4.5E+03$	$6.5E+03$	$9.5E+03$	$1.4E+04$	$2.2E+04$	$3.5E+04$	$5.5E+04$	$9.0E+04$
$3.0E+03$	$3.0E+03$	$4.5E+03$	$6.5E+03$	$1.0E+04$	$1.5E+04$	$2.2E+04$	$3.5E+04$	$5.5E+04$	$9.0E+04$	$1.5E+05$
$5.0E+03$	$5.0E+03$	$7.5E+03$	$1.1E+04$	$1.5E+04$	$2.2E+04$	$3.0E+04$	$4.5E+04$	$7.0E+04$	$1.1E+05$	$1.8E+05$
$6.0E+03$	$6.0E+03$	$9.0E+03$	$1.2E+04$	$1.6E+04$	$2.2E+04$	$3.0E+04$	$4.5E+04$	$7.0E+04$	$1.1E+05$	$1.8E+05$
$6.6E+03$	$6.6E+03$	$9.5E+03$	$1.25E+04$	$1.65E+04$	$2.25E+04$	$3.05E+04$	$4.55E+04$	$7.05E+04$	$1.15E+05$	$1.85E+05$
$7.2E+03$	$7.2E+03$	$9.9E+03$	$1.29E+04$	$1.69E+04$	$2.29E+04$	$3.09E+04$	$4.59E+04$	$7.09E+04$	$1.19E+05$	$1.89E+05$
$7.5E+03$	$7.5E+03$	$1.02E+04$	$1.32E+04$	$1.72E+04$	$2.32E+04$	$3.12E+04$	$4.62E+04$	$7.12E+04$	$1.22E+05$	$1.92E+05$
$7.9E+03$	$7.9E+03$	$1.05E+04$	$1.35E+04$	$1.75E+04$	$2.35E+04$	$3.15E+04$	$4.65E+04$	$7.15E+04$	$1.25E+05$	$1.95E+05$
$8.5E+03$	$8.5E+03$	$1.08E+04$	$1.38E+04$	$1.78E+04$	$2.38E+04$	$3.18E+04$	$4.68E+04$	$7.18E+04$	$1.28E+05$	$1.98E+05$
$9.0E+03$	$9.0E+03$	$1.12E+04$	$1.42E+04$	$1.82E+04$	$2.42E+04$	$3.22E+04$	$4.72E+04$	$7.22E+04$	$1.32E+05$	$2.02E+05$
$9.5E+03$	$9.5E+03$	$1.15E+04$	$1.45E+04$	$1.85E+04$	$2.45E+04$	$3.25E+04$	$4.75E+04$	$7.25E+04$	$1.35E+05$	$2.05E+05$
$1.0E+04$	$1.0E+04$	$1.18E+04$	$1.48E+04$	$1.88E+04$	$2.48E+04$	$3.28E+04$	$4.8E+04$	$7.28E+04$	$1.38E+05$	$2.08E+05$
$1.1E+04$	$1.1E+04$	$1.22E+04$	$1.52E+04$	$1.92E+04$	$2.52E+04$	$3.32E+04$	$4.92E+04$	$7.32E+04$	$1.42E+05$	$2.12E+05$
$1.2E+04$	$1.2E+04$	$1.25E+04$	$1.55E+04$	$1.95E+04$	$2.55E+04$	$3.35E+04$	$5.0E+04$	$7.35E+04$	$1.45E+05$	$2.15E+05$
$1.3E+04$	$1.3E+04$	$1.28E+04$	$1.58E+04$	$1.98E+04$	$2.58E+04$	$3.38E+04$	$5.2E+04$	$7.38E+04$	$1.48E+05$	$2.18E+05$
$1.4E+04$	$1.4E+04$	$1.32E+04$	$1.62E+04$	$2.02E+04$	$2.62E+04$	$3.42E+04$	$5.5E+04$	$7.42E+04$	$1.52E+05$	$2.22E+05$
$1.5E+04$	$1.5E+04$	$1.35E+04$	$1.65E+04$	$2.05E+04$	$2.65E+04$	$3.45E+04$	$5.8E+04$	$7.45E+04$	$1.55E+05$	$2.25E+05$
$1.6E+04$	$1.6E+04$	$1.38E+04$	$1.68E+04$	$2.08E+04$	$2.68E+04$	$3.48E+04$	$6.1E+04$	$7.48E+04$	$1.58E+05$	$2.28E+05$
$1.7E+04$	$1.7E+04$	$1.42E+04$	$1.72E+04$	$2.12E+04$	$2.72E+04$	$3.52E+04$	$6.4E+04$	$7.52E+04$	$1.62E+05$	$2.32E+05$
$1.8E+04$	$1.8E+04$	$1.45E+04$	$1.75E+04$	$2.15E+04$	$2.75E+04$	$3.55E+04$	$6.7E+04$	$7.55E+04$	$1.65E+05$	$2.35E+05$
$1.9E+04$	$1.9E+04$	$1.48E+04$	$1.78E+04$	$2.18E+04$	$2.78E+04$	$3.58E+04$	$7.0E+04$	$7.8E+04$	$1.68E+05$	$2.38E+05$
$2.0E+04$	$2.0E+04$	$1.52E+04$	$1.82E+04$	$2.22E+04$	$2.82E+04$	$3.62E+04$	$7.3E+04$	$8.1E+04$	$1.71E+05$	$2.41E+05$
$2.1E+04$	$2.1E+04$	$1.55E+04$	$1.85E+04$	$2.25E+04$	$2.85E+04$	$3.65E+04$	$7.6E+04$	$8.4E+04$	$1.74E+05$	$2.44E+05$
$2.2E+04$	$2.2E+04$	$1.58E+04$	$1.88E+04$	$2.28E+04$	$2.88E+04$	$3.68E+04$	$7.9E+04$	$8.7E+04$	$1.77E+05$	$2.47E+05$
$2.3E+04$	$2.3E+04$	$1.62E+04$	$1.92E+04$	$2.32E+04$	$2.92E+04$	$3.72E+04$	$8.2E+04$	$9.0E+04$	$1.80E+05$	$2.50E+05$
$2.4E+04$	$2.4E+04$	$1.65E+04$	$1.95E+04$	$2.35E+04$	$2.95E+04$	$3.75E+04$	$8.5E+04$	$9.3E+04$	$1.83E+05$	$2.53E+05$
$2.5E+04$	$2.5E+04$	$1.68E+04$	$1.98E+04$	$2.38E+04$	$2.98E+04$	$3.78E+04$	$8.8E+04$	$9.6E+04$	$1.86E+05$	$2.56E+05$
$2.6E+04$	$2.6E+04$	$1.72E+04$	$2.02E+04$	$2.42E+04$	$3.02E+04$	$3.82E+04$	$9.1E+04$	$9.9E+04$	$1.89E+05$	$2.59E+05$
$2.7E+04$	$2.7E+04$	$1.75E+04$	$2.05E+04$	$2.45E+04$	$3.05E+04$	$3.85E+04$	$9.4E+04$	$1.02E+05$	$1.92E+05$	$2.62E+05$
$2.8E+04$	$2.8E+04$	$1.78E+04$	$2.08E+04$	$2.48E+04$	$3.08E+04$	$3.88E+04$	$9.7E+04$	$1.05E+05$	$1.95E+05$	$2.65E+05$
$2.9E+04$	$2.9E+04$	$1.82E+04$	$2.12E+04$	$2.52E+04$	$3.12E+04$	$3.92E+04$	$1.0E+05$	$1.08E+05$	$1.98E+05$	$2.68E+05$
$3.0E+04$	$3.0E+04$	$1.85E+04$	$2.15E+04$	$2.55E+04$	$3.15E+04$	$3.95E+04$	$1.03E+05$	$1.11E+05$	$2.01E+05$	$2.71E+05$
$3.1E+04$	$3.1E+04$	$1.88E+04$	$2.18E+04$	$2.58E+04$	$3.18E+04$	$3.98E+04$	$1.06E+05$	$1.14E+05$	$2.04E+05$	$2.74E+05$
$3.2E+04$	$3.2E+04$	$1.92E+04$	$2.22E+04$	$2.62E+04$	$3.22E+04$	$4.02E+04$	$1.09E+05$	$1.17E+05$	$2.07E+05$	$2.77E+05$
$3.3E+04$	$3.3E+04$	$1.95E+04$	$2.25E+04$	$2.65E+04$	$3.25E+04$	$4.05E+04$	$1.12E+05$	$1.20E+05$	$2.10E+05$	$2.80E+05$
$3.4E+04$	$3.4E+04$	$1.98E+04$	$2.28E+04$	$2.68E+04$	$3.28E+04$	$4.08E+04$	$1.15E+05$	$1.23E+05$	$2.13E+05$	$2.83E+05$
$3.5E+04$	$3.5E+04$	$2.02E+04$	$2.32E+04$	$2.72E+04$	$3.32E+04$	$4.12E+04$	$1.18E+05$	$1.26E+05$	$2.16E+05$	$2.86E+05$
$3.6E+04$	$3.6E+04$	$2.05E+04$	$2.35E+04$	$2.75E+04$	$3.35E+04$	$4.15E+04$	$1.21E+05$	$1.29E+05$	$2.19E+05$	$2.89E+05$
$3.7E+04$	$3.7E+04$	$2.08E+04$	$2.38E+04$	$2.78E+04$	$3.38E+04$	$4.18E+04$	$1.24E+05$	$1.32E+05$	$2.22E+05$	$2.92E+05$
$3.8E+04$	$3.8E+04$	$2.12E+04$	$2.42E+04$	$2.82E+04$	$3.42E+04$	$4.22E+04$	$1.27E+05$	$1.35E+05$	$2.25E+05$	$2.95E+05$
$3.9E+04$	$3.9E+04$	$2.15E+04$	$2.45E+04$	$2.85E+04$	$3.45E+04$	$4.25E+04$	$1.3E+05$	$1.38E+05$	$2.28E+05$	$2.98E+05$
$4.0E+04$	$4.0E+04$	$2.18E+04$	$2.48E+04$	$2.88E+04$	$3.48E+04$	$4.28E+04$	$1.33E+05$	$1.41E+05$	$2.31E+05$	$3.01E+05$
$4.1E+04$	$4.1E+04$	$2.22E+04$	$2.52E+04$	$2.92E+04$	$3.52E+04$	$4.32E+04$	$1.36E+05$	$1.44E+05$	$2.34E+05$	$3.04E+05$
$4.2E+04$	$4.2E+04$	$2.25E+04$	$2.55E+04$	$2.95E+04$	$3.55E+04$	$4.35E+04$	$1.39E+05$	$1.47E+05$	$2.37E+05$	$3.07E+05$
$4.3E+04$	$4.3E+04$	$2.28E+04$	$2.58E+04$	$2.98E+04$	$3.58E+04$	$4.38E+04$	$1.42E+05$	$1.5E+05$	$2.4E+05$	$3.1E+05$
$4.4E+04$	$4.4E+04$	$2.32E+04$	$2.62E+04$	$3.02E+04$	$3.62E+04$	$4.42E+04$	$1.45E+05$	$1.53E+05$	$2.43E+05$	$3.13E+05$
$4.5E+04$	$4.5E+04$	$2.35E+04$	$2.65E+04$	$3.05E+04$	$3.65E+04$	$4.45E+04$	$1.48E+05$	$1.56E+05$	$2.46E+05$	$3.16E+05$
$4.6E+04$	$4.6E+04$	$2.38E+04$	$2.68E+04$	$3.08E+04$	$3.68E+04$	$4.48E+04$	$1.51E+05$	$1.59E+05$	$2.49E+05$	$3.19E+05$
$4.7E+04$	$4.7E+04$	$2.42E+04$	$2.72E+04$	$3.12E+04$	$3.72E+04$	$4.52E+04$	$1.54E+05$	$1.62E+05$	$2.52E+05$	$3.22E+05$
$4.8E+04$	$4.8E+04$	$2.45E+04$	$2.75E+04$	$3.15E+04$	$3.75E+04$	$4.55E+04$	$1.57E+05$	$1.65E+05$	$2.55E+05$	$3.25E+05$
$4.9E+04$	$4.9E+04$	$2.48E+04$	$2.78E+04$	$3.18E+04$	$3.78E+04$	$4.58E+04$	$1.6E+05$	$1.68E+05$	$2.58E+05$	$3.28E+05$
$5.0E+04$	$5.0E+04$	$2.52E+04$	$2.82E+04$	$3.22E+04$	$3.82E+04$	$4.62E+04$	$1.63E+05$	$1.71E+05$	$2.61E+05$	$3.31E+05$
$5.1E+04$	$5.1E+04$	$2.55E+04$	$2.85E+04$	$3.25E+04$	$3.85E+04$	$4.65E+04$	$1.66E+05$	$1.74E+05$	$2.64E+05$	$3.34E+05$
$5.2E+04$	$5.2E+04$	$2.58E+04$	$2.88E+04$	$3.28E+04$	$3.88E+04$	$4.68E+04$	$1.69E+05$	$1.77E+05$	$2.67E+05$	$3.37E+05$
$5.3E+04$	$5.3E+04$	$2.62E+04$	$2.92E+04$	$3.32E+04$	$3.92E+04$	$4.72E+04$	$1.72E+05$	$1.8E+05$	$2.7E+05$	$3.4E+05$
$5.4E+04$	$5.4E+04$	$2.65E+04$	$2.95E+04$	$3.35E+04$	$3.95E+04$	$4.75E+04$	$1.75E+05$	$1.83E+05$	$2.73E+05$	$3.43E+05$
$5.5E+04$	$5.5E+04$	$2.68E+04$	$2.98E+04$	$3.38E+04$	$3.98E+04$	$4.78E+04$	$1.78E+05$	$1.86E+05$	$2.76E+05$	$3.46E+05$
$5.6E+04$	$5.6E+04$	$2.72E+04$	$3.02E+04$	$3.42E+04$	$4.02E+04$	$5.02E+04$	$1.81E+05$	$1.9E+05$	$2.79E+05$	$3.49E+05$
$5.7E+04$	$5.7E+04$	$2.75E+04$	$3.05E+04$	$3.45E+04$	$4.05E+04$	$5.05E+04$	$1.84E+05$	$1.93E+05$	$2.82E+05$	$3.52E+05$
$5.8E+04$	$5.8E+04$	$2.78E+04$	$3.08E+04$	$3.48E+04$	$4.08E+04$	$5.08E+04$	$1.87E+05$	$1.96E+05$	<	

Table B.20.  $(1/T_0) D_{-}(z/T_0)$  for bremsstrahlung. Units:  $\text{cm}^2/\text{g.}$ 

$z/T_0$	$T_0 = 0.02$	$0.05$	$0.10$	$0.20$	$0.50$	$1.00$	$2.00$	$5.00$	$10.00$	$20.00$
$(\text{g}/\text{cm}^2/\text{MeV})$										
1.0E-03	2.63E-03	1.42E-03	8.34E-04	3.83E-04	2.97E-04	2.20E-04	1.04E-04	8.51E-05	2.54E-04	
1.5E-03	3.78E-03	1.90E-03	4.86E-04	3.86E-04	3.64E-04	2.65E-04	1.38E-04	1.25E-04	4.07E-04	
2.0E-03	4.73E-03	2.30E-03	1.31E-03	5.77E-04	4.13E-04	3.00E-04	1.67E-04	1.63E-04	5.24E-04	
3.0E-03	6.23E-03	3.00E-03	1.66E-03	7.30E-04	4.85E-04	3.52E-04	2.18E-04	2.36E-04	6.59E-04	
4.0E-03	7.44E-03	3.62E-03	1.96E-03	8.55E-04	5.42E-04	3.93E-04	2.63E-04	3.16E-04	7.16E-04	
5.0E-03	8.48E-03	4.16E-03	2.23E-03	9.60E-04	5.91E-04	4.26E-04	3.05E-04	4.01E-04	7.40E-04	
6.0E-03	9.43E-03	4.66E-03	2.44E-03	1.06E-03	6.35E-04	4.54E-04	3.46E-04	4.87E-04	7.55E-04	
8.0E-03	1.15E-02	1.20E-02	5.53E-03	1.20E-03	7.15E-04	5.04E-04	4.23E-04	6.38E-04	8.00E-04	
1.0E-02	1.82E-02	1.25E-02	6.25E-03	3.10E-03	1.32E-03	7.84E-04	5.47E-04	4.96E-04	7.48E-04	
1.5E-02	2.71E-02	1.52E-02	7.50E-03	3.63E-03	1.55E-03	9.31E-04	6.43E-04	6.57E-04	9.19E-04	
2.0E-02	3.19E-02	1.72E-02	8.27E-03	3.99E-03	1.70E-03	1.05E-03	7.29E-04	7.87E-04	1.05E-03	
3.0E-02	2.68E-02	1.86E-02	9.29E-03	4.49E-03	1.91E-03	1.21E-03	8.80E-04	9.85E-04	1.30E-03	
4.0E-02	2.20E-02	1.80E-02	9.94E-03	4.89E-03	2.04E-03	1.30E-03	1.00E-03	1.14E-03	1.55E-03	
5.0E-02	1.80E-02	1.80E-02	1.02E-02	5.19E-03	2.15E-03	1.38E-03	1.09E-03	1.26E-03	1.76E-03	
6.0E-02	1.52E-02	1.62E-02	9.94E-03	5.34E-03	2.23E-03	1.44E-03	1.15E-03	1.37E-03	1.94E-03	
8.0E-02	1.12E-02	1.02E-02	8.57E-03	5.25E-03	2.36E-03	1.53E-03	1.26E-03	1.55E-03	2.22E-03	
1.0E-01	8.61E-03	7.54E-03	6.89E-03	4.82E-03	2.43E-03	1.60E-03	1.34E-03	1.69E-03	2.43E-03	
1.5E-01	5.37E-03	4.27E-03	4.08E-03	3.51E-03	2.51E-03	2.30E-03	1.66E-03	1.47E-03	1.93E-03	
2.0E-01	3.82E-03	3.05E-03	2.76E-03	1.91E-03	1.54E-03	1.54E-03	1.47E-03	1.47E-03	2.03E-03	
3.0E-01	2.37E-03	2.02E-03	1.65E-03	1.43E-03	1.22E-03	1.17E-03	1.27E-03	1.27E-03	1.99E-03	
4.0E-01	1.71E-03	1.51E-03	1.19E-03	9.48E-04	7.49E-04	6.50E-04	8.73E-04	1.05E-03	1.80E-03	
5.0E-01	1.33E-03	1.19E-03	9.88E-04	7.96E-04	6.27E-04	5.31E-04	6.78E-04	8.91E-04	1.62E-03	
6.0E-01	1.09E-03	9.88E-04	6.09E-04	4.89E-04	3.98E-04	3.98E-04	4.39E-04	5.56E-04	7.76E-04	
8.0E-01	7.90E-04	7.39E-04	5.90E-04	4.94E-04	4.02E-04	3.28E-04	3.85E-04	6.44E-04	1.28E-03	
1.0E+00	6.80E-04	6.20E-04	5.90E-04	4.94E-04	4.02E-04	3.28E-04	3.85E-04	5.81E-04	1.51E-03	
1.5E+00	3.63E-04	3.85E-04	3.85E-04	3.32E-04	2.82E-04	2.43E-04	3.01E-04	4.82E-04	2.80E-03	
2.0E+00	2.41E-04	2.81E-04	2.47E-04	2.14E-04	2.00E-04	2.52E-04	4.13E-04	4.82E-04	3.72E-03	
3.0E+00	1.26E-04	1.79E-04	1.63E-04	1.44E-04	1.48E-04	1.96E-04	3.22E-04	5.37E-04	1.31E-03	
4.0E+00	7.83E-05	1.28E-04	1.20E-04	1.08E-04	1.19E-04	1.62E-04	2.59E-04	3.93E-04	2.72E-03	
5.0E+00	5.40E-05	9.79E-05	9.48E-05	8.64E-05	8.64E-05	9.98E-05	1.39E-04	2.15E-04	2.91E-04	
6.0E+00	3.95E-05	7.86E-05	7.82E-05	7.20E-05	7.20E-05	8.70E-05	1.22E-04	1.80E-04	2.15E-04	
8.0E+00	2.30E-05	5.51E-05	5.74E-05	6.93E-05	6.93E-05	9.55E-05	1.30E-04	1.30E-04	1.52E-04	
1.0E+01	1.42E-05	4.17E-05	4.48E-05	4.32E-05	5.76E-05	7.68E-05	9.41E-05	9.41E-05	9.97E-04	
1.5E+01	4.79E-06	2.45E-05	2.78E-05	2.87E-05	3.96E-05	4.65E-05	4.38E-05	4.38E-05	6.20E-04	
2.0E+01	1.89E-06	1.57E-05	1.92E-05	1.92E-05	2.11E-05	2.85E-05	2.91E-05	2.91E-05	2.91E-05	
3.0E+01	4.26E-07	7.34E-06	1.09E-05	1.09E-05	1.32E-05	1.32E-05	1.32E-05	1.32E-05	1.32E-05	
4.0E+01	1.44E-07	4.17E-06	6.91E-06	8.96E-06	8.79E-06	8.79E-06	8.79E-06	8.79E-06	8.79E-06	
5.0E+01	6.69E-08	2.73E-06	4.71E-06	6.32E-06	6.32E-06	5.09E-06	5.09E-06	5.09E-06	5.09E-06	
6.0E+01	3.91E-08	1.94E-06	3.36E-06	4.56E-06	4.56E-06	3.00E-06	3.00E-06	3.00E-06	3.00E-06	
8.0E+01	2.16E-08	9.97E-07	1.86E-06	2.49E-06	2.49E-06	1.71E-06	1.71E-06	1.71E-06	1.71E-06	
1.0E+02	1.19E-08	4.57E-07	1.09E-06	1.09E-06	1.41E-06	1.41E-06	1.41E-06	1.41E-06	1.41E-06	
1.5E+02	2.68E-09	6.11E-08	3.13E-08	3.13E-08	3.83E-07	3.83E-07	3.83E-07	3.83E-07	3.83E-07	
2.0E+02	6.06E-10	1.70E-08	1.70E-08	1.70E-08	2.76E-20	2.76E-20	2.76E-20	2.76E-20	2.76E-20	
3.0E+02	3.09E-11	1.06E-14	4.08E-15	4.08E-15	9.43E-27	9.43E-27	9.43E-27	9.43E-27	9.43E-27	

## Appendix C. Sample Run

### 1. Input Data

Below is a listing of the input data for the run producing the results shown in figure 12 of Appendix A. Note that the monoenergetic depth-dose data set is read from unit 9.

1	9	2					
42	2						
0.03000	0.04000	0.05000	0.06000	0.08000	0.10000		
0.15000	0.20000	0.30000	0.40000	0.50000	0.60000		
0.80000	1.00000	1.25000	1.50000	1.75000	2.00000		
2.50000	3.00000	3.50000	4.00000	4.50000	5.00000		
5.50000	6.00000	6.50000	7.00000	7.50000	8.00000		
8.50000	9.00000	9.50000	10.00000	12.50000	15.00000		
17.50000	20.00000	22.50000	25.00000	27.50000	30.00000		
2.000	1000.000	2.000	1000.000	301	0.100	7.000	101
GEOSTAT, 35790 KM, INCL=0, PLONG=160W; SP:1AL(95%), TP:NONE, EL:AEI7-HI(79)							
3	0	28	1.00000E 03	3.15360E 07			
0.0000E 00	0.0000E 00	0.0000E 00					
2.6500E 01	2.4500E 10	0.0000E 00					
1.0000E-01	2.0000E-01	3.0000E-01	4.0000E-01	5.0000E-01	6.0000E-01		
7.0000E-01	8.0000E-01	9.0000E-01	1.0000E 00	1.2500E 00	1.5000E 00		
1.7500E 00	2.0000E 00	2.2500E 00	2.5000E 00	2.7500E 00	3.0000E 00		
3.2500E 00	3.5000E 00	3.7500E 00	4.0000E 00	4.2500E 00	4.5000E 00		
4.7500E 00	5.0000E 00	5.5000E 00	6.0000E 00	6.5000E 00	7.0000E 00		
7.5343E 04	5.7226E 04	3.5768E 04	2.0637E 04	1.2084E 04	7.7592E 03		
5.3738E 03	4.0677E 03	3.3050E 03	2.0840E 03	9.4707E 02	4.4939E 02		
2.2097E 02	1.0413E 02	5.1592E 01	2.6350E 01	1.2667E 01	5.7739E 00		
2.9428E 00	1.8846E 00	1.4374E 00	1.1547E 00	8.4948E-01	6.2276E-01		
4.8761E-01	3.4227E-01	2.1946E-01	1.2189E-02	0.0	0.0		

### 2. Output Data

The output listing, the significant portions of which are given below, is mostly self-explanatory. In addition to monitoring the input data, the total flux and the average energy is given, both for the protons and electron incident fluxes:

$$\text{INT SPEC} \equiv \int_{T_{\min}}^{T_{\max}} \psi_{4\pi}(T_0) dT_0$$

$$\text{EAV} \equiv \int_{T_{\min}}^{T_{\max}} T_0 \psi_{4\pi}(T_0) dT_0 \quad / \quad \int_{T_{\min}}^{T_{\max}} \psi_{4\pi}(T_0) dT_0$$

Sample output listing:

IMAX	IUNT							
42	2							
SHIELD DEPTH (G/CM2)								
0.03000	0.04000	0.05000	0.06000	0.08000	0.10000			
0.15000	0.20000	0.30000	0.40000	0.50000	0.60000			
0.80000	1.00000	1.25000	1.50000	1.75000	2.00000			
2.50000	3.00000	3.50000	4.00000	4.50000	5.00000			
5.50000	6.00000	6.50000	7.00000	7.50000	8.00000			
8.50000	9.00000	9.50000	10.00000	12.50000	15.00000			
17.50000	20.00000	22.50000	25.00000	27.50000	30.00000			
EMINS	EMAXS	EMINP	EMAXP	NPTSP	EMINE	EMAXE	NPTSE	
2.000	1000.000	2.000	1000.000	301	0.100	7.000	101	
2.000	999.999	2.000	999.999	301	0.100	7.000	101	ADJUSTED VALUES
GEOSTAT, 35790 KM, INCL=0, PLONG=160W; SP:1AL(95%), TP:NONE, EL:AEI7-HI(79)								
JSMAX	JPMAX	JEMAX	EUNIT	TINTER				
3	0	28	1.00000E+03	3.15360E+07				
E(MEV)								
0.0	0.0	0.0						
SOLAR PROTON SPECTRUM (/ENERGY/CM2)								
2.6500E+01	2.4500E+10	0.0						
INT SPEC	EAV(MEV)							
2.2719E+10	28.50006							
E(MEV)								
1.0000E-01	2.0000E-01	3.0000E-01	4.0000E-01	5.0000E-01	6.0000E-01			
7.0000E-01	8.0000E-01	9.0000E-01	1.0000E+00	1.2500E+00	1.5000E+00			
1.7500E+00	2.0000E+00	2.2500E+00	2.5000E+00	2.7500E+00	3.0000E+00			
3.2500E+00	3.5000E+00	3.7500E+00	4.0000E+00	4.2500E+00	4.5000E+00			
4.7500E+00	5.0000E+00	5.5000E+00	6.0000E+00					
ELECTRON SPECTRUM (/ENERGY/CM2/TIME)								
7.5343E+04	5.7226E+04	3.5768E+04	2.0637E+04	1.2084E+04	7.7592E+03			
5.3738E+03	4.0677E+03	3.3050E+03	2.0840E+03	9.4707E+02	4.4939E+02			
2.2097E+02	1.0413E+02	5.1592E+01	2.6350E+01	1.2667E+01	5.7739E+00			
2.9428E+00	1.8846E+00	1.4374E+00	1.1547E+00	8.4948E-01	6.2276E-01			
4.8761E-01	3.4227E-01	2.1946E-01	1.2189E-02					
INT SPEC	EAV(MEV)							
1.9162E+07	0.34290							

## DOSE AT TRANSMISSION SURFACE OF FINITE ALUMINUM SLAB SHIELDS

RADS AL	Z(MM)	Z(G/CM2)	ELECTRON	BREMS	EL+BR	TRP PROT	SOL PROT	EL+BR+TRP	TOTAL
4.374	0.111	0.030	4.130E+06	2.719E+03	4.133E+06	0.0	3.638E+03	4.133E+06	4.136E+06
5.833	0.148	0.040	3.186E+06	2.470E+03	3.189E+06	0.0	3.402E+03	3.189E+06	3.192E+06
7.291	0.185	0.050	2.534E+06	2.252E+03	2.537E+06	0.0	3.209E+03	2.537E+06	2.540E+06
8.749	0.222	0.060	2.063E+06	2.064E+03	2.065E+06	0.0	2.907E+03	2.065E+06	2.068E+06
11.665	0.296	0.080	1.440E+06	1.759E+03	1.442E+06	0.0	2.673E+03	1.442E+06	1.445E+06
14.581	0.370	0.100	1.059E+06	1.530E+03	1.061E+06	0.0	2.250E+03	1.061E+06	1.064E+06
21.872	0.556	0.150	5.683E+05	1.155E+03	5.695E+05	0.0	1.419E+05	5.695E+05	5.717E+05
29.163	0.741	0.200	3.410E+05	9.277E+02	3.419E+05	0.0	1.399E+05	3.419E+05	3.439E+05
43.744	1.111	0.300	1.393E+05	6.600E+02	1.399E+05	0.0	1.568E+03	1.399E+05	1.415E+05
58.326	1.481	0.400	6.246E+04	5.077E+02	6.296E+04	0.0	1.310E+03	6.296E+04	6.427E+04
72.907	1.852	0.500	3.040E+04	4.125E+02	3.081E+04	0.0	1.123E+03	3.081E+04	3.194E+04
87.489	2.222	0.600	1.546E+04	3.493E+02	1.581E+04	0.0	9.811E+02	1.581E+04	1.679E+04
116.652	2.963	0.800	4.411E+03	2.727E+02	4.683E+03	0.0	7.749E+02	4.683E+03	5.458E+03
145.815	3.704	1.000	1.436E+03	2.279E+02	1.664E+03	0.0	6.329E+02	1.664E+03	2.297E+03
182.269	4.630	1.250	4.360E+02	1.919E+02	6.279E+02	0.0	5.069E+02	6.279E+02	1.135E+03
218.722	5.556	1.500	1.736E+02	1.673E+02	3.409E+02	0.0	4.153E+02	3.409E+02	7.562E+02
255.176	6.481	1.750	8.030E+01	1.492E+02	2.295E+02	0.0	3.473E+02	2.295E+02	5.769E+02
291.630	7.407	2.000	3.669E+01	1.353E+02	1.720E+02	0.0	2.937E+02	1.720E+02	4.657E+02
364.537	9.259	2.500	5.603E+00	1.149E+02	1.205E+02	0.0	2.179E+02	1.205E+02	3.385E+02
637.445	11.111	3.000	3.263E-01	1.005E+02	1.009E+02	0.0	1.673E+02	1.009E+02	2.682E+02
510.352	12.963	3.500	9.898E-04	8.968E+01	8.969E+01	0.0	1.314E+02	8.969E+01	2.210E+02
583.260	14.815	4.000	1.070E-08	8.110E+01	8.110E+01	0.0	1.047E+02	8.110E+01	1.858E+02
656.167	16.667	4.500	0.0	7.405E+01	7.405E+01	0.0	8.459E+01	7.405E+01	1.586E+02
729.074	18.519	5.000	0.0	6.812E+01	6.812E+01	0.0	6.959E+01	6.812E+01	1.377E+02
801.982	20.370	5.500	0.0	6.302E+01	6.302E+01	0.0	5.784E+01	6.302E+01	1.209E+02
874.889	22.222	6.000	0.0	5.855E+01	5.855E+01	0.0	4.804E+01	5.855E+01	1.066E+02
947.797	24.074	6.500	0.0	5.459E+01	5.459E+01	0.0	4.051E+01	5.459E+01	9.510E+01
1020.704	25.926	7.000	0.0	5.104E+01	5.104E+01	0.0	3.438E+01	5.104E+01	8.542E+01
1093.612	27.778	7.500	0.0	4.784E+01	4.784E+01	0.0	3.927E+01	4.784E+01	7.711E+01
1166.519	29.630	8.000	0.0	4.493E+01	4.493E+01	0.0	2.524E+01	4.493E+01	4.975E+01
1239.427	31.481	8.500	0.0	4.227E+01	4.227E+01	0.0	2.187E+01	4.227E+01	3.462E+01
1312.334	33.333	9.000	0.0	3.983E+01	3.983E+01	0.0	1.886E+01	3.983E+01	5.870E+01
1385.241	35.185	9.500	0.0	3.758E+01	3.758E+01	0.0	1.642E+01	3.758E+01	5.400E+01
1458.149	37.037	10.000	0.0	3.550E+01	3.550E+01	0.0	1.425E+01	3.550E+01	4.975E+01
1822.686	46.296	12.500	0.0	2.709E+01	2.709E+01	0.0	7.524E+00	2.709E+01	8.757E+00
2187.223	55.556	15.000	0.0	2.102E+01	2.102E+01	0.0	4.227E+00	2.102E+01	5.530E+00
2551.760	64.815	17.500	0.0	1.648E+01	1.648E+01	0.0	2.527E+00	1.648E+01	1.901E+01
2916.298	74.074	20.000	0.0	1.300E+01	1.300E+01	0.0	1.532E+00	1.300E+01	1.453E+01
3280.835	83.333	22.500	0.0	1.028E+01	1.028E+01	0.0	9.578E-01	1.028E+01	1.244E+01
3645.372	92.593	25.000	0.0	8.137E+00	8.137E+00	0.0	6.197E-01	8.137E+00	8.757E+00
4009.910	101.852	27.500	0.0	6.440E+00	6.440E+00	0.0	3.963E-01	6.440E+00	6.836E+00
4374.445	111.111	30.000	0.0	5.094E+00	5.094E+00	0.0	2.679E-01	5.094E+00	5.362E+00

ALUMINUM WHITE SEMI-TRANSPARENT

## 1/2 DOSE AT CENTER OF ALUMINUM SPHERES

RADS AL	Z(MILS)	Z(MM)	Z(G/CM2)	ELECTRON	BREMS	EL+BR	TRP PROT	SOL PROT	EL+BR+TRP	TOTAL
4.374	0.111	0.030	1.150E+07	6.162E+03	1.150E+07	0.0	4.994E+03	1.150E+07	1.151E+07	1.151E+07
5.833	0.148	0.040	9.510E+06	5.675E+03	9.516E+06	0.0	4.694E+03	9.516E+06	9.521E+06	9.521E+06
7.291	0.185	0.050	7.972E+06	5.239E+03	7.977E+06	0.0	4.464E+03	7.977E+06	7.982E+06	7.982E+06
8.749	0.222	0.060	6.766E+06	4.852E+03	6.771E+06	0.0	4.264E+03	6.771E+06	6.775E+06	6.775E+06
11.665	0.296	0.080	5.019E+06	4.177E+03	5.023E+06	0.0	3.956E+03	5.023E+06	5.027E+06	5.027E+06
14.581	0.370	0.100	3.848E+06	3.633E+03	3.852E+06	0.0	3.723E+03	3.852E+06	3.855E+06	3.855E+06
21.872	0.556	0.150	2.240E+06	2.714E+03	2.242E+06	0.0	3.280E+03	2.242E+06	2.246E+06	2.246E+06
29.163	0.741	0.200	1.471E+06	2.171E+03	1.473E+06	0.0	2.955E+03	1.473E+06	1.476E+06	1.476E+06
43.744	1.111	0.300	7.227E+05	1.541E+03	7.243E+05	0.0	2.496E+03	7.243E+05	7.268E+05	7.268E+05
58.326	1.481	0.400	3.664E+05	1.170E+03	3.676E+05	0.0	2.175E+03	3.676E+05	3.697E+05	3.697E+05
72.907	1.852	0.500	1.975E+05	9.265E+02	1.984E+05	0.0	1.927E+03	1.984E+05	2.003E+05	2.003E+05
87.489	2.222	0.600	1.11E+05	7.619E+02	1.118E+05	0.0	1.737E+03	1.118E+05	1.136E+05	1.136E+05
116.652	2.963	0.800	3.658E+04	5.709E+02	3.715E+04	0.0	1.648E+03	3.715E+04	3.860E+04	3.860E+04
145.815	3.704	1.000	1.293E+04	4.699E+02	1.340E+04	0.0	1.232E+03	1.340E+04	1.463E+04	1.463E+04
182.269	4.630	1.250	3.855E+03	3.951E+02	4.250E+03	0.0	1.040E+03	4.250E+03	5.290E+03	5.290E+03
218.722	5.556	1.500	1.429E+03	3.456E+02	1.775E+03	0.0	8.824E+02	1.775E+03	2.657E+03	2.657E+03
255.176	6.481	1.750	0.022E+02	3.095E+02	0.012E+03	0.0	6.728E+02	0.012E+03	1.779E+03	1.779E+03
291.630	7.407	2.000	3.843E+02	2.817E+02	6.660E+02	0.0	6.660E+02	6.660E+02	1.339E+03	1.339E+03
364.537	9.259	2.500	9.336E+01	2.422E+02	3.356E+02	0.0	5.214E+02	3.356E+02	8.570E+02	8.570E+02
437.445	11.111	3.000	1.130E+01	2.153E+02	2.266E+02	0.0	4.200E+02	2.266E+02	6.465E+02	6.465E+02
510.352	12.963	3.500	9.096E-02	1.954E+02	1.955E+02	0.0	3.459E+02	1.955E+02	5.415E+02	5.415E+02
583.260	14.815	4.000	1.677E-06	1.799E+02	0.0	2.897E+02	1.799E+02	4.696E+02	4.696E+02	4.696E+02
656.167	16.667	4.500	0.0	1.671E+02	1.671E+02	0.0	2.401E+02	1.671E+02	4.073E+02	4.073E+02
729.074	18.519	5.000	0.0	1.563E+02	1.563E+02	0.0	1.999E+02	1.563E+02	3.561E+02	3.561E+02
801.982	20.370	5.500	0.0	1.469E+02	1.469E+02	0.0	1.768E+02	1.469E+02	3.236E+02	3.236E+02
874.889	22.222	6.000	0.0	1.386E+02	1.386E+02	0.0	1.510E+02	1.386E+02	2.896E+02	2.896E+02
947.797	24.074	6.500	0.0	1.312E+02	1.312E+02	0.0	1.276E+02	1.312E+02	2.587E+02	2.587E+02
1020.704	25.926	7.000	0.0	1.245E+02	1.245E+02	0.0	1.233E+02	1.245E+02	2.378E+02	2.378E+02
1093.612	27.778	7.500	0.0	1.186E+02	1.186E+02	0.0	9.724E+01	1.186E+02	2.158E+02	2.158E+02
1166.519	29.630	8.000	0.0	1.132E+02	1.132E+02	0.0	9.803E+01	1.132E+02	1.963E+02	1.963E+02
1239.427	31.481	8.500	0.0	1.084E+02	1.084E+02	0.0	7.656E+01	1.084E+02	1.850E+02	1.850E+02
1312.334	33.333	9.000	0.0	1.040E+02	1.040E+02	0.0	6.740E+01	1.040E+02	1.714E+02	1.714E+02
1385.241	35.185	9.500	0.0	1.000E+02	1.000E+02	0.0	5.999E+01	1.000E+02	1.600E+02	1.600E+02
1458.149	37.037	10.000	0.0	9.632E+01	9.632E+01	0.0	5.446E+01	9.632E+01	1.508E+02	1.508E+02
1822.686	46.296	12.500	0.0	8.142E+01	8.142E+01	0.0	2.981E+01	8.142E+01	1.122E+01	1.122E+01
2187.223	55.556	15.000	0.0	6.969E+01	6.969E+01	0.0	1.818E+01	6.969E+01	8.787E+01	8.787E+01
2551.760	64.815	17.500	0.0	5.946E+01	5.946E+01	0.0	1.158E+01	5.946E+01	7.104E+01	7.104E+01
2916.298	74.074	20.000	0.0	5.022E+01	5.022E+01	0.0	7.526E+00	5.022E+01	5.775E+01	5.775E+01
3280.835	83.333	22.500	0.0	4.197E+01	4.197E+01	0.0	4.197E+01	4.197E+01	4.676E+01	4.676E+01
3645.372	92.593	25.000	0.0	3.480E+01	3.480E+01	0.0	3.480E+01	3.480E+01	3.818E+01	3.818E+01
4009.910	101.852	27.500	0.0	2.872E+01	2.872E+01	0.0	2.258E+00	2.872E+01	3.098E+01	3.098E+01
4374.445	111.111	30.000	0.0	1.318E+01	1.318E+01	0.0	1.318E+01	1.318E+01	1.363E+01	1.363E+01

## Appendix D. Listing of the computer code.

```

C SHIELDOSE, 12 FEB 80. A 10
C DEVELOPED BY S. M. SELTZER, NATIONAL BUREAU OF STANDARDS. A 15
C C
C IDET = 1, AL DETECTOR A 20
C 2, H2-O DETECTOR A 30
C 3, SI DETECTOR A 40
C 4, SI-02 DETECTOR A 50
C C INCIDENT OMNIDIRECTIONAL FLUX IN /ENERGY/CM2/UNIT TIME A 70
C (SOLAR-FLARE FLUX IN /ENERGY/CM2). A 80
C EUNIT IS CONVERSION FACTOR FROM /ENERGY TO /MEV, A 90
C E.G., EUNIT = 1000 IF FLUX IS /KEV. A 100
C TINTER IS MISSION DURATION IN MULTIPLES OF UNIT TIME. A 110
C C
C DIMENSION EP(30),RP(30),DP(30,51),ZP(51),ER(80),RE(80),EE(10), A 120
1 DE(10,41,2),ZE(41),ZB(60),EB(10),DB(10,60,2),ZM(50),Z(50), A 130
2 TPL(301),TP(301),RINP(301),TEL(101),TE(101),RINE(101),SOL(301), A 140
3 EPS(101),S(101),SPG(301),G(301),SEG(101),DOSOL(50,2), A 150
4 DOSP(50,2),DIN(60,301),GP(301,50),GE(101,50,2),GB(101,50,2), A 160
5 DOSE(50,2,2),DOSB(50,2,2),ZMM(50),ZL(50),GARB(60) A 170
CALL ERRSET (208,256,-1,1) A 180
ZCON=0.001*2.540005*2.70 A 190
ZMCON=10.0/2.70 A 200
RADCON=1.6021892E-08 A 210
PRINT 10 A 220
10 FORMAT ('0 IDET NUT IPRNT') A 230
READ 30, IDET,NUT,IPRNT A 240
PRINT 30, IDET,NUT,IPRNT A 250
IDEI1=IDEI+1 A 260
REWIND NUT A 270
PRINT 20 A 280
20 FORMAT ('0MPMAX LPMAX KMAX MEMAX LEMAX MBMAX LBMAX') A 290
READ (NUT,30) MPMAX,LPMAX,KMAX,MEMAX,LEMAX,MBMAX,LBMAX A 300
PRINT 30, MPMAX,LPMAX,KMAX,MEMAX,LEMAX,MBMAX,LBMAX A 310
30 FORMAT (12I6) A 320
PRINT 40 A 330
40 FORMAT ('0PROTON DOSE DATA (ENERGIES INCREASING)') A 340
PRINT 50 A 350
50 FORMAT ('0 E(MEV) R(G/CM2)') A 360
DO 110 M=1,MPMAX A 370
READ (NUT,60) EP(M),RP(M) A 380
PRINT 60, EP(M),RP(M) A 390
60 FORMAT (1P6E12.4) A 400
EP(M)= ALOG(EP(M)) A 410
RP(M)= ALOG(RP(M)) A 420
DO 70 ID=1,IDEI A 430
READ (NUT,60) (DP(M,L),L=1,LPMAX) A 440
70 CONTINUE A 450
GO TO (80,90), IPRNT A 460
80 PRINT 60, (DP(M,L),L=1,LPMAX) A 470
90 IF (IDEI1.GT.4) GO TO 110 A 480
DO 100 ID=IDEI1,4 A 490
READ (NUT,60) (GARB(L),L=1,LPMAX) A 500
100 CONTINUE A 510
110 CONTINUE A 520
ZPFAC=1.0/FLOAT(LPMAX-1) A 530
DO 120 L=1,LPMAX A 540
120 ZP(L)=FLOAT(L-1)*ZPFAC A 550
PRINT 130 A 560
130 FORMAT ('0ELECTRON DOSE DATA') A 570
PRINT 140 A 580
140 FORMAT ('0E(MEV)') A 590
READ (NUT,150) (ER(K),K=1,KMAX) A 600
PRINT 150, (ER(K),K=1,KMAX) A 610
150 FORMAT (6F12.5) A 620
PRINT 160 A 630
160 FORMAT ('0ORANGE(G/CM2)') A 640
READ (NUT,60) (RE(K),K=1,KMAX) A 650
PRINT 60, (RE(K),K=1,KMAX) A 660
A 670

```

```

DO 170 K=1,KMAX A 680
ER(K)=ALOG(ER(K)) A 690
170 RE(K)=ALOG(RE(K)) A 700
PRINT 180 A 710
180 FORMAT ('0E(MEV), THEN R0*D/E (ENERGIES INCREASING)') A 720
DO 270 M=1,MEMAX A 730
READ (NUT,150) EE(M) A 740
PRINT 150, EE(M) A 750
EE(M)=ALOG(EE(M)) A 760
DO 210 ID=1, IDET A 770
DO 200 N=1,2 A 780
READ (NUT,190) (DE(M,L,N),L=1,LEMAX) A 790
190 FORMAT (1P8E10.3) A 800
200 CONTINUE A 810
210 CONTINUE A 820
GO TO (220,240), IPRNT A 830
220 DO 230 N=1,2 A 840
PRINT 190, (DE(M,L,N),L=1,LEMAX) A 850
230 CONTINUE A 860
240 IF (IDET1.GT.4) GO TO 270 A 870
DO 260 ID=IDET1,4 A 880
DO 250 N=1,2 A 890
READ (NUT,190) (GARB(L),L=1,LEMAX) A 900
250 CONTINUE A 910
260 CONTINUE A 920
270 CONTINUE A 930
ZEFAC=1.0/FLOAT(LEMAX-1) A 940
DO 280 L=1,LEMAX A 950
280 ZE(L)=FLOAT(L-1)*ZEFAC A 960
PRINT 290 A 970
290 FORMAT ('OBREMSSTRAHLUNG DOSE DATA (ENERGIES INCREASING)') A 980
PRINT 300 A 990
300 FORMAT ('0Z/E (G/CM2 KEV)') A 1000
READ (NUT,310) (ZB(L),L=1,LBMAX) A 1010
PRINT 310, (ZB(L),L=1,LBMAX) A 1020
310 FORMAT (1P8E9.2) A 1030
DO 320 L=1,LBMAX A 1040
320 ZB(L)=ALOG(1000.0*ZB(L)) A 1050
PRINT 330 A 1060
330 FORMAT ('0E(MEV), THEN D/E (CM2/G)') A 1070
DO 420 M=1,MBMAX A 1080
READ (NUT,150) EB(M),RENORM A 1090
PRINT 150, EB(M),RENORM A 1100
EB(M)=ALOG(EB(M)) A 1110
DO 350 ID=1, IDET A 1120
DO 340 N=1,2 A 1130
READ (NUT,310) (DB(M,L,N),L=1,LBMAX) A 1140
340 CONTINUE A 1150
350 CONTINUE A 1160
GO TO (360,380), IPRNT A 1170
360 DO 370 N=1,2 A 1180
PRINT 310, (DB(M,L,N),L=1,LBMAX) A 1190
370 CONTINUE A 1200
380 DO 390 N=1,2 A 1210
DO 390 L=1,LBMAX A 1220
390 DB(M,L,N)=ALOG(RENORM*DB(M,L,N)) A 1230
IF (IDET1.GT.4) GO TO 420 A 1240
DO 410 ID=IDET1,4 A 1250
DO 400 N=1,2 A 1260
READ (NUT,310) (GARB(L),L=1,LBMAX) A 1270
400 CONTINUE A 1280
410 CONTINUE A 1290
420 CONTINUE A 1300
PRINT 430 A 1310
430 FORMAT ('0 IMAX IUNT') A 1320
READ 30, IMAX,IUNT A 1330
PRINT 30, IMAX,IUNT A 1340
GO TO (440,470,500), IUNT A 1350
440 PRINT 450 A 1360
450 FORMAT ('OSHIELD DEPTH (MILS)') A 1370

```

```

READ 150, (ZM(I),I=1,IMAX) A 1380
PRINT 150, (ZM(I),I=1,IMAX) A 1390
DO 460 I=1,IMAX A 1400
Z(I)=ZCON*ZM(I) A 1410
460 ZMM(I)=Z(I)*ZMCON A 1420
GO TO 530 A 1430
470 PRINT 480 A 1440
480 FORMAT ('0SHIELD DEPTH (G/CM2)') A 1450
READ 150, (Z(I),I=1,IMAX) A 1460
PRINT 150, (Z(I),I=1,IMAX) A 1470
DO 490 I=1,IMAX A 1480
ZM(I)=Z(I)/ZCON A 1490
490 ZMM(I)=Z(I)*ZMCON A 1500
GO TO 530 A 1510
500 PRINT 510 A 1520
510 FORMAT ('0SHIELD DEPTH (MM}') A 1530
READ 150, (ZMM(I),I=1,IMAX) A 1540
PRINT 150, (ZMM(I),I=1,IMAX) A 1550
DO 520 I=1,IMAX A 1560
Z(I)=ZMM(I)/ZMCON A 1570
520 ZM(I)=Z(I)/ZCON A 1580
530 DO 540 I=1,IMAX A 1590
540 ZL(I)=ALOG(Z(I)) A 1600
PRINT 550 A 1610
550 FORMAT ('0      EMIN S     EMAX S     EMIN P     EMAX P   NPTSP     EMIN E
1      EMAX E NPTSE')
READ 560, EMIN S, EMAX S, EMIN P, EMAX P, NPTSP, EMIN E, EMAX E, NPTSE A 1620
PRINT 560, EMIN S, EMAX S, EMIN P, EMAX P, NPTSP, EMIN E, EMAX E, NPTSE A 1630
560 FORMAT (4F10.3,I6,2F10.3,I6) A 1640
EMINU=AMIN1(EMIN P,EMIN S) A 1650
EMAXU=AMAX1(EMAX P,EMAX S) A 1660
DEP=ALOG(EMAXU/EMINU)/FLOAT(NPTSP-1) A 1670
NFSTS=ALOG(EMIN S/EMINU)/DEP+0.5 A 1680
NFSTS=NFSTS+1 A 1690
NLSTS=ALOG(EMAX S/EMINU)/DEP+0.5 A 1700
NLSTS=NLSTS+1 A 1710
NLENS=NLSTS-NFSTS+1 A 1720
NFSTP=ALOG(EMIN P/EMINU)/DEP+0.5 A 1730
NFSTP=NFSTP+1 A 1740
NLSTP=ALOG(EMAX P/EMINU)/DEP+0.5 A 1750
NLSTP=NLSTP+1 A 1760
NLENP=NLSTP-NFSTP+1 A 1770
EMINUL=ALOG(EMINU) A 1780
DELP=DEP/3.0 A 1790
ICALL=1 A 1800
DO 570 NP=1,NPTSP A 1810
TPL(NP)=EMINUL+FLOAT(NP-1)*DEP A 1820
TP(NP)=EXP(TPL(NP)) A 1830
CALL SPOL (TPL(NP),EP,RP,MPMAX,ICALL,ANS) A 1840
570 RINP(NP)=EXP(ANS) A 1850
PRINT 580, TP(NFSTS),TP(NLSTS),TP(NFSTP),TP(NLSTP),NPTSP,EMINE,EMA
1XE,NPTSE A 1860
A 1870
580 FORMAT (4F10.3,I6,2F10.3,I6,' ADJUSTED VALUES') A 1880
DO 620 L=1,LPMAX A 1890
ICALL=1 A 1900
DO 610 NP=1,NPTSP A 1910
IF (TPL(NP).LT.EP(MPMAX)) GO TO 590 A 1920
DIN(L,NP)=DP(MPMAX,L) A 1930
GO TO 610 A 1940
590 IF (TPL(NP).GT.EP(1)) GO TO 600 A 1950
DIN(L,NP)=DP(1,L) A 1960
GO TO 610 A 1970
600 CALL SPOL (TPL(NP),EP,DP(1,L),MPMAX,ICALL,DIN(L,NP)) A 1980
610 CONTINUE A 1990
620 CONTINUE A 2000
DO 660 NP=1,NPTSP A 2010
ICALL=1 A 2020
DO 650 I=1,IMAX A 2030
ZRIN=Z(I)/RINP(NP) A 2040
IF (ZRIN.LT.1.0) GO TO 640 A 2050
A 2060
A 2070

```

```

630 GP(NP,I)=0.0 A 2080
GO TO 650 A 2090
640 CALL SPOL (ZRIN,ZP,DIN(1,NP),LPMAX,ICALL,ANS) A 2100
IF (ANS.LT.0.0) GO TO 630 A 2110
GP(NP,I)=TP(NP)*ANS/RINP(NP) A 2120
650 CONTINUE A 2130
660 CONTINUE A 2140
EMINEL=ALOG(EMINE) A 2150
DEE=(ALOG(EMAXE)-EMINEL)/FLOAT(NPTSE-1) A 2160
DELE=DEE/3.0 A 2170
ICALL=1 A 2180
DO 670 NE=1,NPTSE A 2190
TEL(NE)=EMINEL+FLOAT(NE-1)*DEE A 2200
TE(NE)=EXP(TEL(NE)) A 2210
CALL SPOL (TEL(NE),ER,RE,KMAX,ICALL,ANS) A 2220
670 RINE(NE)=EXP(ANS) A 2230
DO 820 N=1,2 A 2240
DO 710 L=1,LEMAX A 2250
ICALL=1 A 2260
DO 700 NE=1,NPTSE A 2270
IF (TEL(NE).LT.EE(MEMAX)) GO TO 680 A 2280
DIN(L,NE)=DE(MEMAX,L,N) A 2290
GO TO 700 A 2300
680 IF (TEL(NE).GT.EE(1)) GO TO 690 A 2310
DIN(L,NE)=DE(1,L,N) A 2320
GO TO 700 A 2330
690 CALL SPOL (TEL(NE),EE,DE(1,L,N),MEMAX,ICALL,DIN(L,NE)) A 2340
700 CONTINUE A 2350
710 CONTINUE A 2360
DO 750 NE=1,NPTSE A 2370
ICALL=1 A 2380
DO 740 I=1,IMAX A 2390
ZRIN=Z(I)/RINE(NE) A 2400
IF (ZRIN.LT.1.0) GO TO 730 A 2410
720 GE(NE,I,N)=0.0 A 2420
GO TO 740 A 2430
730 CALL SPOL (ZRIN,ZE,DIN(1,NE),LEMAX,ICALL,ANS) A 2440
IF (ANS.LT.0.0) GO TO 720 A 2450
GE(NE,I,N)=TE(NE)*ANS/RINE(NE) A 2460
740 CONTINUE A 2470
750 CONTINUE A 2480
DO 790 L=1,LBMAX A 2490
ICALL=1 A 2500
DO 780 NE=1,NPTSE A 2510
IF (TEL(NE).LT.EB(MBMAX)) GO TO 760 A 2520
DIN(L,NE)=DB(MBMAX,L,N) A 2530
GO TO 780 A 2540
760 IF (TEL(NE).GT.EB(1)) GO TO 770 A 2550
DIN(L,NE)=DB(1,L,N) A 2560
GO TO 780 A 2570
770 CALL SPOL (TEL(NE),EB,DB(1,L,N),MBMAX,ICALL,DIN(L,NE)) A 2580
780 CONTINUE A 2590
790 CONTINUE A 2600
DO 810 NE=1,NPTSE A 2610
ICALL=1 A 2620
DO 800 I=1,IMAX A 2630
ZBIN=ALOG(Z(I)/TE(NE)) A 2640
CALL SPOL (ZBIN,ZB,DIN(1,NE),LBMAX,ICALL,ANS) A 2650
800 GB(NE,I,N)=TE(NE)*EXP(ANS) A 2660
810 CONTINUE A 2670
820 CONTINUE A 2680
830 PRINT 840 A 2690
840 FORMAT ('1') A 2700
PRINT 850 A 2710
850 FORMAT ('0') A 2720
READ (5,860,END=1420) A 2730
PRINT 860 A 2740
860 FORMAT (72H A 2750
1 ) A 2760
PRINT 870 A 2770

```

```

870 FORMAT ('0JSMAX JPMAX JEMAX      EUNIT      TINTER')
          READ 880, JSMAX, JPMAX, JEMAX, EUNIT, TINTER
          PRINT 880, JSMAX, JPMAX, JEMAX, EUNIT, TINTER
880 FORMAT (3I6,1P2E12.5)
          IF (TINTER.LE.0.0) TINTER=1.0
          DELTAS=RADCON*DELP/4.0
          DELTAP=TINTER*RADCON*DELP/4.0
          DELTAE=TINTER*RADCON*DELE/4.0
          IF (EUNIT.LE.0.0) EUNIT=1.0
          ISOL=2
          IF (JSMAX.LT.3) GO TO 900
          ISOL=1
          PRINT 140
          READ 60, (EPS(J),J=1,JSMAX)
          PRINT 60, (EPS(J),J=1,JSMAX)
          PRINT 890
890 FORMAT ('0SOLAR PROTON SPECTRUM (/ENERGY/CM2)')
          READ 60, (S(J),J=1,JSMAX)
          PRINT 60, (S(J),J=1,JSMAX)
          CALL SPECTR (JSMAX,EPS,S,EUNIT,DELP,NLENS,TP(NFSTS),TPL(NFSTS),SOL
1(NFSTS))
900 ITRP=2
          IF (JPMAX.LT.3) GO TO 920
          ITRP=1
          PRINT 140
          READ 60, (EPS(J),J=1,JPMAX)
          PRINT 60, (EPS(J),J=1,JPMAX)
          PRINT 910
910 FORMAT ('0TRAPPED PROTON SPECTRUM (/ENERGY/CM2/TIME)')
          READ 60, (S(J),J=1,JPMAX)
          PRINT 60, (S(J),J=1,JPMAX)
          CALL SPECTR (JPMAX,EPS,S,EUNIT,DELP,NLENP,TP(NFSTP),TPL(NFSTP),SPG
1(NFSTP))
920 ILEC=2
          IF (JEMAX.LT.3) GO TO 940
          ILEC=1
          PRINT 140
          READ 60, (EPS(J),J=1,JEMAX)
          PRINT 60, (EPS(J),J=1,JEMAX)
          PRINT 930
930 FORMAT ('0ELECTRON SPECTRUM (/ENERGY/CM2/TIME)')
          READ 60, (S(J),J=1,JEMAX)
          PRINT 60, (S(J),J=1,JEMAX)
          CALL SPECTR (JEMAX,EPS,S,EUNIT,DELE,NPTSE,TE,TEL,SEG)
940 GO TO (980,950), ISOL
950 DO 960 NP=NFSTS,NLSTS
960 SOL(NP)=0.0
          DO 970 J=1,2
          DO 970 I=1,IMAX
970 DOSOL(I,J)=0.0
          GO TO 1010
980 DO 1000 I=1,IMAX
          DO 990 NP=NFSTS,NLSTS
990 G(NP)=SOL(NP)*GP(NP,I)
          CALL INT (DELTAS,G(NFSTS),NLENS,DOSOL(I,1))
1000 CONTINUE
          CALL SPHERE (ZL,DOSOL(1,1),IMAX,DOSOL(1,2))
1010 GO TO (1050,1020), ITRP
1020 DO 1030 NP=NFSTP,NLSTP
1030 SPG(NP)=0.0
          DO 1040 J=1,2
          DO 1040 I=1,IMAX
1040 DOSP(I,J)=0.0
          GO TO 1080
1050 DO 1070 I=1,IMAX
          DO 1060 NP=NFSTP,NLSTP
1060 G(NP)=SPG(NP)*GP(NP,I)
          CALL INT (DELTAP,G(NFSTP),NLENP,DOSP(I,1))
1070 CONTINUE
          CALL SPHERE (ZL,DOSP(1,1),IMAX,DOSP(1,2))

```

```

1080 GO TO (1110,1090), ILEC A 3480
1090 DO 1100 J=1,2 A 3490
   DO 1100 N=1,2 A 3500
   DO 1100 I=1,IMAX A 3510
   DOSE(I,N,J)=0.0 A 3520
1100 DOSB(I,N,J)=0.0 A 3530
   GO TO 1160 A 3540
1110 DO 1150 N=1,2 A 3550
   DO 1130 I=1,IMAX A 3560
   DO 1120 NE=1,NPTSE A 3570
   G(NE)=SEG(NE)*GE(NE,I,N) A 3580
1120 SPG(NE)=SEG(NE)*GB(NE,I,N) A 3590
   CALL INT (DELTAE,G,NPTSE,DOSE(I,N,1)) A 3600
   CALL INT (DELTAE,SPG,NPTSE,DOSB(I,N,1)) A 3610
1130 CONTINUE A 3620
   GO TO (1150,1140), N A 3630
1140 CALL SPHERE (ZL,DOSE(1,N,1),IMAX,DOSE(1,N,2)) A 3640
   CALL SPHERE (ZL,DOSB(1,N,1),IMAX,DOSB(1,N,2)) A 3650
1150 CONTINUE A 3660
1160 J=1 A 3670
   DO 1340 N=1,2 A 3680
   GO TO (1170,1190), N A 3690
1170 PRINT 1180 A 3700
1180 FORMAT ('1DOSE AT TRANSMISSION SURFACE OF FINITE ALUMINUM SLAB SHI A 3710
1ELDS')
   GO TO 1210 A 3720
1190 PRINT 1200 A 3730
1200 FORMAT ('1DOSE IN SEMI-INFINITE ALUMINUM MEDIUM') A 3750
1210 GO TO (1220,1240,1260,1280), IDET A 3760
1220 PRINT 1230 A 3770
1230 FORMAT ('0RAD'S AL') A 3780
   GO TO 1300 A 3790
1240 PRINT 1250 A 3800
1250 FORMAT ('0RAD'S H2O') A 3810
   GO TO 1300 A 3820
1260 PRINT 1270 A 3830
1270 FORMAT ('0RAD'S SI') A 3840
   GO TO 1300 A 3850
1280 PRINT 1290 A 3860
1290 FORMAT ('0RAD'S SI-02') A 3870
1300 PRINT 1310 A 3880
1310 FORMAT ('0 Z(MILS)      Z(MM)      Z(G/CM2)      ELECTRON      BREMS A 3890
1 EL+BR      TRP PROT      SOL PROT      EL+BR+TRP      TOTAL')
   PRINT 850 A 3900
   DO 1330 I=1,IMAX A 3910
   DOSEB=DOSE(I,N,J)+DOSB(I,N,J) A 3920
   DOSEBP=DOSEB+DOSP(I,J) A 3930
   DOST=DOSEBP+DOSOL(I,J) A 3940
   PRINT 1320, ZM(I),ZMM(I),Z(I),DOSE(I,N,J),DOSB(I,N,J),DOSEB,DOSP(I A 3950
   ,J),DOSOL(I,J),DOSEBP,DOST A 3960
1320 FORMAT (0P3F11.3,1P7E11.3) A 3970
1330 CONTINUE A 3980
1340 CONTINUE A 3990
   J=2 A 4000
   N=2 A 4010
   PRINT 1350 A 4020
1350 FORMAT ('11/2 DOSE AT CENTER OF ALUMINUM SPHERES') A 4030
   GO TO (1360,1370,1380,1390), IDET A 4040
1360 PRINT 1230 A 4050
   GO TO 1400 A 4060
1370 PRINT 1250 A 4070
   GO TO 1400 A 4080
1380 PRINT 1270 A 4090
   GO TO 1400 A 4100
1390 PRINT 1290 A 4110
1400 PRINT 1310 A 4120
   PRINT 850 A 4130
   DO 1410 I=1,IMAX A 4140
   DOSEB=DOSE(I,N,J)+DOSB(I,N,J) A 4150
   DOSEBP=DOSEB+DOSP(I,J) A 4160
                                         A 4170

```

```

DOST=DOSEBP+DOSOL(I,J) A 4180
PRINT 1320, ZM(I),ZMM(I),Z(I),DOSE(I,N,J),DOSB(I,N,J),DOSEB,DOSP(I A 4190
1,J),DOSOL(I,J),DOSEBP,DOST A 4200
1410 CONTINUE A 4210
GO TO 830 A 4220
1420 STOP A 4230
END A 4240

```

```

C      SUBROUTINE SPECTR (JMAX,EPS,S,EUNIT,DELTA,NPTS,T,TL,SP), 1 NOV 79. B 10
SUBROUTINE SPECTR (JMAX,EPS,S,EUNIT,DELTA,NPTS,T,TL,SP) B 20
DIMENSION EPS(1),S(1),T(1),TL(1),SP(1),G(301) B 30
IF (EPS(1).GT.0.0) GO TO 20 B 40
ALPHA=S(1) B 50
BETA=S(2) B 60
IF (BETA.LE.0.0) BETA=1.0 B 70
BETA=BETA/ALPHA B 80
DO 10 N=1,NPTS B 90
SP(N)=T(N)*BETA*EXP(-T(N)/ALPHA) B 100
10 G(N)=T(N)*SP(N) B 110
GO TO 50 B 120
20 DO 30 J=1,JMAX B 130
EPS(J)= ALOG(EPS(J)) B 140
30 S(J)= ALOG(EUNIT*S(J)) B 150
ICALL=1 B 160
DO 40 N=1,NPTS B 170
CALL SPOL (TL(N),EPS,S,JMAX,ICALL,ANS) B 180
SP(N)=T(N)*EXP(ANS) B 190
40 G(N)=T(N)*SP(N) B 200
50 CALL INT (DELTA,SP,NPTS,SIN) B 210
CALL INT (DELTA,G,NPTS,EBAR) B 220
EBAR=EBAR/SIN B 230
PRINT 60 B 240
60 FORMAT ('0    INT SPEC     EAV(MEV)') B 250
PRINT 70, SIN,EBAR B 260
70 FORMAT (1PE12.4,0PF12.5) B 270
RETURN B 280
END B 290

```

```

C      SUBROUTINE SPOL (S,X,Y,N,IN,T), 15 JAN 71. C 10
SUBROUTINE SPOL (S,X,Y,N,IN,T) C 20
C      CUBIC SPLINE INTERPOLATION WITH PARABOLIC RUNOUT. C 30
DIMENSION X(1),Y(1),E(101),U(101) C 40
GO TO (10,50), IN C 50
10 IN=2 C 60
N1=N-1 C 70
E(1)=1.0 C 80
U(1)=0.0 C 90
B1=X(2)-X(1) C 100
C1=(Y(2)-Y(1))/B1 C 110
DO 20 J=2,N1 C 120
B2=X(J+1)-X(J) C 130
C2=(Y(J+1)-Y(J))/B2 C 140
B=X(J+1)-X(J-1) C 150
D=(C2-C1)/B C 160
C=B1/B C 170
B1=B2 C 180
C1=C2 C 190
P=C*E(J-1)+2.0 C 200
E(J)=(C-1.0)/P C 210
20 U(J)=(D-C*U(J-1))/P C 220
E(N)=U(N1)/(1.0-E(N1)) C 230
DO 30 KK=1,N1 C 240
K=N-KK C 250
30 E(K)=E(K)*E(K+1)+U(K) C 260

```

```

IF (X(1).GT.X(N)) GO TO 40          C 270
IDIR=0                                C 280
MLB=0                                  C 290
MUB=N                                  C 300
GO TO 50                                C 310
40 IDIR=1                                C 320
MLB=N                                  C 330
MUB=0                                  C 340
50 IF (S.GE.X(MUB+IDIR)) GO TO 90      C 350
IF (S.LE.X(MLB+1-IDIR)) GO TO 100     C 360
ML=MLB                                C 370
MU=MUB                                C 380
GO TO 70                                C 390
60 IF (IABS(MU-ML).LE.1) GO TO 110     C 400
70 MAV=(ML+MU)/2                      C 410
IF (S.LT.X(MAV)) GO TO 80            C 420
ML=MAV                                C 430
GO TO 60                                C 440
80 MU=MAV                                C 450
GO TO 60                                C 460
90 MU=MUB+2*IDIR                      C 470
GO TO 120                               C 480
100 MU=MLB+2*(1-IDIR)                  C 490

C
C      SUBROUTINE INT(DELTA,G,N,RESULT), (N=1).
C      SUBROUTINE INT (DELTA,G,N,RESULT)
C      DIMENSION G(1)                      D 10
C      NL1=N-1                            D 20
C      NL2=N-2                            D 30
C      IF (FLOAT(N)-2.0*FLOAT(N/2)) 90,90,10   D 40
10     IF (N-1) 20,20,30                  D 50
20     SIGMA=0.0                          D 60
      GO TO 80                            D 70
30     IF (N-3) 40,40,50                  D 80
40     SIGMA=G(1)+4.0*G(2)+G(3)          D 90
      GO TO 80                            D 100
50     SUM4=0.0                          D 110
      DO 60 K=2,NL1,2                    D 120
60     SUM4=SUM4+G(K)                   D 130
      SUM2=0.0                          D 140
      DO 70 K=3,NL2,2                    D 150
70     SUM2=SUM2+G(K)                   D 160
      SIGMA=G(1)+4.0*SUM4+2.0*SUM2+G(N)    D 170
80     RESULT=DELTA*SIGMA              D 180
      RETURN                             D 190
90     IF (N-2) 100,100,110             D 200
100    SIGMA=1.5*(G(1)+G(2))           D 210
      GO TO 80                            D 220
110    IF (N-4) 120,120,130             D 230
120    SIGMA=1.125*(G(1)+3.0*G(2)+3.0*G(3)+G(4)) D 240
      GO TO 80                            D 250
130    IF (N-6) 140,140,150             D 260
140    SIGMA=G(1)+3.875*G(2)+2.625*G(3)+2.625*G(4)+3.875*G(5)+G(6) D 270
      GO TO 80                            D 280
150    IF (N-8) 160,160,170             D 290
160    SIGMA=G(1)+3.875*G(2)+2.625*G(3)+2.625*G(4)+3.875*G(5)+2.0*G(6)+4. D 300
      10*G(7)+G(8)                     D 310
      GO TO 80                            D 320
170    SIGMA=G(1)+3.875*G(2)+2.625*G(3)+2.625*G(4)+3.875*G(5)+G(6)       D 330
      SUM4=0.0                          D 340
      DO 180 K=7,NL1,2                  D 350
180    SUM4=SUM4+G(K)                   D 360
      SUM2=0.0                          D 370
      DO 190 K=8,NL2,2                  D 380
190    SUM2=SUM2+G(K)                   D 390
      SIGMA=SIGMA+G(6)+4.0*SUM4+2.0*SUM2+G(N)    D 400
      GO TO 80                            D 410
      END                                D 420
                                         D 430
                                         D 440

```

```

C      SUBROUTINE SPHERE (ZL,DOSE,IMAX,DOSPH), 30 AUG 79      E   10
      SUBROUTINE SPHERE (ZL,DOSE,IMAX,DOSPH)                   E   20
      DIMENSION ZL(1),DOSE(1),DOSL(50),DERV(50),DOSPH(1)       E   30
      DO 10 I=1,IMAX                                         E   40
      IF (DOSE(I).LE.0.0) GO TO 20                           E   50
10    DOSL(I)=ALOG(DOSE(I))                                E   60
      I=IMAX+1                                              E   70
20    IMIX=I-1                                              E   80
      IF (IMIX.LT.3) GO TO 40                               E   90
      CALL SPLDRV (ZL,DOSL,DERV,IMIX)                      E  100
      DO 30 I=1,IMIX                                         E  110
30    DOSPH(I)=DOSE(I)*(1.0-DERV(I))                     E  120
40    IMIX1=IMIX+1                                         E  130
      IF (IMIX1.GT.IMAX) RETURN                            E  140
      DO 50 I=IMIX1,IMAX                                    E  150
50    DOSPH(I)=0.0                                         E  160
      RETURN                                                 E  170
      END                                                   E  180

```

```

C      SUBROUTINE SPLDRV (X,Y,U,N), 28 AUG 79.      F   10
C      SUBROUTINE SPLDRV (X,Y,U,N)                   F   20
C      CUBIC SPLINE WITH PARABOLIC RUNDOUT.        F   30
C          U CONTAINS DERIVATIVES AT KNOTS           F   40
C      DIMENSION X(1),Y(1),E(101),U(1)              F   50
      N1=N-1                                           F   60
      E(1)=1.0                                         F   70
      U(1)=0.0                                         F   80
      B1=X(2)-X(1)                                     F   90
      C1=(Y(2)-Y(1))/B1                                F  100
      DO 10 J=2,N1                                      F  110
      B2=X(J+1)-X(J)                                    F  120
      C2=(Y(J+1)-Y(J))/B2                                F  130
      B=X(J+1)-X(J-1)                                  F  140
      D=(C2-C1)/B                                     F  150
      C=B1/B                                         F  160
      B1=B2                                         F  170
      C1=C2                                         F  180
      P=C*E(J-1)+2.0                                 F  190
      E(J)=(C-1.0)/P                                  F  200
10    U(J)=(D-C*U(J-1))/P                            F  210
      E(N)=U(N1)/(1.0-E(N1))                         F  220
      DO 20 KK=1,N1                                      F  230
      K=N-KK                                         F  240
      E(K)=E(K)*E(K+1)+U(K)                          F  250
      B2=X(K+1)-X(K)                                    F  260
      U(K)=(Y(K+1)-Y(K))/B2-B2*(2.0*E(K)+E(K+1))  F  270
20    CONTINUE                                         F  280
      U(N)=(Y(N)-Y(N1))/B2+B2*(2.0*E(N)+E(N1))  F  290
      RETURN                                            F  300
      END                                               F  310

```

U.S. DEPT. OF COMM. BIBLIOGRAPHIC DATA SHEET		1. PUBLICATION OR REPORT NO.  TN 1116	2. Gov't. Accession No.	3. Recipient's Accession No.
4. TITLE AND SUBTITLE  SHIELDOSE: A Computer Code for Space-Shielding Radiation Dose Calculations			5. Publication Date  May 1980	
7. AUTHOR(S)  Stephen Seltzer			6. Performing Organization Code	
9. PERFORMING ORGANIZATION NAME AND ADDRESS  NATIONAL BUREAU OF STANDARDS DEPARTMENT OF COMMERCE WASHINGTON, DC 20234			10. Project/Task/Work Unit No.	8. Performing Organ. Report No.
12. SPONSORING ORGANIZATION NAME AND COMPLETE ADDRESS (Street, City, State, ZIP)  Office of Naval Research, Arlington, Va. 22217  NASA Goddard Space Flight Center, Greenbelt, Md. 20771			13. Type of Report & Period Covered  Final	14. Sponsoring Agency Code
15. SUPPLEMENTARY NOTES  <input type="checkbox"/> Document describes a computer program; SF-185, FIPS Software Summary, is attached.				
16. ABSTRACT (A 200-word or less factual summary of most significant information. If document includes a significant bibliography or literature survey, mention it here.)  A computer code, SHIELDOSE, has been developed for the calculation of absorbed dose as a function of depth in aluminum shielding material of spacecraft, given the electron and proton fluences encountered in orbit. Absorbed dose, for small volumes of the detector materials Al, H <sub>2</sub> O, Si, and SiO <sub>2</sub> , is evaluated in three geometries: (1) in a semi-infinite plane medium, (2) at the transmission surface of a finite-thickness slab, and (3) at the center of a solid sphere. Use of the code is described, and an extensive set of monoenergetic depth-dose data for the various detector materials and geometries is tabulated.				
17. KEY WORDS (six to twelve entries; alphabetical order; capitalize only the first letter of the first key word unless a proper name; separated by semicolons)  Computer code; depth-dose data; electrons; electron bremsstrahlung; protons; space shielding.				
18. AVAILABILITY  <input checked="" type="checkbox"/> Unlimited  <input type="checkbox"/> For Official Distribution. Do Not Release to NTIS  <input checked="" type="checkbox"/> Order From Sup. of Doc., U.S. Government Printing Office, Washington, DC 20402,  <input type="checkbox"/> Order From National Technical Information Service (NTIS), Springfield, VA. 22161		19. SECURITY CLASS (THIS REPORT)  <input checked="" type="checkbox"/> UNCLASSIFIED	21. NO. OF PRINTED PAGES  72	
		20. SECURITY CLASS (THIS PAGE)  UNCLASSIFIED	22. Price  \$3.75	

USCOMM-DC

# NBS TECHNICAL PUBLICATIONS

## PERIODICALS

**JOURNAL OF RESEARCH**—The Journal of Research of the National Bureau of Standards reports NBS research and development in those disciplines of the physical and engineering sciences in which the Bureau is active. These include physics, chemistry, engineering, mathematics, and computer sciences. Papers cover a broad range of subjects, with major emphasis on measurement methodology and the basic technology underlying standardization. Also included from time to time are survey articles on topics closely related to the Bureau's technical and scientific programs. As a special service to subscribers each issue contains complete citations to all recent Bureau publications in both NBS and non-NBS media. Issued six times a year. Annual subscription: domestic \$17; foreign \$21.25. Single copy, \$3 domestic; \$3.75 foreign.

**NOTE:** The Journal was formerly published in two sections: Section A "Physics and Chemistry" and Section B "Mathematical Sciences."

**DIMENSIONS/NBS**—This monthly magazine is published to inform scientists, engineers, business and industry leaders, teachers, students, and consumers of the latest advances in science and technology, with primary emphasis on work at NBS. The magazine highlights and reviews such issues as energy research, fire protection, building technology, metric conversion, pollution abatement, health and safety, and consumer product performance. In addition, it reports the results of Bureau programs in measurement standards and techniques, properties of matter and materials, engineering standards and services, instrumentation, and automatic data processing. Annual subscription: domestic \$11; foreign \$13.75.

## NONPERIODICALS

**Monographs**—Major contributions to the technical literature on various subjects related to the Bureau's scientific and technical activities.

**Handbooks**—Recommended codes of engineering and industrial practice (including safety codes) developed in cooperation with interested industries, professional organizations, and regulatory bodies.

**Special Publications**—Include proceedings of conferences sponsored by NBS, NBS annual reports, and other special publications appropriate to this grouping such as wall charts, pocket cards, and bibliographies.

**Applied Mathematics Series**—Mathematical tables, manuals, and studies of special interest to physicists, engineers, chemists, biologists, mathematicians, computer programmers, and others engaged in scientific and technical work.

**National Standard Reference Data Series**—Provides quantitative data on the physical and chemical properties of materials, compiled from the world's literature and critically evaluated. Developed under a worldwide program coordinated by NBS under the authority of the National Standard Data Act (Public Law 90-396).

**NOTE:** The principal publication outlet for the foregoing data is the Journal of Physical and Chemical Reference Data (JPCRD) published quarterly for NBS by the American Chemical Society (ACS) and the American Institute of Physics (AIP). Subscriptions, reprints, and supplements available from ACS, 1155 Sixteenth St., NW, Washington, DC 20056.

**Building Science Series**—Disseminates technical information developed at the Bureau on building materials, components, systems, and whole structures. The series presents research results, test methods, and performance criteria related to the structural and environmental functions and the durability and safety characteristics of building elements and systems.

**Technical Notes**—Studies or reports which are complete in themselves but restrictive in their treatment of a subject. Analogous to monographs but not so comprehensive in scope or definitive in treatment of the subject area. Often serve as a vehicle for final reports of work performed at NBS under the sponsorship of other government agencies.

**Voluntary Product Standards**—Developed under procedures published by the Department of Commerce in Part 10, Title 15, of the Code of Federal Regulations. The standards establish nationally recognized requirements for products, and provide all concerned interests with a basis for common understanding of the characteristics of the products. NBS administers this program as a supplement to the activities of the private sector standardizing organizations.

**Consumer Information Series**—Practical information, based on NBS research and experience, covering areas of interest to the consumer. Easily understandable language and illustrations provide useful background knowledge for shopping in today's technological marketplace.

*Order the above NBS publications from: Superintendent of Documents, Government Printing Office, Washington, DC 20402.*

*Order the following NBS publications—FIPS and NBSIR's—from the National Technical Information Services, Springfield, VA 22161.*

**Federal Information Processing Standards Publications (FIPS PUB)**—Publications in this series collectively constitute the Federal Information Processing Standards Register. The Register serves as the official source of information in the Federal Government regarding standards issued by NBS pursuant to the Federal Property and Administrative Services Act of 1949 as amended, Public Law 89-306 (79 Stat. 1127), and as implemented by Executive Order 11717 (38 FR 12315, dated May 11, 1973) and Part 6 of Title 15 CFR (Code of Federal Regulations).

**NBS Interagency Reports (NBSIR)**—A special series of interim or final reports on work performed by NBS for outside sponsors (both government and non-government). In general, initial distribution is handled by the sponsor; public distribution is by the National Technical Information Services, Springfield, VA 22161, in paper copy or microfiche form.

## BIBLIOGRAPHIC SUBSCRIPTION SERVICES

The following current-awareness and literature-survey bibliographies are issued periodically by the Bureau:

**Cryogenic Data Center Current Awareness Service.** A literature survey issued biweekly. Annual subscription: domestic \$25; foreign \$30.

**Liquefied Natural Gas.** A literature survey issued quarterly. Annual subscription: \$20.

**Superconducting Devices and Materials.** A literature survey issued quarterly. Annual subscription: \$30. Please send subscription orders and remittances for the preceding bibliographic services to the National Bureau of Standards, Cryogenic Data Center (736) Boulder, CO 80303.

**U.S. DEPARTMENT OF COMMERCE**  
**National Bureau of Standards**  
Washington, D.C. 20234

OFFICIAL BUSINESS

Penalty for Private Use, \$300

POSTAGE AND FEES PAID  
U.S. DEPARTMENT OF COMMERCE  
COM-215



SPECIAL FOURTH-CLASS RATE  
BOOK

---